Functional analysis of the membrane-fusion machinery mediating cell-plate formation in dividing cells of the flowering plant *Arabidopsis thaliana*

Dissertation

der Mathematisch-Naturwissenschaftlichen Fakultät

der Eberhard Karls Universität Tübingen

zur Erlangung des Grades eines

Doktors der Naturwissenschaften

(Dr. rer. nat.)

vorgelegt von

Matthias Ulrich Karnahl

aus Ludwigsburg

Tübingen

2017

Gedruckt mit Genehmigung der Mathematisch-Naturwissenschaftlichen Fakultät der Eberhard Karls Universität Tübingen.

Tag der mündlichen Qualifikation:	18. August 2017
Dekan:	Prof. Dr. Wolfgang Rosenstiel
1. Berichterstatter:	Prof. Dr. Gerd Jürgens
2. Berichterstatter:	Prof. Dr. Klaus Harter

I. Table of Contents

II. Figure List

1. Abstract

The mechanism of plant cytokinesis strongly differs from cell division in other eukaryotic organisms. The expanding cell plate grows from the centre of the division plane towards the maternal plasma membrane. The formation of this vesicular-tubular network is arranged through the delivery of large amounts of membrane vesicles, which fuse with one another in the division plane and requires the activity of SNARE proteins and regulatory proteins that belong to the Sec1/Munc18 family (SM). The SM protein KEULE functions in *Arabidopsis* cell division through the positive regulation of the cytokinesis-specific Qa-SNARE KNOLLE and its Qb-, Qc- (or Qbc-) R-SNARE partners. In a current model, the following mechanism was proposed: KNOLLE is delivered to the cell plate in an inactive form. Upon arrival in the plane of cell division, it becomes activated and this fusion-competent state of KNOLLE is stabilized by KEULE. In this primed state, KNOLLE can form *trans*-SNARE complexes, which initiates the fusion process. However, it is so far unknown in which form interacting SNAREs are trafficked through the endomembrane system and reach their destination at the cell plate, whether as monomeric SNAREs or in pre-assembled, inactive complexes. To evaluate this, transgenic seedlings were engineered to analyse exclusively newly synthesised SNARE proteins upon blocking secretory traffic at either the Endoplasmic Reticulum (ER) or the Trans-Golgi-Network (TGN) by treating seedlings with the fungal toxin brefeldin A. Co-Immunoprecipitation experiments on extracts from these seedlings revealed the presence of pre-assembled KNOLLE *cis*-SNARE complexes at both blocked sites. Hence, these experiments suggest that inactive, cytokinesis-specific KNOLLE-*cis*-SNARE complexes assemble already at ER membranes and are maintained during their passage *via* Golgi/TGN to the plane of cell division, where they are transformed into fusogenic SNAREs. This mechanism can ensure the delivery of large, stoichiometric amounts of fusion components to the division plane. This mode of SNARE trafficking could be: (i) specific to cell division, (ii) generally employed in biological contexts of rapid membrane expansion, or (iii) represent the default mechanism to deliver newly synthesised SNAREs to their destination. First evidence for a more generally employed mechanism provided the analogous analysis of Qa-SNAREs PEN1 and SYP132. Similar to KNOLLE, both plasma-membrane-localized Qa-SNAREs were detected in pre-assembled SNARE complexes in extracts from ER or TGN membranes.

In line with the essential function of the SM protein KEULE during cytokinesis, in *keule* mutants cell division is impaired, which results in their developmental arrests at an early seedling stage. However, this relatively late arrest of *keule* mutants suggests the presence of functionally overlapping SM proteins that act in related pathways during earlier stages of development. In

contrast to gymnosperms and the basal angiosperm *Amborella*, which harbour only a single *SEC1* gene, *Arabidopsis* and most other angiosperms encode for three SEC1-related SM proteins. SEC1B, the closest homologue of KEULE in *Arabidopsis,* was functionally analysed and its function evaluated for overlapping and/or specialized roles compared to KEULE. In contrast to *keule* mutants that are severely impaired in the development during a seedling stage, homozygous *sec1b* mutants were viable and developed entirely normally. The *sec1b keule* double mutant displayed near-gametophytic lethality revealing their genetic interaction and implying functional overlap between SEC1B and KEULE. Both SM proteins were detected at the cell plate of dividing cells and interacted with cytokinesis-specific Qa-SNARE KNOLLE or cytokinesis-relevant Qa-SNARE SYP132, supporting a combined function in vesicle fusion during cytokinesis. Furthermore, SEC1B, but not KEULE, accumulated at the plasma membrane of interphase cells and it preferentially interacted with SYP132, rather than with KNOLLE. This suggests a preferential role of SEC1B in the regulation of plasma-membrane-localized SYP132 during secretory traffic in interphase cells. The analyses of different Qa-SNARE-SM protein double mutants revealed that among the four analysed fusion factors, including SM proteins KEULE and SEC1B, and Qa-SNAREs KNOLLE and SYP132, only the positive regulation of KNOLLE by KEULE can sustain cytokinesis during early embryo development. These data suggest that SEC1B and the evolutionary more ancient SYP132 exert their major, conserved function in the secretory trafficking pathway of interphase cells, while KEULE might have co-evolved a cytokinesis-specific function together with KNOLLE during angiosperm evolution

The R-SNAREs VAMP721 and VAMP722 equally contribute to vesicle fusion during cell plate formation as part of two described cytokinesis-specific SNARE complexes in *Arabidopsis*. However, even in the absence of both proteins in *vamp721 vamp722* double mutants, cell division is not entirely abolished and mutants develop to an early seedling stage, indicating the involvement of further R-SNAREs. VAMP721 and VAMP722 are part of the VAMP72 clade that contains seven members, among which VAMP724 is the only member that is expressed during vegetative plant growth, localizes to the plasma membrane and is not yet characterized. Thus, VAMP724 was functionally analysed and tested for its involvement in vesicle fusion during cell division and putative overlapping or distinct functions with VAMP721 and VAMP722 were evaluated. The *vamp724* mutant developed entirely normal, suggesting VAMP724 to be non-essential during normal plant growth. However, the *vamp721 vamp722 vamp724* triple-homozygous mutant did not develop to a seedling stage, implying developmental arrest during earlier developmental stages and overlapping functions of VAMP724 with VAMP721 and VAMP722. This functional overlap was supported by the ability of overexpressed *VAMP724* to partially complement the *vamp721 vamp722* double mutant phenotype. VAMP724 localized to the cell plate of dividing cells and interacted with cytokinesis-specific Qa-SNARE KNOLLE in

co-immunoprecipitation experiments. Furthermore, VAMP724 interacted with plasma-membrane Qa-SNARE SYP132 and upon strong accumulation, it was detected at the plasma membrane of interphase cells. By this, VAMP724 overlapped in both localization and interaction partners with VAMP721 and VAMP722. Together, this suggests that the R-SNARE VAMP724 is functionally very similar to its close homologues VAMP721 and VAMP722. As such, it is - at least in their absence - involved in vesicle fusion during cytokinesis and at the plasma membrane of interphase cells during secretory trafficking.

2. Zusammenfassung

Der Mechanismus der Zellteilung in Pflanzen unterscheidet sich grundlegend von dem anderer eukaryotischer Organismen. Es entsteht eine Zellplatte, die vom Zentrum der Zellteilungsebene aus in Richtung der parentalen Plasmamembran expandiert, mit der sie fusioniert und dadurch die Tochterzellen voneinander separiert. Dafür werden Membranvesikel zunächst ins Zentrum und später entsprechend an die Ränder des expandierenden tubolo-vesikulären Netzwerks der wachsenden Zellplatte geliefert, wo sie miteinander und mit der Zellplatte fusionieren. Da die Zellplatte etwa ein Drittel der parentalen Plasmamembran umfasst, werden große Mengen an Membranvesikeln benötigt um die separierende Membran auszubilden. Proteine der SNARE und der SEC1/Munc18 (SM) Familie spielen bei der Fusion von Membranen eine essenzielle Rolle. Das SM-Protein KEULE fungiert während der Zellteilung in *Arabidopsis* als positiver Regulator des Qa-SNAREs KNOLLE. Ein aktuelles mechanistisches Modell besagt, dass KNOLLE in einer inaktiven Form zur Zellplatte transportiert wird, dort in einem energieabhängigen Schritt durch α-SNAP/NSF aktiviert wird und die resultierende, aktive Form durch KEULE stabilisiert wird. In dieser aktiven Form kann KNOLLE *trans*-SNARE-Komplexe ausbilden, die die gegenüberliegenden Membranen benachbarter Vesikel überbrücken, was deren Fusion initiiert. Jedoch bisher unbekannt war, in welcher Form KNOLLE in die Zellteilungsebene gelangt und ob es als monomeres Qa-SNARE oder als voll-assemblierter, inaktiver Qa-,Qb-Qc-R-SNARE Komplex durch das Endomembransystem transportiert wird. Dies wurde getestet, indem transgene Linien konzipiert wurden, die es erlaubten, den sekretorischen Transportweg an ER oder TGN, jeweils durch Behandlung mit dem pilzlichen Inhibitor Brefeldin A (BFA), zu blockieren und ausschließlich neusynthetisierte SNAREs an den blockierten Membranen zu analysieren. Keimlingsextrakte dieser Linien wurden mittels Co-Immunopräzipitation auf die Präsenz von SNARE-Komplexen getestet und sowohl am ER, als auch am TGN wurden assemblierte KNOLLE-haltige *cis*-SNARE-Komplexe nachgewiesen. Dies deutet darauf hin, dass zellteilungsspezifische SNARE-Proteine bereits am ER in inaktiven *cis*-SNARE-Komplexen

assemblieren, die entlang des sekretorischen Transportweges *via* Golgi/TGN zur Zellteilungsebene transportiert werden, wo sie aktiviert werden. Diese Form des SNARE Transports garantiert den einheitlichen Transport großer Mengen an Fusionskomponenten in die Zellteilungsebene und stellt dadurch einen hocheffizienten Mechanismus dar. Dieser Transportmodus könnte speziell während der Zellteilung Anwendung finden (i), einen generellen Mechanismus darstellen, der eine Rolle in biologischen Zusammenhängen spielt in denen Membranen rapide expandieren (ii), oder grundsätzlich für neusynthetisierte SNARE Proteine genutzt werden, die auf diesem Wege an ihre Zielmembran geliefert werden (iii). Einen ersten Hinweis auf die Verallgemeinerung dieses Transportmodus lieferte die analoge Analyse der beiden Qa-SNAREs PEN1 und SYP132, die ebenfalls am ER und im TGN als Komplex mit Qb- oder Qbc-SNARE detektiert wurden.

Das SM Protein KEULE spielt eine essentielle Rolle während der Zellteilung in *Arabidopsis*, indem es das Qa-SNARE KNOLLE positiv reguliert. Interessanterweise blockiert jedoch der Ausfall von KEULE nicht die weitere Embryonalentwicklung, wie bei einem Ausfall der Zellteilung zu erwarten wäre. Daher war zu vermuten, dass weitere mit KEULE funktionell überlappende Proteine an der Zellteilung beteiligt sind. Im Gegensatz zu den Gymnospermen und der basalen Angiosperme *Amborella,* die nur ein SEC1-Homolog enthalten, kodieren *Arabidopsis* und die meisten anderen Angiospermen für zwei weitere SEC1-ähnliche SM Proteine zusätzlich zu KEULE. Unter ihnen ist SEC1B am nächsten verwandt mit KEULE, daher wurde SEC1B funktional charakterisiert und auf überlappende, bzw. spezialisierte Funktionen mit KEULE untersucht. Im Gegensatz zur stark beeinträchtigten Entwicklung von *keule* Mutanten waren *sec1b* Mutanten homozygot überlebensfähig und entwickelten sich wild-typisch. Doppelmutanten der beiden SM Proteine waren jedoch gametophytisch nahezu letal, was deren funktionalen Überlapp indiziert. Beide SM Proteine wurden an der Zellplatte detektiert und eine Interaktion mit dem zytokinese-spezifischen Qa-SNARE KNOLLE oder dem zytokinese-assoziierten Qa-SNARE SYP132 konnte nachgewiesen werden, was stark auf eine überlappende Rolle der beiden SM Proteine während der Zellteilung hindeutet. Außerdem akkumulierte SEC1B, im Gegensatz zu KEULE, an der Plasmamembran in Interphase-Zellen und es interagierte präferenziell mit SYP132, verglichen mit KNOLLE. Dies wiederum spricht dafür, dass SEC1B hauptsächlich an der Regulation von SYP132 beteiligt ist und für eine Rolle im sekretorischen Transportweg in Interphase-Zellen spricht. Die Analyse verschiedener Kombinationen an SM protein – SNARE Protein Doppelmutanten hat ergeben, dass von den analysierten Fusionskomponenten, die die SM Proteine KEULE und SEC1B und die Qa-SNARE Proteine KNOLLE und SYP132 umfassen, ausschließlich die Kombination aus KEULE und KNOLLE ausreicht, um die Zellteilung in Embryonen aufrecht zu erhalten. Diese Ergebnisse deuten darauf hin, dass SEC1B und das evolutionär gesehen ältere SYP132 ihre Hauptrolle im konservierten Transportweg zur Plasmamembran in Interphase-Zellen

ausprägen, während KEULE zusammen mit KNOLLE in Angiospermen co-evolviert sein könnte, um eine spezifische Funktion während der Zellteilung auszuprägen.

Die Immunlokalisierung der beiden Proteine deren Kolokalisierung an der Zellplatte sich teilender Zellen, konsistent mit deren Aktivität während der Zellteilung. In Interphase-Zellen hingegen, akkumulierte KEULE zytosolisch, während SEC1B an der Plasmamembran detektiert wurde. Weiterhin zeigte SEC1B eine starke Präferenz für die Interaktion mit dem evolutionär älteren Qa-SNARE SYP132, während KEULE mit Qa-SNAREs SYP132 und KNOLLE gleichermaßen interagierte, und diese Präferenz wurde ebenfalls in genetischen Interaktionsstudien nachgewiesen. Dies deutet darauf hin, dass die Hauptaktivität des SM Proteins SEC1B darin liegt, das Qa-SNARE SYP132 zu regulieren und impliziert damit eine vorrangige Rolle im sekretorischen Transportweg zur Plasmamembran. KEULE hingegen interagierte mit KNOLLE und SYP132 gleichermaßen und könnte mit dem evolutionär jüngeren KNOLLE zusammen co-evolvieren, um eine spezifische Aktivität während der Zellteilung auszuprägen.

Die R-SNAREs VAMP721 und VAMP722 sind gleichermaßen beteiligt an der Vesikelfusion an der Zellplatte. Jedoch ist die Zellteilung in *vamp721 vamp722* Doppelmutanten nicht komplett inhibiert, was auf funktionell überlappende R-SNAREs hinweist. VAMP721/VAMP722 gehören zur VAMP72 Familie, die sieben Mitglieder in *Arabidopsis* beinhaltet. Unter ihnen ist VAMP724 das einzige Mitglied, dem bislang keine spezifische Funktion zugewiesen wurde, das an der Plasmamembran lokalisiert und das in relevanten, vegetativen Entwicklungsphasen exprimiert wird. Daher wurde VAMP724 funktional charakterisiert und in Hinsicht auf überlappende bzw. spezialisierte biologische Rollen evaluiert. VAMP724 ist nicht essentiell für die Entwicklung von Pflanzen, was sich in homozygot-vitalen *vamp724* Mutanten ausdrückte. Im Gegensatz dazu arretieren *vamp721 vamp722* Doppelmutanten in frühen Keimlingsstadien. Die *vamp721 vamp722 vamp724* Tripelmutanten waren in ihrer Entwicklung bereits in früheren Stadien beeinträchtigt, was auf eine überlappende Funktionalität dieser drei R-SNAREs hinweist. Entsprechend konnte die *vamp721 vamp722* Mutante phänotypisch durch die Überexpression von VAMP724 während der Zellteilung - unter der Kontrolle des *KNOLLE* Promoters - komplementiert werden. Subzellulär wurde VAMP724 an der Zellplatte detektiert und die Interaktion mit dem zytokinese-spezifischen Qa-SNARE KNOLLE wurde nachgewiesen, was die Funktionalität von VAMP724 in der Vesikelfusion während der Zellteilung belegt. Weiterhin wurde VAMP724 an der Plasmamembran in Interphase-Zellen lokalisiert und eine Interaktion mit dem Plasmamembran-Qa-SNARE SYP132 nachgewiesen, was auf eine weitere Funktion im sekretorischen Transportweg hindeutet. Demnach weist das R-SNARE VAMP724 eine ähnliche Funktionalität zu der, seiner beiden Homologe VAMP721/VAMP722 auf und trägt zumindest in deren Abwesenheit zur Vesikelfusion an der Zellplatte sich teilender Zellen und im sekretorischen Transportweg zur Plasmamembran bei.

3. General Introduction

3.1 Plant Endomembrane compartments and their communication network through vesicle trafficking

The plant endomembrane system and their trafficking pathways

Maintaining a functional cell requires the spatial separation of chemical processes into separated functional units such as endosomes and other organelles. The lumen of organelles is separated by lipid bilayer membranes from the lumen of the cell (cytosol), which generates chemically unique environments that allow the functional specification of these environments. The integrity of this endomembrane system requires active transport pathways for the delivery of membrane-bound and intra-luminal material, called cargo, from one compartment to another. Newly synthesised membrane-bound proteins are co-translationally or post-translationally inserted into the Endoplasmic Reticulum (ER) membrane, whereas intraluminal proteins are pass through ER membranes and accumulate inside the ER lumen. Membrane-bound proteins, lipids, cell-wall material and intraluminal proteins are delivered from the ER to their destination in the endomembrane system. Two major anterograde trafficking pathways are well established in plant cells (Figure 1). One is the secretory pathway that describes cargo delivery from ER through the stacks of the Golgi apparatus, *via* the Trans-Golgi-Network (TGN) to the plasma membrane. The other route diverges after the TGN towards the vacuole *via* Multi-Vesicular-Bodies (MVBs). Endocytosis a major retrograde trafficking pathway retrieves extracellular and plasma-membrane-bound material cargo from the plasma membrane back to the TGN/ early endosomes. From there, endocytosed cargo can be either delivered through MVBs to the vacuole for degradation or trafficked back to the plasma membrane in the recycling pathway (Park and Jurgens 2011). The endocytic pathway that delivers cargo to the vacuole is important to remove obsolete material from the plasma membrane, for example receptor-ligand complexes that transmitted their signal already to downstream targets, like FLS2 that is endocytosed and degraded upon flg22 binding (Robatzek et al. 2006). In contrast, receptors or transporters, which activities are still needed at the plasma membrane are recycled back to the plasma membrane for reuse. In response to environmental stimuli, the pathway that is chosen for specific cargo can vary, to allow cells to respond to the detected environmental changes. This was shown, for instance, for the boron exporter REQUIRES HIGH BORON1 (BOR1). Under low boron conditions, BOR1 is abundant at the plasma membrane and undergoes continues cycling, whereas it is rapidly internalized and delivered

to the vacuole for degradation under high boron concentrations to avoid toxicity by high intracellular boron levels (Takano et al. 2005). The recycling pathway is important for the establishment of cell polarity through the polar delivery of previously endocytosed cargo back to specific sectors at the plasma membrane. For instance, the basal accumulation of the auxin efflux carrier PIN1 is essential for the directional flow of auxin, which in turn is involved in several developmental aspects, like phototropism, gravitropism, apical dominance and root formation (Steinmann et al. 1999).

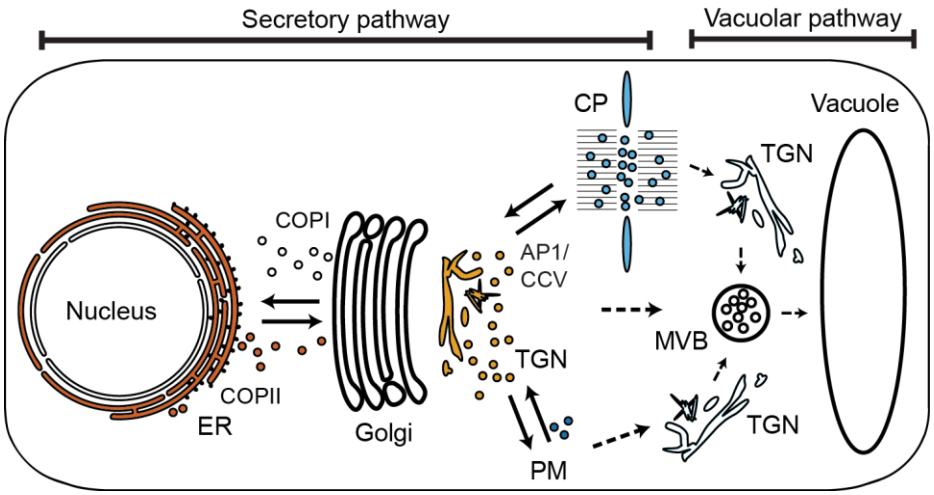

Figure 1 Major trafficking routes in plant cells (simplified).

Newly synthesised membrane-bound and intraluminal cargo is transported along the secretory trafficking pathway towards its destination in the endomembrane system. From their site of synthesis at the Endoplasmic Reticulum (ER) they pass through the Golgi stacks, *via* the Trans-Golgi-Network (TGN) to their destination at the plasma membrane (PM). During plant cell division, this trafficking pathway is reorganised to deliver newly synthesised and endocytosed cargo from the PM to the forming cell plate (CP). In the vacuolar pathway, newly synthesised and endocytosed cargo from the PM or the CP are delivered from the TGN through Multi-Vesicular-Bodies (MVBs) to the vacuole, usually for degradation (Park and Jurgens 2011). COPI, COPII, AP1/CCV, membrane vesicles with specific coat complexes; CCV, clathrin-coated vesicles.

Vesicular trafficking

In these trafficking pathways, small, spherical membrane structures, called vesicles, are formed to pass lipids and other membrane associated cargo through the lipophobic space of the cytosol. Vesicle formation is initiated through the activation of small G-proteins of the ARF or SAR1 family by specific ARF guanine-nucleotide exchange factors (ARF-GEFs), which exchange protein-internal GDP for GTP (Memon 2004). ARF and SAR1 proteins cycle between an inactive, soluble GDP-bound state and an active, membrane-associated GTP-bound state. Upon activation, they accumulate at the site of vesicle formation in the donor membrane and recruit downstream effectors, including adaptor and coat protein complexes that are specific to distinct membranes (Cherfils 2014). At the ER-Golgi interface, vesicles coated with COPI (coat protein I) mediate intra-Golgi and retrograde Golgi-ER trafficking,

whereas the anterograde ER-Golgi transport is mediated by COPII-coated transport vesicles (Figure 1) (Lee et al. 2004). Clathrin, a third class of coat proteins, is recruited to distinct membranes by different adaptor complexes (Hirst and Robinson 1998). In plants, clathrin was detected at the TGN, MVB and the plasma membrane (Ito et al. 2012) and is involved in intra-endosomal, secretory and endocytic trafficking pathways (Robinson 2015). The recruitment of adaptor and coat complexes further leads to the selective accumulation of soluble and membrane-bound cargo into the forming vesicle and initiates membrane curvature. Once membrane curvature progresses, vesicles are pinched off by dynamin-related proteins and are now free to travel through the cytoplasm towards the destined target membrane (Park and Jurgens 2011).

Active sorting processes at the vesicle formation site accumulate specific components of the trafficking machinery into the forming vesicle, which ensures specificity of the targeting process to defined target membranes. These components include the RAB protein family of small GTPases that undergo a similar GDP- or GTP-bound cycle as ARF/SAR1 (Stenmark 2009). Active RAB-GTP can recruit a variety of effectors that include sorting adaptors, motors, kinases, phosphatases and tethering factors. Through the recruitment of these effectors, they are involved in the establishment of membrane identity, vesicle budding, uncoating, motility and vesicle fusion with the plasma membrane. Thus, RAB proteins recruit specific motor proteins that promote vesicle delivery along actin filaments or microtubules to defined target membranes. Upon arrival, tethering factors at target membrane and at vesicles, including RABs, initiate the tethering process (Stenmark 2009). Subsequently, fusion is initiated through the interaction of SNARE (soluble N-ethylmaleimide-sensitive-factor attachment receptor) proteins located at each of the opposing membranes and their formation of membrane-spanning *trans*-SNARE complexes. The assembly in these highly stable SNARE complexes releases a substantial amount of energy, which was suggested to be essential to overcome the energy barrier between the two opposing polar membrane surfaces (Lipka et al. 2007).

3.2 The mechanism of SNARE protein activity and its regulation through SEC1/Munc18 (SM) proteins

SNARE protein characteristics

SNARE proteins belong to a superfamily that is conserved among all eukaryotic kingdoms and are, for instance, represented by about 60 members in *Arabidopsis thaliana*. They are characterized by a conserved helical SNARE domain of about 60-70 amino acids (Figure 2) (Lipka et al. 2007). A central conserved amino acid within this domain allows for the

classification into Q-SNAREs, carrying a glutamine (Q), and R-SNAREs, carrying an arginine (R) at this position (Fasshauer et al. 1998). Prior to fusion, Q-SNAREs usually form a receptive tri-helical SNARE complex at the target membrane (t-SNARE), while R-SNAREs arrive on the vesicle (v-SNARE) (Sollner et al. 1993, Rothman 1994). The conservation of divergent SNARE domains further subdivides Q-SNAREs into Qa-, Qb- or Qc-SNAREs (Bock et al. 2001). Additionally, Qb- and Qc-SNARE domains can be included in the same protein, which is classified as Qbc-SNARE. Fusogenic SNARE complexes contain one SNARE domain each, resulting in either Qa-Qb-Qc-R-SNARE or Qa-Qbc-R-SNARE complexes (Bock et al. 2001).

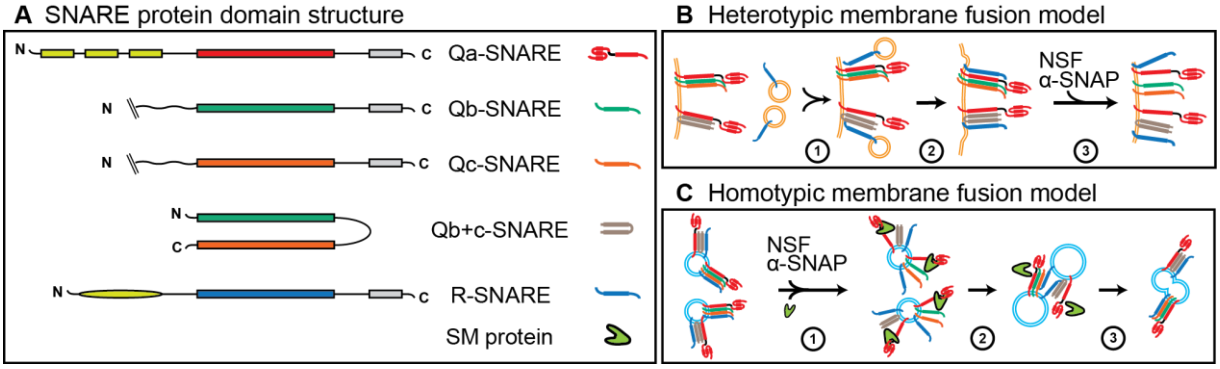

Figure 2 Model for heterotypic and. homotypic vesicle fusion

Schematic representation of Qa-, Qb-, Qc-, Qbc- and R-SNARE protein domain structure (A), helices of Qa-SNAREs (yellow), the longin domain of R-SNAREs (yellow), transmembrane domains (grey), and SNARE domains (different colours) are indicated. (B) During heterotypic membrane fusion: vesicles arrive at their destination, fusion is initiated through the formation of membrane-spanning (*trans*)-SNARE complexes (1) and after vesicle fusion (2) they locate together (*cis*) at the target membrane. Resulting *cis*-SNARE complexes are dissociated by α-SNAP/NSF (B-3), and R-SNAREs recycled for further fusion events. During homotypic vesicle fusion (C), vesicles containing similar SNARE complexes arrive at their site of fusion. SNAREs are activated by α-SNAP/NSF (1) and the active form of the Qa-SNARE stabilized by the SM protein (in some cases), trans-SNARE complexes form (2) to promote vesicle fusion (3).

The mechanism of vesicle fusion was originally and extensively studied during neurotransmitter release at the mammalian synapse. Syntaxin-1, which acts in synaptic vesicle exocytosis was the first identified Qa-SNARE (Bennett et al. 1992), and thus Qa-SNAREs are often referred to as ‘syntaxin’. The domain structure of Qa-SNAREs includes a regulatory N-peptide, followed by three N-terminal helices, a flexible linker domain, the SNARE domain and a hydrophobic C-terminal transmembrane domain (Figure 2) (Lerman et al. 2000). The three helices at the N-terminus (H_{abc} motif) form a three-helical bundle (Fernandez et al. 1998) that can fold back onto the SNARE domain, mimicking the assembled SNARE complex (Dulubova et al. 1999, Munson et al. 2000). This “closed” conformation abolishes binding to other SNARE proteins and confers auto-inhibitory properties (Dulubova et al. 2007). Qa-SNAREs localize at specific membranes but can interact with promiscuous Qbc- or Qb-, Qc- and R-SNARE partners. Therefore Qa-SNAREs are considered to confer specificity to membrane fusion events (Sanderfoot 2007, Bassham et al. 2008).

SNARE protein mechanism and regulation by Sec1/Munc18 proteins

In synaptic vesicle exocytosis, Munc18-1 was identified as regulator of syntaxin-1 and its SNARE partners Qbc-SNARE SNAP-25 and R-SNARE synaptobrevin (Garcia et al. 1994, Pevsner et al. 1994). Munc18-1 is a member of the SEC1/Munc18 protein family (SM proteins), which is conserved among all eukaryotes and comprises four clades that act at different subcellular locations (Koumandou et al. 2007). Munc18-1 regulates the function of Qa-SNARE syntaxin-1 through two distinct mechanisms (Sollner et al. 1993, Pevsner et al. 1994). Firstly, it binds syntaxin-1 in its closed conformation, preventing SNARE complex formation (Burkhardt et al. 2008, Chen et al. 2008). Secondly, Munc18-1 binds to the assembled SNARE complex and promotes its assembly during vesicle fusion (Shen et al. 2007, Rodkey et al. 2008). These opposite regulatory effects of Munc18-1 on syntaxin-1 were recently combined into a model that could explain the precise function and the mechanism that underlies the regulatory effect of Mun18-1 (Rizo and Sudhof 2012): First, Munc18-1 binds to the N-peptide and the H_{abc} motif of newly synthesised syntaxin-1 and keeps the protein in a closed, inactive form, which prevents unspecific interactions and fusion during its path through the secretory trafficking pathway. Subsequently, another fusion factor, MUN13 dissociates the complex and induces a conformational change in syntaxin-1 that results in its open form. Munc18-1 then binds syntaxin-1 at the SNARE motif and initiates the incorporation of Qbc-SNARE SNAP-25. This primed complex consisting of syntaxin-1 and SNAP-25, which resides at the plasma membrane, can then interact with the vesicle-associated R-SNARE synaptobrevin in *trans*-SNARE complexes to bridge the opposing membranes, thus promoting fusion (compare figure 2B) (Rizo and Sudhof 2012). However, this mode of regulation cannot be applied to all SNARE-SM protein partners and differs among tissues and species (Rizo and Sudhof 2012). One example for the diversity of the interaction mechanism represents Sec1p, the SM protein involved in yeast exocytosis that interacts solely with previously assembled SNARE complexes, but not with its monomeric cognate Qa-SNARE Sso1p (Togneri et al. 2006).

3.3 The plant-specific mechanism of cell division

During cell division, parental cells are partitioned into two daughter cells by a newly formed membrane. In this aspect of cell division, the mechanism in plant cells differs considerably from that in other eukaryotes, in which an actomyosin ring constricts the parental plasma membrane in the plane of cell division until only a small gap remains. This gap appears to be filled by vesicles fusion, likely depending on the secretory trafficking pathway (Guizetti and Gerlich 2010). In contrast, plant cells form the dividing membrane (aka cell plate) by TGN-derived vesicles fusing with one another in the centre of the division plane to generate a vesicular-

tubular network that laterally expands towards the parental membrane, where it eventually fuses to separate the two daughter cells (Boruc and Van Damme 2015).

In plant cytokinesis, a circular array of microtubules and actin filaments, called preprophase band (PPB), is established at the cell cortex underneath the plasma membrane. This array initially defines the plane of cell division and the future fusion site between the forming cell plate and the plasma membrane (Valster et al. 1997, Granger and Cyr 2001). Site markers are recruited to the PPB, and upon disassembly of the PPB, these markers are retained to transduce the positional information. These markers include cytoskeleton-interacting and reorganizing proteins like the PHRAGMOPLAST-ORINTING KINESIN 1 (POK1) and outline, after PPB disassembly, the so-called cortical division zone, which retains the positional information of the future fusion zone (Walker et al. 2007, Xu et al. 2008, Lipka et al. 2014). Vesicles are delivered to the expanding cell plate through a dynamic cytoskeletal array, called phragmoplast. During the lateral expansion of the cell plate, microtubules of the phragmoplast depolymerise in the centre and polymerise at the margins of the expanding cell plate, in coordination with proteins from the cortical division zone (Austin et al. 2005). Through this permanent reorganization of the phragmoplast, vesicles reach specifically into the growing margins of the cell plate, where they fuse to expand the cell plate. Eventually, the growing membrane approaches the plasma membrane at the cortical division zone where cell plate and plasma membrane fuse to separate the two daughter cells (Muller and Jurgens 2016).

Secretory traffic during plant cytokinesis

The formation of a novel membrane compartment, like the cell plate, requires large amounts of membrane material including lipids, cell wall material and plasma membrane proteins. To meet this high demand during cytokinesis, endocytosed proteins from the plasma membrane and *de novo* synthesised proteins converge at the TGN and are delivered to the cell plate in a default pathway. Few exceptions are specifically targeted elsewhere, for instance the auxin-efflux carrier PIN1 that is still recycled and polarly delivered to the plasma membrane (Touihri et al. 2011, Richter et al. 2014). Notably, *de novo* synthesised material is absolutely required during cell plate formation, as was shown by blocking ER-Golgi traffic in the ARF-GEF mutant *gnl1* by the fungal toxin BFA, which abolished cell plate formation and resulted in multinucleate cells (Reichardt et al. 2007). Vesicles destined for the cell plate are formed at the TGN, depending on redundantly acting ARF-GEFs BIG1 to BIG4 and the adaptor complex AP-1 (Richter et al. 2014). Removing either of these trafficking-related proteins results in multinucleate cells, a clear sign of impaired cell plate formation (Park et al. 2013, Teh et al. 2013, Richter et al. 2014). Upon arrival in the plane of cell division, vesicle tethering requires the activity of RAB-A GTPases, the EXOCYST and the TRAPII tethering complexes and is

followed by SNARE-dependent vesicle fusion (Chow et al. 2008, Fendrych et al. 2010, Qi et al. 2011, Rybak et al. 2014).

Vesicle fusion during cytokinesis

In flowering plants, the Qa-SNARE KNOLLE has evolved a specialized functional that is essential to vesicle fusion during cytokinesis. It is expressed specifically during late G2/M-phase of the cell cycle and strongly labels the cell plate of dividing cells (Lauber et al. 1997). After cytokinesis, it is rapidly sequestered from the plasma membrane and targeted *via* the MVB towards the vacuole for degradation (Reichardt et al. 2007). KNOLLE forms SNARE complexes with promiscuous SNARE partners and assembles into two distinct SNARE complexes that provide the majority of SNARE activity during cell plate formation. These two complexes contain either Qbc-SNARE SNAP33 and R-SNARE VAMP721 or its close paralogue VAMP722 (further referred to as VAMP721/VAMP722), or Qb-SNARE NPSN11, Qc-SNARE SYP71 and R-SNARE VAMP721/VAMP722 (El Kasmi et al. 2013).

The SM protein KEULE (aka SEC11) was identified as an essential component of the vesicle fusion machinery during plant cytokinesis and positively regulates the function of Qa-SNARE KNOLLE (Lukowitz et al. 1996, Assaad et al. 2001). The mechanism of this regulation differs from that described for mammalian or yeast homologues. Like mammalian syntaxin-1, KNOLLE can assume at least two distinct conformations. In its closed form, the N-terminal helical domain folds back onto the SNARE domain, inhibiting SNARE complex formation, whereas the two domains are physically apart in the open form (Park et al. 2012). Introducing two point mutations into the linker domain that connects the SNARE domain with the N-terminal helices stabilizes the open conformation of Qa-SNAREs (Dulubova et al. 1999). Similar point mutations in KNOLLE increased its susceptibility to trypsin degradation, suggestion a more open conformation (Park et al. 2012). It was shown in yeast-two-hybrid and pull-down experiments that KEULE interacts preferentially with the constitutively open form of KNOLLE. In contrast, in *Arabidopsis* seedling extracts, the converse was observed and KEULE interacted exclusively with the wild-type form of KNOLLE. In seedling extracts, cognate SNARE partners of KNOLLE are present, which outcompete KEULE for the interaction with the KNOLLE open form. This suggests that the open conformation represents the reactive form of KNOLLE that assembles into SNARE complexes *in vivo*. This was confirmed by the preferential interaction of Qbc-SNARE partner SNAP33 with the open form of KNOLLE compared to its wild-type variant. Interestingly, overexpressing the open form of KNOLLE in *keule* mutants could fully complement the mutant phenotype. This indicates that KEULE function was bypassed by this constitutively active form of KNOLLE, rendering the positive regulation by KEULE unnecessary. This led to the formulation of a functional model in which KNOLLE is delivered to the cell plate in an inactive form. In an energy-dependent step, likely

involving α-SNAP/NSF, KNOLLE changes its conformation into the active, open form, which can be stabilized by KEULE (Park et al. 2012). Subsequently, KEULE is displaced during fusion by cognate SNARE partners that exhibit higher affinity for the open form of KNOLLE to form fusogenic *trans*-SNARE complexes (Park et al. 2012).

Abrogation of both KNOLLE-containing complexes strongly impairs cytokinesis, consequently *knolle* mutants or *syp71 snap33* double mutants arrest at an early seedling stage, displaying cytokinetic defects. These defects are characterized by unfused vesicles in the division plane, cell wall stubs and enlarged, multinucleate cells. Notably cell division is not fully abolished in these double mutants and plants can develop to a seedling stage (El Kasmi et al. 2013). Similarly, in *keule* mutants, in which the SM protein KEULE no longer regulates the formation of SNARE complexes, a comparable phenotype was observed (Assaad et al. 1996). Ongoing cell division activity during the early development of these mutants suggests that for both fusion factors, SNARE proteins and SM proteins, functionally overlapping components promote vesicle fusion in their absence. In contrast, the *knolle keule* double mutant phenotype displays developmental arrest at the zygote stage, resulting in a single multinucleate cells, which corresponds to fully abolished cytokinesis due to the absence of both, Qa-SNARE KNOLLE and its regulatory SM protein KEULE (Waizenegger et al. 2000).

3.4 Aim of thesis

In plants, cell division requires the delivery of large amounts of TGN-derived vesicles that fuse with one-another in the plane of cell division to generate the tubular-vesicular of the expanding cell plate that upon completion separates the two daughter cells. Membrane fusion is initiated by the formation of membrane spanning *trans*-SNARE complexes, which is regulated by members of the Sec1-/Munc18 (SM) protein family. In *Arabidopsis* cytokinesis, SM protein KEULE positively regulates the cytokinesis-specific Qa-SNARE KNOLLE and its promiscuous SNARE partners. To further understand underlying mechanisms and their regulation, three questions were addressed in this work by analysing members of these protein families: (i) A current model predicts the arrival of inactive KNOLLE in the fusion plane, where it is activated and the fusogenic form stabilized by KEULE. However unknown is, in which form KNOLLE and relevant SNARE partners are transported through the endomembrane system. This issue was addressed by analysing SNAREs that were extracted from specific sites along the secretory trafficking pathway and analysed for either their monomeric form or their pre-assembly in *cis*-SNARE-complexes. (ii) The KEULE deficient mutant advances to an early seedling stage before it arrests. This suggests that during earlier developmental stages other SM proteins compensate for the loss of KEULE during in cytokinesis. Thus, closely related members of the SM protein family in *Arabidopsis* were functionally analysed and tested for their involvement

during cell division. They were further evaluated for putative functional overlap or specialization in an evolutionary perspective. (iii) The R-SNAREs VAMP721 and VAMP722 are equally involved in SNARE complex formation during cytokinesis and as such essential components of the vesicle fusion machinery during *Arabidopsis* cell division. However, the *vamp721 vamp722* double mutant develops to a seedling stage, like the *keule* mutant, suggesting the involvement of further R-SNAREs during cytokinesis. In the attempt to identify this or these R-SNARE(s), the *Arabidopsis* VAMP72 clade - of which VAMP721 and VAMP722 are part - was evaluated for possible candidates. The single candidate, VAMP724, was tested for its involvement in cytokinesis and functionally analysed. The results were interpreted for overlapping and distinct functions among the members of this R-SNARE clade.

4. ER assembly of *cis*-SNARE complexes mediates unimpeded passage through the endomembrane system

4.1 Introduction

In regular endosomal trafficking, the membrane identity of vesicles is defined by the composition of the donor compartments and the membrane material that is specifically sorted into the forming vesicle. Through this sorting step, specific components of the membrane fusion machinery, including RAB GTPases and SNARE proteins, decorate the vesicles and confer specificity to the subsequent fusion process with the target membrane. In this so-called heterotypic membrane fusion, specific t-SNAREs (usually Q-SNARE complexes) on the target membrane form *trans*-SNARE complexes with v-SNAREs (usually the R-SNARE) on the arriving vesicle (Lipka et al. 2007). In contrast, during homotypic membrane fusion, similar membranes face each other that contain identical fusion components, which thus requires additional layers of regulation to limit vesicle fusion to the desired site (compare figure 2B-C). During plant cytokinesis, near-identical vesicles from the Golgi/TGN arrive in the plane of cell division and fuse with one another to generate the expanding cell plate (Richter et al. 2014). These secretory vesicles deliver *de novo* synthesised and endocytosed material to the cell plate, including proteins of the fusion machinery, like the cytokinesis-specific Qa-SNARE KNOLLE and its SNARE partners. During cell division, KNOLLE forms two distinct SNARE complexes that contain either the Qbc-SNARE SNAP33 and R-SNAREs VAMP721 or VAMP722 or Qb-SNARE NPSN11, Qc-SNARE SYP71 and R-SNARE VAMP721 or VAMP722 (El Kasmi et al. 2013). A current model describes the arrival of KNOLLE in the fusion plane in

an inactive, fusion-incompetent form. Vesicle fusion can only proceed through the activation of KNOLLE by NSF/α-SNAP and the stabilization of the open, fusion-competent form of KNOLLE by the SM protein KEULE (Park et al. 2012). However, it is unknown in which form these SNAREs are trafficked through the endomembrane system and reach the plane of cell division. Individual SNARE proteins could be sorted into different vesicle subpopulations and by this be spatially separated during transport. SNAREs could also reside on transport vesicles in a monomeric or oligomeric form and be kept inactive by unknown components, in a comparable mechanism to the mammalian SM protein Munc18-1 and its cognate Qa-SNARE syntaxin-1 (Medine et al. 2007). Alternatively, vesicles could contain highly stable, pre-assembled *cis*-SNARE complexes prior to fusion that are activated in the fusion plane as suggested by Park et al. (2012).

To address this question experimentally, specific mutants were used to block secretory traffic in *Arabidopsis* seedlings at either the ER-Golgi interface or at the TGN by treatment with the fungal toxin brefeldin A (BFA). During cytokinesis, newly synthesised SNARE proteins, including KNOLLE, are inserted into the membrane of the ER and trafficked along the secretory pathway *via* the Golgi stacks and the TGN to the plane of cell division. Towards the end of cytokinesis, KNOLLE is endocytosed and targeted *via* MVBs to the vacuole for degradation (see Figure 3A) (Reichardt et al. 2007). Thus, blocking secretory traffic at the ER-Golgi interface or at the TGN captures KNOLLE and other *de novo* synthesised SNAREs at those sites before they can assemble in SNARE complexes during membrane fusion. To ensure that during the experiments exclusively newly synthesised SNAREs would be detected and post-fusion SNARE complexes could be excluded, transgenic lines in respective mutant backgrounds (see below) were generated that expressed SNAREs from an estradiol-inducible promoter and expression was only induced after the trafficking block was fully established. Such expressed SNAREs included either Qb-SNARE NPSN11 or Qbc-SNARE SNAP33, as representatives for both KNOLLE-containing SNARE complexes. By testing precipitates from these transgenic lines for SNARE interaction, either (i) monomeric or (ii) pre-assembled *cis*-SNARE complexes would be observed for newly synthesised SNAREs at both sites the ER or the TGN. Thus, the observation can elucidate in which form KNOLLE and its partners are delivered through the endomembrane system, following their path along the secretory pathway.

To evaluate, whether a general mode of SNARE trafficking would be observed, or rather a mechanism specific to the delivery of KNOLLE during cell division, the analysis was extended to additional Qa-SNAREs and precipitates were tested for the presence of PEN1 and SYP132. PEN1 was found in SNARE complexes together with Qb-SNARE NPSN11 or Qbc-SNARE SNAP33. It continuously cycles between the TGN and the plasma membrane, where it participates in the secretory trafficking pathway during regular plant growth. It is additionally

involved in plant defence responses against, for instance, the infection by powdery mildew (Assaad et al. 2004, Kwon et al. 2008b, Pajonk et al. 2008, Reichardt et al. 2011, Fujiwara et al. 2014). SYP132 is known to interact with Qb-SNARE NPSN11 and localizes at the plasma membrane, where it remains stably associated upon delivery. It also participates in regular secretory trafficking and is further involved in plant resistance against bacterial pathogens. Recently, it was additionally functionally implicated in vesicle fusion during cytokinesis. (Reichardt et al. 2011, Fujiwara et al. 2014, Park et al. in submission)

For blocking secretory traffic, the fungal toxin brefeldin A (BFA) was employed, which inhibits the ARF-activating guanine-nucleotide exchange reaction of sensitive ARF-GEFs. Secretory traffic in *Arabidopsis* is normally insensitive to BFA, unlike the situation in mammals, yeast and most flowering plants (Mossessova et al. 2003, Renault et al. 2003, Richter et al. 2014). However, ARF-GEF sensitivity to BFA depends on a single amino acid within the catalytic SEC7 domain and mutation of this amino acid renders the ARF-GEFs sensitive or insensitive, without impairing protein function (Peyroche et al. 1999). In *Arabidopsis,* ER-Golgi traffic is jointly regulated by the BFA-insensitive ARF-GEF GNL1 and the BFA-sensitive ARF-GEF GNOM (Richter et al. 2007). In *gnl1* mutants that express a sensitive variant of GNL1, both relevant ARF-GEFs are rendered sensitive to BFA. Thus, treating these plants with BFA prevents the recruitment of the COPI coat complex and induces collapse of ER-Golgi traffic, which subsequently results in the fusion of Golgi stacks with the ER (see Figure 3A) (Richter et al. 2007). Late-secretory traffic from the TGN to the plane of cell division requires the formation of AP-1 complex-coated transport vesicles, which is regulated by four functionally overlapping ARF-GEFs, BIG1 to BIG4 (Park et al. 2013, Richter et al. 2014). Among these, BIG3 is the sole BFA-resistant protein. Hence, mutational inactivation of the *BIG3* gene renders late-secretory traffic BFA-sensitive and treatment of *big3* mutants with BFA causes the accumulation of TGN-derived membranes in aggregates, so-called BFA compartments, in which endocytosed and secretory proteins accumulate (Figure 3A) (Richter et al. 2014). Consistent, with blocked traffic and the failure to deliver fusion components to the plane of cell division, BFA-treated *big3* and *gnl1* mutant seedlings displayed binucleate cells and cell wall stubs, indicative of impaired cell plate formation (Richter et al. 2007, Richter et al. 2014).

4.2 Results

4.2.1 SNAREs in TGN-derived membranes are assembled into SNARE complexes

For the interpretation of the transport form of captured SNAREs, proteins must be excluded that already went through the fusion cycle and contaminate the results with post-fusion *cis*-SNARE complexes. *Arabidopsis* seedling cells divide asynchronously and BFA treatment would inhibit secretory traffic only in cells entering the division phase, but not in cells of later mitotic stages, in which the complexes are assembled. Therefore, N-terminally YFP-tagged NPSN11 and GFP-tagged SNAP33 were expressed from an inducible expression system that is sensitive to β-estradiol (EST) (Zuo et al. 2000), only after 30 minutes BFA pre-treatment. Importantly, neither YFP-NPSN11 nor GFP-SNAP33 were expressed from this promoter without EST treatment, which is a prerequisite for the detection of newly-made SNAREs that are blocked at the ER or the TGN. This was confirmed by the failure to detect GFP signal in non-induced seedlings by immunostaining with anti-GFP antiserum and by the absence of GFP-tagged protein in anti-GFP precipitates from these from those plants (Figure 6A).

Arabidopsis *big3* mutant seedlings were treated with BFA for 30 min, followed by 210 minutes of combined BFA and EST treatment to induce expression of YFP-NPSN11 or GFP-SNAP33. Upon BFA treatment, both fusion proteins and KNOLLE were exclusively detected in TGN-containing BFA compartments, in contrast to the strong labelling of cell plates in *big3* mutant seedlings not treated with BFA (Figure 3B,C). The frequency of cells undergoing cytokinesis was not altered by BFA treatment of wild-type or mutant seedlings, which was determined by immunostaining of phragmoplast microtubules (Figure 4A,B).

Co-immunoprecipitation analysis of BFA-treated *big3* mutant seedlings, expressing estradiol -(EST-) inducible YFP-NPSN11 revealed the presence of Qb-SNARE NPSN11 fused to YFP, Qa-SNARE KNOLLE, Qc-SNARE SYP71 and R-SNARE VAMP721/722, as well as the absence of Qbc-SNARE SNAP33 in the anti-GFP precipitate (Figure 5A). Thus, only members of the KNOLLE-NPSN11-SYP71-VAMP721/722 complex were co-immunoprecipitated, whereas SNAP33 – a member of the other KNOLLE-containing SNARE complex – was not. The converse was observed in the co-immunoprecipitation analysis of *big3* mutant seedlings, expressing the EST-inducible Qbc-SNARE member, GFP-SNAP33, of the other KNOLLE complex. Qc-SNARE SYP71 was not detected in the co-immunoprecipitate, in contrast to the members of the trimeric KNOLLE complex Qbc-SNARE GFP-SNAP33, Qa-SNARE KNOLLE and R-SNARE VAMP721/722 (Figure 5B). Thus, the interaction detected by co-immunoprecipitation was exclusively confined to members of specific SNARE complexes that

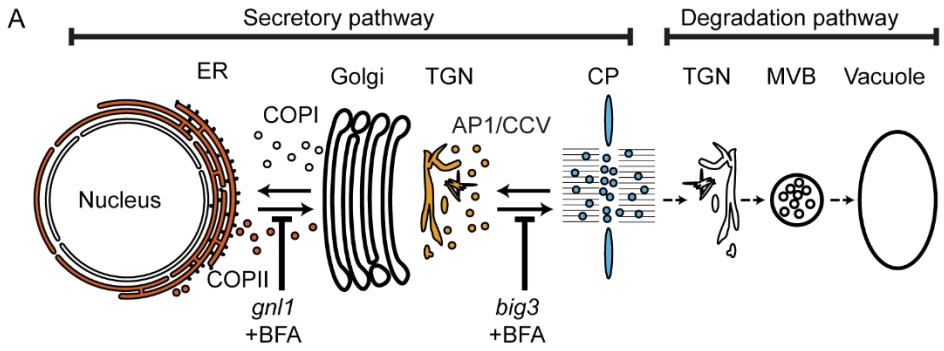

Co-accumulation of *de novo* synthesised KNOLLE and SNARE partners in TGN- or ER-/Golgi-derived membranes through site-specific inhibition of the secretory trafficking pathway

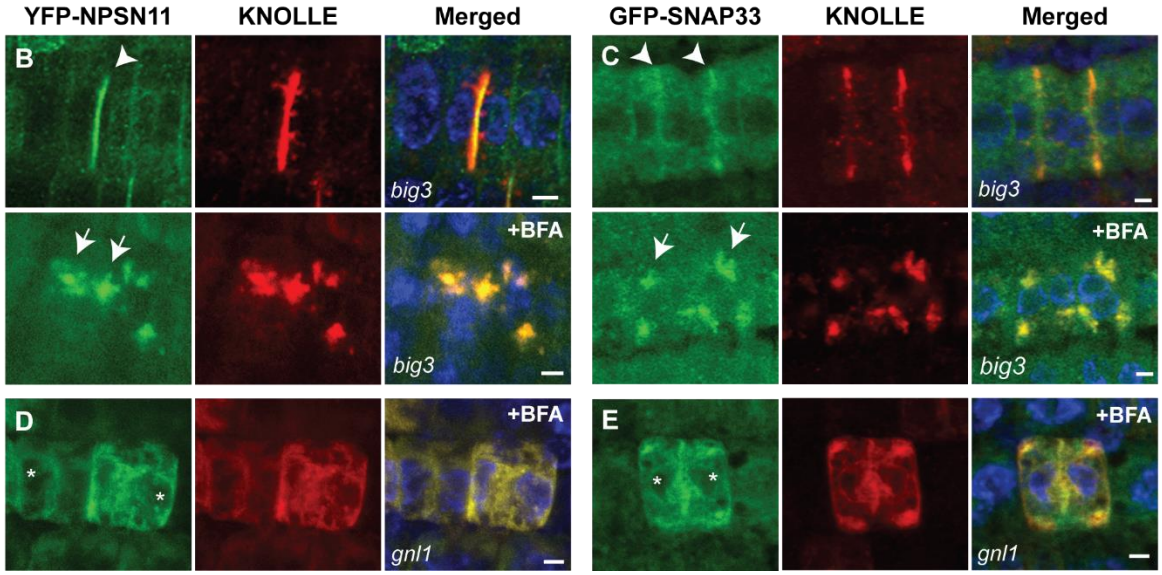

Figure 3 Site-specific inhibition of SNARE protein trafficking to the cell-division plane.

(**A**) The trafficking route of the Qa-SNARE KNOLLE in cytokinesis follows the secretory pathway, from the ER, through Golgi/TGN to the CP and the degradation pathway through TGN, MVBs to vacuoles (Reichardt et al. 2007). ER, endoplasmic reticulum; TGN, *trans*-Golgi network; CP, cell plate; MVB, multivesicular body; COPI, COPII, AP1/CCV, membrane vesicles with specific coat protein complexes; *gnl1*, *big3*, knockout mutations of ARF-GEFs rendering those trafficking steps sensitive to brefeldin A (BFA). (**B-E**) Subcellular localisation of estradiol-inducible YFP-NPSN11 (**B, D**, green) and GFP-SNAP33 (**C**, **E**, green), and KNOLLE (**B-E**; red) in *big3* (**B, C**) and *gnl1 GNL1*$^{BFA\text{-}sens.}$ (**D**) mutant seedling roots treated with 50 µM BFA for 30 min, followed by 50 µM BFA + 20 µM estradiol for 210 min. Note that YFP-NPSN11 or GFP-SNAP33 accumulates with KNOLLE at the BFA compartments in BFA-treated *big3* mutant whereas YFP-NPSN11 or GFP-SNAP33 colocalises with KNOLLE at the ER in BFA-treated *gnl1 GNL1*$^{BFA\text{-}sens.}$ mutant. Nuclei of overlays (**B–D**) were counterstained with DAPI (blue). -BFA, mock treatment; +BFA, BFA treatment; -EST, no estradiol treatment. Arrowheads, cell plates; arrows, BFA compartments; asterisks, ER. Scale bar, 5 µm. The experiments were technically repeated three times.

contained the EST-induced SNARE partner, which strongly suggests that only direct interactions between SNARE complex members were detected. To rule out complex formation during the immunoprecipitation procedure, varying amounts of extracts from *KNOLLE::mCherry-KNOLLE* transgenic seedlings were added to extracts expressing either YFP-NSPN11 or GFP-SNAP33 before immunoprecipitation with anti-GFP beads. The amount

A

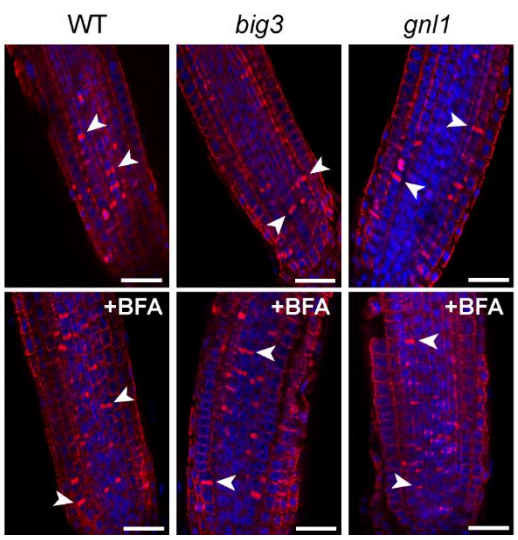

B Frequency of cells undergoing cytokinesis

Genotype	-BFA (± SD)	+BFA (± SD)
WT (Col-0)	35 (± 6)	35 (± 9)
big3	38 (± 6)	40 (± 6)
gnl1 GNL1$^{BFA\text{-}sens.}$	32 (± 10)	32 (± 9)

Figure 4 Cytokinetic cells in *big3* and *gnl1 GNL1*$^{BFA\text{-}sens.}$ mutant seedling roots.

Mutant seedling roots were treated with 50 µM BFA for 30 min followed by 50 µM BFA + 20 µM estradiol for 210 min. (A) Anti- α-tubulin-labeling of microtubule phragmopasts (red, arrowhead) suggests unchanged populations of cytokinetic cells in BFA treated mutant or wild-type (WT) seedling roots. Nuclei were counterstained with DAPI (blue). (B) Quantification of the frequency of cytokinetic cells further excluded negative effects of either mutation or BFA treatment in two technical replicates. +BFA, BFA treatment. scale bar, 25 µm

of KNOLLE-containing SNARE complexes changed neither with additional 1x nor 10x mCherry-KNOLLE (Figure 6B). To exclude the possibility that BFA might induce ectopic SNARE complex formation, KNOLLE co-precipitation with GFP-SNAP33 or YFP-NSPN11, and thus complex formation, was compared between BFA-treated and -untreated wild-type seedlings, through semi-quantitative band intensity evaluation. No obvious difference in KNOLLE complex formation was observed for treated and untreated seedlings, ruling out BFA-induced complexes (Figure 6C). As an additional control, immunoprecipitates from EST-induced KNOLLE-partners GFP-SNAP33 and YFP-NPSN11 were tested for the presence of the Qa-SNARE PEP12 (aka SYP21), which is normally located at the MVB and absent from the plane of cell division (da Silva Conceicao et al. 1997, Muller et al. 2003). Upon BFA treatment of *big3* mutant seedlings, PEP12 relocated to the same BFA compartments as GFP-SNAP33 and YFP-NPSN11 (Figure 7A). Neither SNAP33 nor NPSN11 interacted with mRFP-tagged PEP12 whereas both did interact with KNOLLE, further confirming the specificity of the co-immunoprecipitation assay (Figure 7B). These results indicate that in dividing cells two distinct KNOLLE-containing SNARE complexes are already assembled as *cis*- (in one membrane) SNARE complexes at the TGN, i.e. before the initiation of the fusion process at the plane of cell division, and that they comprise either (i) KNOLLE, SNAP33 and VAMP721/722 or (ii) KNOLLE, NPSN11, SYP71 and VAMP721/722.

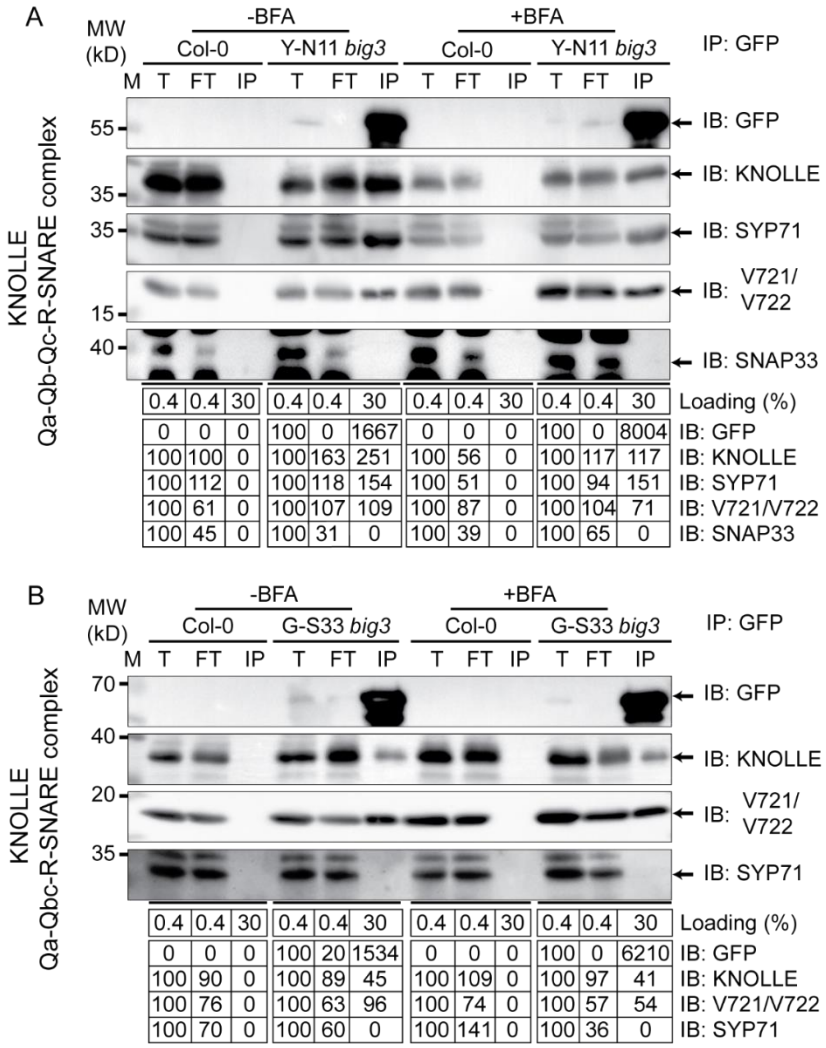

Figure 5 Interaction analysis of cytokinetic SNAREs with traffic blocked at the TGN.

Wild-type (WT) and *big3* mutant seedlings carrying estradiol-inducible *YFP-NPSN11* (A) or *GFP-SNAP33* (B) transgenes were treated with 50 µM BFA for 30 min followed by 50 µM BFA + 20 µM estradiol for 210 min (see Fig. 2B–C). Protein extracts were subjected to immunoprecipitation with anti-GFP beads, protein blots were probed with the antisera indicated on the right (IB): GFP, anti-GFP; KN, anti-KNOLLE; V721/V722, anti-VAMP721/722; SYP71, anti-SYP71; SNAP33, anti-SNAP33; kDa, protein size (left); MW, molecular weight; -BFA, mock treatment; +BFA, BFA treatment; T, total extract; UB, unbound; IP, immunoprecipitate. Loading (%), relative loading volume to total volume; relative signal intensity are indicated below (input signal = 100% for UB and IP). The experiments were technically repeated more than six times.

Figure 6 Confirmation of *de novo* synthesised KNOLLE SNARE partners and other control experiments for co-immunoprecipitation analyses of SNARE complex formation. (next page)

(A) No signal of KNOLLE SNARE partners was detected without EST induction, during GFP imaging analysis and notably, no tagged protein accumulated after immunoprecipitation with anti-GFP beads. *big3* mutant seedlings carrying YFP-NPSN11 (A, left) or GFP-SNAP33 (A, right) transgenes were treated or not treated with 50 µM BFA for 240 min and observed for GFP fluorescence (A, upper panel, green; compare Figure 2B,C) or tested by immunoprecipitation with anti-GFP beads (A, lower panel). For the immunofluorescence analysis seedlings were stained with anti-KNOLLE and DAPI. Precipitates from non-induced seedlings were loaded on protein blots, together with positive controls that were induced and treated with 20 µM estradiol and 50 µM BFA for 210 min. Blots were probed with indicated antisera on the right (IB) (B) *In vitro* mixing of experimental extract with different amounts of extract from

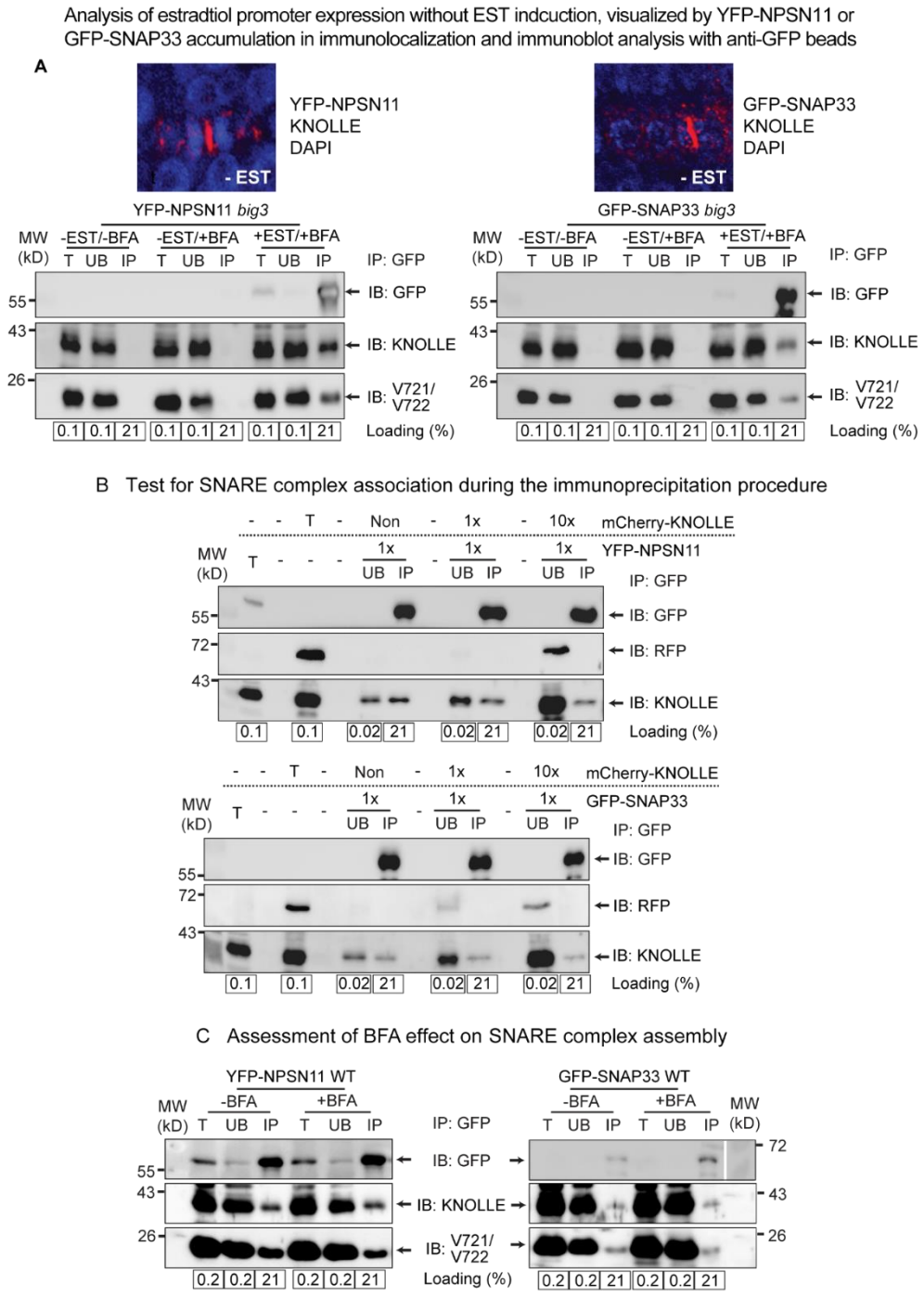

tagged KNOLLE seedlings. Cleared protein extracts of YFP-N11 (B, upper panel) or GFP-SNAP33 (B, lower panel) and the cleared protein extracts of mCherry-KNOLLE were mixed and subjected to immunoprecipitation with anti-GFP beads. Protein blots were probed with the antisera indicated on the right (IB). Note that the addition of mCherry-KNOLLE protein does not alter the amount of endogenous KNOLLE co-immunoprecipitated with YFP-N11 or GFP-SNAP33. Non, no addition of mCherry-KNOLLE protein lysate; 1x, equal amounts; 10x, 10x excess. Seedlings of wild-type (WT) background carrying YFP-NPSN11 (C, left panel) or GFP-SNAP33 (C, right panel) transgenes were treated with 50 µM BFA + 20 µM estradiol for 210 min. Protein extracts were subjected to immunoprecipitation with anti-GFP beads and protein blots probed with the antisera indicated on the right (IB). GFP, anti-GFP; RFP, anti-RFP; KNOLLE, anti-KNOLLE; V721/V722, anti-VAMP721/722; kDa, protein size; MW, molecular weight; -EST, no estradiol; -BFA, mock treatment; +BFA, BFA treatment; T, total extract; UB, unbound; IP, immunoprecipitate; Loading (%), relative loading volume to total volume; relative signal intensity (input signal = 100% for UB and IP).

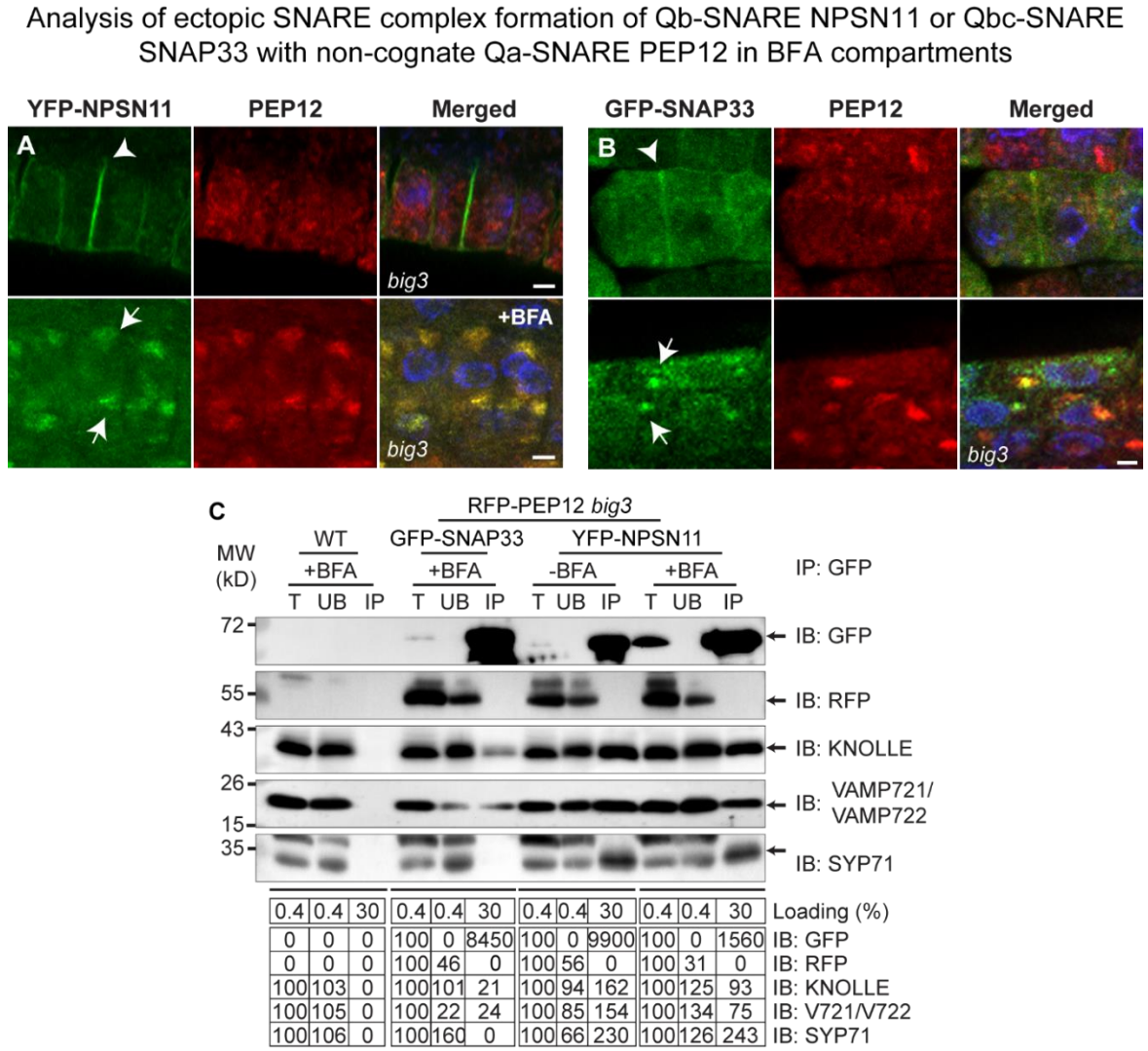

Figure 7 Subcellular localization and co-immunoprecipitation analysis of PEP12 (aka SYP21) in *big3* mutant seedling root cells, co-expressing estradiol-inducible YFP-NPSN11 and GFP-SNAP33.

(A,B) mRFP-PEP12, expressed from the *KNOLLE* promoter, coaccumulates with YFP-NPSN11 (A) and GFP-SNAP33 (B) in *big3* mutant seedlings in BFA compartments (A,B, arrow), after treatment with 50 µM BFA for 30 min followed by 50 µM BFA + 20 µM estradiol for 210 min. PEP12 was absent from GFP precipitates (C), when seedling extracts were subjected to immunoprecipitation with anti-GFP beads. Protein blots were probed with the antisera indicated on the right (IB): GFP, anti-GFP; RFP, anti-RFP; KNOLLE, anti-KNOLLE; V721/V722, anti-VAMP721/722; SYP71, anti-SYP71. G:S33, GFP:SNAP33; R:P12, mRFP:PEP12; Y:N11, YFP:NPSN11. kDa, molecular weight in kilodalton; MW, molecular weight; -BFA, mock treatment; +BFA, BFA treatment; T, total extract; UB, unbound; IP, immunoprecipitate. Loading (%), relative loading volume to total volume; relative signal intensity (input signal = 100% for UB and IP). Nuclei of merged images (A,B) were counterstained with DAPI (blue). Arrowheads, cell plates; arrows, BFA compartments. Scale bar, 5 µm. The experiments were technically repeated three times.

Figure 8 COPI dissociation from Golgi membranes in BFA-treated gnl1 *GN$^{BFA\text{-}sens.}$ seedlings* and interaction analysis of cytokinetic SNAREs with site-specifc traffic blocked at the ER.

(see **next page**) Wild-type (WT) and *gnl1* mutant seedlings complemented with GNL1$^{BFA\text{-}sens.}$ encoding a BFA-sensitive variant of GNL1 and carrying estradiol-inducible *YFP-NPSN11* (A,C) or *GFP-SNAP33* (B,D) transgenes were treated with 50 µM BFA for 30 min followed by 50 µM BFA + 20 µM estradiol for 210 min (see Fig. 2, D). Note cytosolic localisation of gCOP in BFA-treated cells whereas YFP-NPSN11

(A) and GFP-SNAP33 (B) were trapped in the ER (A,B asterisk). Nuclei of merged images were counterstained with DAPI (blue). +BFA, BFA treatment. Arrowheads, cell plates; asterisks, ER. Scale bar, 5 µm. The experiments were technically repeated three times. Protein extracts were subjected to immunoprecipitation with anti-GFP beads, protein blots were probed with the antisera indicated on the right (IB): GFP, anti-GFP; KNOLLE, anti-KNOLLE; V721/V722, anti-VAMP721/VAMP722; SYP71, anti-SYP71; SNAP33, anti-SNAP33; kDa, molecular weight in kilodalton; MW, molecular weight; -BFA, mock treatment; +BFA, BFA treatment; T, total extract; UB, unbound; IP, immunoprecipitate. Loading (%), relative loading volume to total volume; relative signal intensity (input signal = 100% for UB and IP). The experiments were technically repeated more than six times.

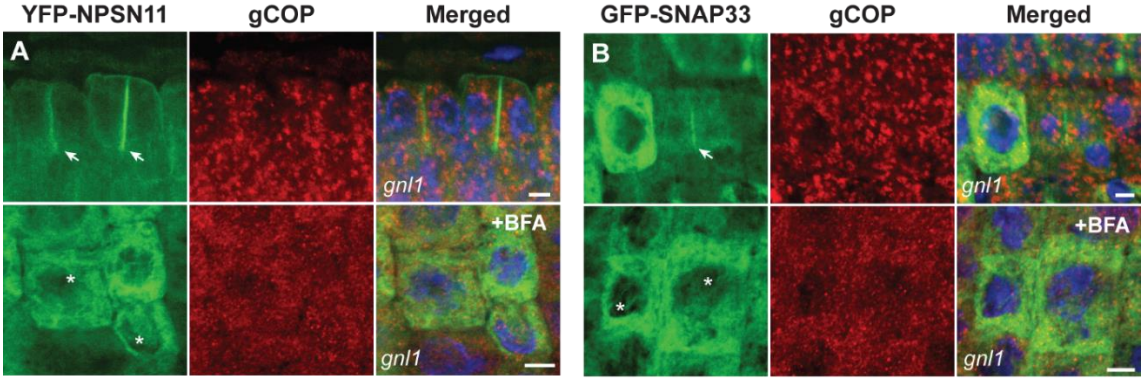

C

MW (kD)	-BFA						+BFA						
	Col-0			Y-N11 *gnl1*			Col-0			Y-N11 *gnl1*			IP: GFP
M	T	FT	IP	T	FT	IP	T	FT	IP	T	FT	IP	
55													IB: GFP
35													IB: KNOLLE
35													IB: SYP71
25													IB: V721/V722
40													IB: SNAP33
	0.4	0.4	30	0.4	0.4	30	0.4	0.4	30	0.4	0.4	30	Loading (%)
	0	0	0	100	25	293	0	0	0	100	0	381	IB: GFP
	100	86	0	100	60	111	100	57	0	100	92	95	IB: KNOLLE
	100	61	0	100	72	100	100	47	0	100	88	120	IB: SYP71
	100	49	0	100	129	81	100	93	0	100	90	58	IB: V721/V722
	100	147	0	100	107	0	100	73	0	100	105	0	IB: SNAP33

KNOLLE Qa-Qb-Qc-R-SNARE complex

D

MW (kD)	-BFA						+BFA						
	Col-0			G-S33 *gnl1*			Col-0			G-S33 *gnl1*			IP: GFP
M	T	FT	IP	T	FT	IP	T	FT	IP	T	FT	IP	
70													IB: GFP
40													IB: KNOLLE
20													IB: V721/V722
35													IB: SYP71
	0.4	0.4	30	0.4	0.4	30	0.4	0.4	30	0.4	0.4	30	Loading (%)
	0	0	0	100	4	1230	0	0	0	100	0	1839	IB: GFP
	100	89	0	100	78	166	100	113	0	100	84	100	IB: KNOLLE
	100	183	0	100	67	99	100	130	0	100	77	116	IB: V721/V722
	100	119	0	100	103	0	100	60	0	100	120	0	IB: SYP71

KNOLLE Qa-Qbc-R-SNARE complex

4.2.2 SNAREs travel through the endomembrane system from the ER onwards in inactive *cis*-SNARE complexes

To determine, where along the secretory pathway KNOLLE-containing *cis*-SNARE complexes are assembled, traffic was blocked already at the ER-Golgi interface by BFA treatment of *gnl1* mutant seedlings expressing BFA-sensitive GNL1$^{BFA\text{-}sens}$ (Richter et al. 2007) and subsequent EST-inducible expression of either YFP-NSPN11 or GFP-SNAP33 after 30 minutes of BFA treatment. Subcellular localisation revealed both fusion proteins, together with KNOLLE, in ER-like structures, indicating the effective inhibition of traffic between ER and Golgi stacks by BFA (Figure 3B). To further verify effective trafficking inhibition at the ER-Golgi interface, the subcellular localisation of γCOP was analysed. The COPI coat-complex subunit γCOP normally associates with *cis*-Golgi membranes and acts in the retrograde Golgi-ER traffic (Richter et al. 2007). Upon BFA treatment γCOP was no longer recruited from the cytosol, indicating the disruption of ER-Golgi traffic (Figure 8A,B). The co-immunoprecipitation analyses with anti-GFP beads from protein extracts of these seedlings showed a comparable interaction pattern between the different SNAREs to that observed in *big3* mutant seedlings indicating that KNOLLE already exists as part of *cis*-SNARE complexes at the ER together with YFP-NPSN11 or GFP-SNAP33. Furthermore, the detected interactions were specific to members of each cytokinetic SNARE complex, excluding recovery of non-interacting proteins from the same membrane compartment (Figure 8C,D). Thus, these data showed that analysed SNARE proteins from the two distinct KNOLLE-containing complexes assembled already at the ER in *cis*-SNARE complexes.

4.2.3 Complex formation of plasma membrane-located Qa-SNAREs along the secretory pathway

To analyse whether *cis*-SNARE complex formation at ER membranes and their maintenance during secretory trafficking is represented a mechanism, exclusive to cytokinetic KNOLLE-containing SNARE complexes, Qa-SNAREs SYP132 and PEN1 were analogously analysed and tested for complex formation at distinct sites along the secretory trafficking route. It was previously shown that both Qa-SNAREs are trapped in BFA compartments in *big3* mutant seedlings or at ER membranes in *gnl1* mutant seedlings upon BFA treatment (Reichardt et al. 2011, Richter et al. 2014). Thus, testing the immunoprecipitates from above described experiments for the presence of SYP132 or PEN1 would indicate whether also these Qa-SNAREs are assembled into SNARE complexes at those distinct sites. Both YFP-NPSN11 and GFP-SNAP33 precipitates, extracted from BFA-treated and subsequently EST-induced *big3* mutant seedlings, revealed the presence of Qa-SNAREs SYP132 and PEN1, indicating their assembly in complexes at the TGN (Figure 9A,B).

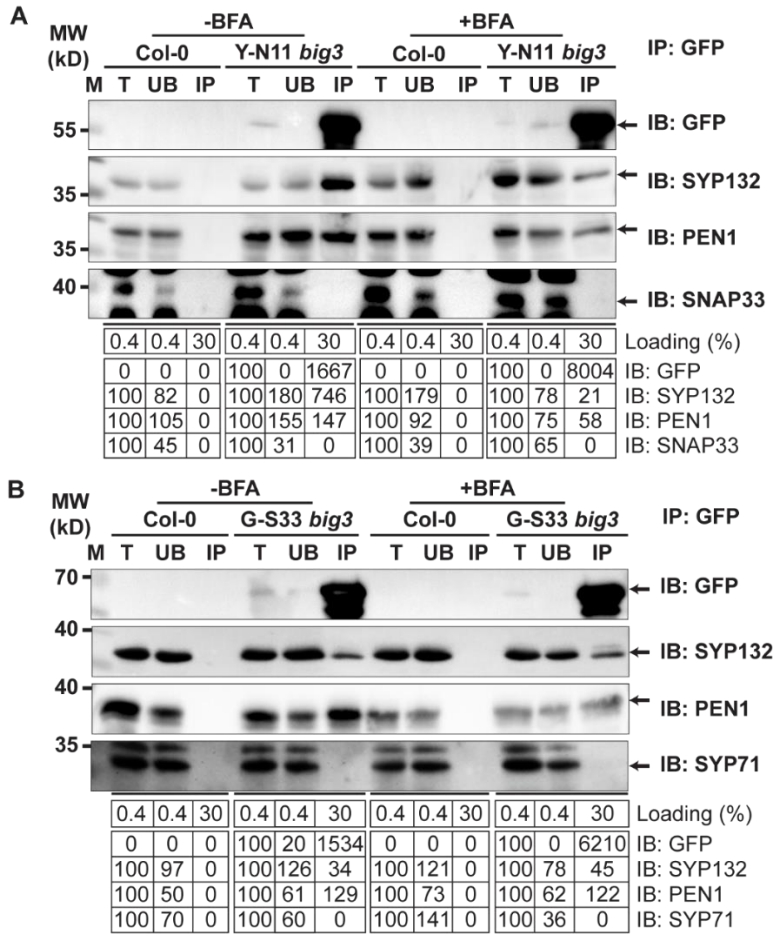

Figure 9 Interaction analysis of NPSN11 and SNAP33 with plasma membrane Qa-SNAREs SYP132 and PEN1 with traffic blocked at the TGN.

Wild-type (WT) and *big3* mutant seedlings carrying estradiol-inducible *YFP-NPSN11* (A) or *GFP-SNAP33* (B) transgenes were treated with 50 µM BFA for 30 min followed by 50 µM BFA + 20 µM estradiol for 210 min. Protein extracts were subjected to immunoprecipitation with anti-GFP beads, protein blots were probed with the antisera indicated on the right (IB): GFP, anti-GFP; SYP132, anti-SYP132; PEN1, anti-PEN1 (aka SYP121); SNAP33, anti-SNAP33; SYP71,anti-SYP71. kDa, molecular weight in kilodalton size (left); MW, molecular weight; -BFA, mock treatment; +BFA, BFA treatment; T, total extract; UB, unbound; IP, immunoprecipitate. Loading (%), relative loading volume to total volume; relative signal intensity are indicated below (input signal = 100% for UB and IP). The experiments were technically repeated more than six times.

Also precipitates from BFA-treated *gnl1* mutant seedlings, expressing *GNL1*$^{BFAres.}$ together with EST-inducible YFP-NSPN11 or GFP-SNAP33 revealed the presence of PEN1 and SYP132 (Figure 10A,B). These results indicate that, like KNOLLE, also PEN1 and SYP132 form complexes at the ER that contain at least Qb-SNARE NPSN11 or Qbc-SNARE SNAP33. Whether the R-SNARE was present in these complexes could not be determined by these experiments, because of the precipitation from the Qb- or Qbc-SNARE and the simultaneous detection of several Qa-SNAREs.

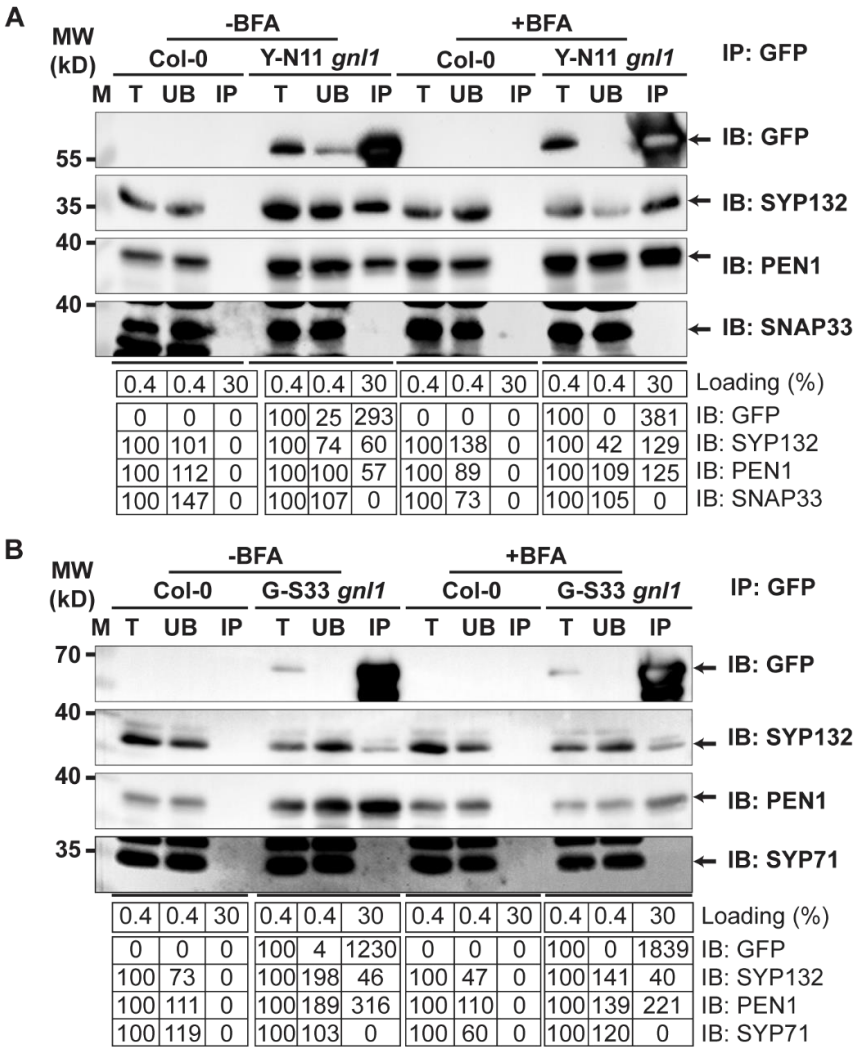

Figure 10 Interaction analysis of NPSN11 and SNAP33 with plasma membrane Qa-SNAREs SYP132 and PEN1 with traffic blocked at the ER.

Wild-type (WT) and *gnl1* mutant seedlings complemented with GNL1$^{BFA\text{-}sens.}$ encoding a BFA-sensitive variant of GNL1 and carrying estradiol-inducible *YFP:NPSN11* (A,C) or *GFP:SNAP33* (B,D) transgenes were treated with 50 µM BFA for 30 min followed by 50 µM BFA + 20 µM estradiol for 210 min. Protein extracts were subjected to immunoprecipitation with anti-GFP beads, protein blots were probed with the antisera indicated on the right (IB): GFP, anti-GFP; SYP132, anti-SYP132; PEN1, anti-PEN1 (aka SYP121); SNAP33, anti-SNAP33; SYP71,anti-SYP71. kDa, molecular weight in kilodalton; MW, molecular weight; -BFA, mock treatment; +BFA, BFA treatment; T, total extract; UB, unbound; IP, immunoprecipitate. Loading (%), relative loading volume to total volume; relative signal intensity are indicated below (input signal = 100% for UB and IP). The experiments were technically repeated more than six times.

4.3 Discussion

4.3.1 Cytokinetic SNAREs are transported as inactive *cis*-SNARE complexes to the plane of cell division

Fully assembled KNOLLE-containing cis-SNARE complexes were detected at either ER membranes or TGN-derived BFA compartments prior to their delivery to the cell plate. These SNARE complexes comprised either Qa-Qb-Qc-R-SNAREs KNOLLE-NPSN11-SYP71-VAMP721/VAMP722, or Qa-Qbc-R-SNAREs KNOLLE/SNAP33-VAMP721/VAMP722 and were exclusively formed by newly synthesised SNAREs. This implies that detected proteins could not yet have taken part in any membrane fusion events and excludes the detection of *cis*-SNARE complexes that usually occur after membrane fusion. Thus, these results clearly indicate that inactive *cis*-SNARE complexes are assembled at the ER and that SNAREs are maintained in complexes during their passage through the secretory trafficking route, that is *via* Golgi stacks and the TGN towards the cell plate (Figure 11). Hence, vesicles that arrive in the plane of cell division contain inactive *cis*-SNARE complexes that must be dissociated and rearranged into membrane-bridging *trans*-SNARE complexes that link the apposed membranes to promote fusion. These observations shed light on the requirement of the SM protein KEULE during cell plate formation. In heterotypic membrane fusion, trans-SNARE complexes are formed between the arriving vesicle and the target membrane, which result in *cis*-SNARE complexes after fusion. These complexes are disassembled by the ATPase NSF to allow the recycling of SNARE components to the respective donor membrane, which makes them available for further vesicle trafficking in the respective pathway. After disassembly Qa-SNAREs can fold back onto themselves to avoid reassembly into the complex (Jahn and Scheller 2006). In contrast, during the homotypic-like membrane fusion of cytokinetic vesicles, SNAREs arrive in the plane of cell division in pre-assembled *cis*-SNARE complexes, which requires their disassembly before fusion, likely facilitated by NSF/α-SNAP. After complex dissociation, the SM protein KEULE interacts with Qa-SNARE KNOLLE to maintain its open, fusion-competent form as a prerequisite for the formation of *trans*-SNARE complexes (Park et al. 2012).

Trafficking in the form of *cis*-SNARE complexes benefits the process of homotypic membrane fusion in several ways. First, a very stable and energetically favoured conformation is assumed (Fasshauer et al. 2002) that abolishes untimely interactions during transport and thus represents an important regulatory mechanism. Second, large amounts of membrane fusion components are delivered to the plane of cell division simultaneously. Thus, this from of SNARE transport might reflect an economic way of meeting the rising need for membrane material and membrane-fusion capacity during plant cytokinesis. This dividing membrane that

separates the future daughter cells accounts for about one-third of the total cell surface and is formed within the narrow time frame of about 30 minutes (Lipka et al. 2014). Unlike plant cytokinesis, other eukaryotes have their parental plasma membrane constricted in the plane of cell division and the remaining gap in the centre is likely closed by the secretory trafficking pathway mediated by SNARE proteins that reside at the plasma membrane throughout the cell cycle (Low et al. 2003). Nevertheless, any major expansion of the eukaryotic cell surface area requires enhanced membrane-fusion capacity that cannot easily be matched by the local recycling of plasma membrane-resident SNARE proteins. Thus, the long-distance delivery of inactive *cis*-SNARE complexes proposed here could meet the requirement and represent a general mode of SNARE trafficking during these processes.

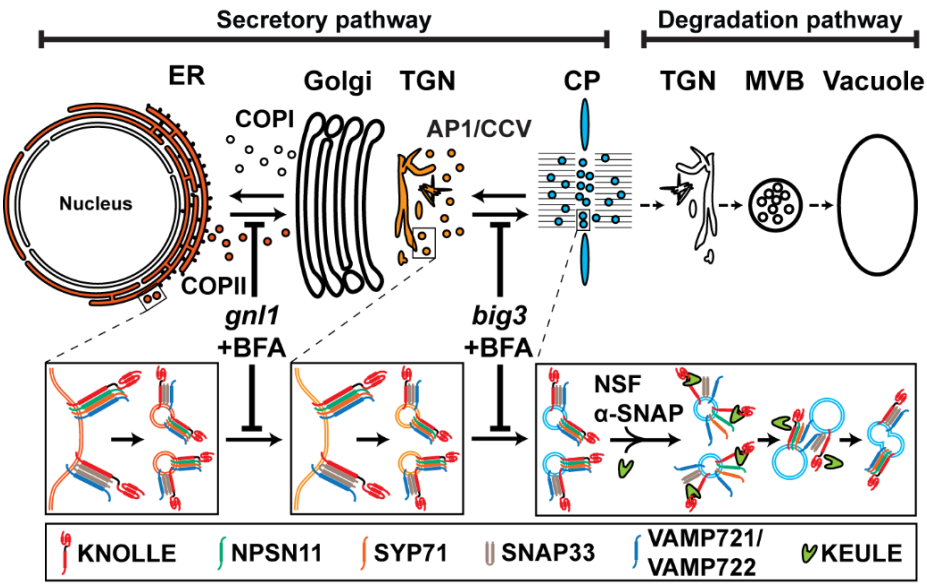

Figure 11 Trafficking of *cis*-SNARE complexes during cytokinesis (model).

Two different types of cytokinetic *cis*-SNARE complexes are assembled on the ER, recruited into COPII vesicles and passed on to the Golgi stack/TGN. At the TGN, they are incorporated into AP1/CCV vesicles for delivery to the division plane. Following their disassembly by NSF ATPase, monomeric Qa-SNARE KNOLLE is assisted by SM protein KEULE in the formation of trans-SNARE complexes mediating fusion of adjacent vesicles during cell-plate formation and expansion (Park et al., 2012).

4.3.2 A general mode of SNARE trafficking?

The Qa-SNAREs PEN1 and SYP132 were both detected in the precipitates of GFP-SNAP33 and YFP-NPSN11 after blocking traffic at either the ER or the TGN. This suggests that, like KNOLLE, they are assembled in *cis*-SNARE-complexes at the ER, before they are passaged *via* the secretory pathway to their destination. Newly synthesised SYP132 is targeted to the plasma membrane (or the cell plate), where it remains stably associated, implying that detected SYP132 in precipitates from seedlings blocked at either the ER or the TGN represented newly synthesised SYP132 (Reichardt et al. 2011). In contrast, PEN1 continuously cycles between

TGN and plasma membrane, which allows no distinction between endocytosed and newly synthesised Qa-SNAREs in the TGN-derived precipitates from *big3* mutant seedlings (Reichardt et al. 2011). However, extracts, in which traffic was blocked at the ER revealed the presence of PEN1-containing SNARE complexes, strongly suggesting that also PEN1 assembles in complexes at the ER that are maintained during their passage through the TGN. It could be argued that BFA-induced alterations in the membrane composition led to an ectopic accumulation of previously synthesised PEN1 or SYP132 at the ER or the TGN and these were assembled in post-fusion cis-SNARE complexes. However, such ectopically localized complexes would include endogenous Qb- or Qbc-SNARE partners that are GFP-untagged and would not appear during the experiment performed with anti-GFP beads. Thus, detected complexes, including SYP132 and PEN1, in-most-likelihood represented *cis*-SNARE complexes that assembled at ER prior to fusion.

The R-SNAREs VAMP721 or VAMP722 were detected in the precipitates from Qb-SNARE NPSN11 and Qbc-SNARE SNAP33, suggesting fully assembled complexes consisting of either Qa-, Qb-, Qc- and R-SNARE or Qa-, Qbc- and R-SNARE. However, the simultaneous detection of several Qa-SNAREs blurs the interpretation of the exact composition of these complexes, because the R-SNARE could have been exclusively precipitated in either PEN1-, SYP132- or KNOLLE-containing complexes. However, considering that during cytokinesis, near-identical vesicles fuse with one-another, containing all the members of KNOLLE-SNARE complexes, suggests that the detection of R-SNAREs in KNOLLE-containing complexes during the experiments is the most likely scenario. In contrast, SYP132 and PEN1 participate in heterotypic membrane fusion at the plasma membrane, during which the vesicle-associated SNARE(s) - usually the R-SNARE - continuously recycle. Thus, for these two Qa-SNAREs it remains uncertain whether the R-SNARE was part of the detected complexes and the experiments could not fully resolve the composition, in which they were found at ER or TGN membranes. Hence, following scenarios are possible: (i) PEN1 and SYP132 assemble at ER membranes into t-SNARE complexes (receptive target-SNARE complex), apart from the R-SNARE and traverse in that form to their target membrane destination, or (ii) fully assembled *cis*-SNARE complexes are formed at the ER, which need to be activated at their destination, involving a mechanism comparable to the one required for KNOLLE-containing complexes. After the first round of fusion and disassembly, the t-SNARE fraction of the complex members would remain at the target membrane, while the vesicle-associated SNAREs enter the recycling process to the TGN and back to promote subsequent fusion events at the plasma membrane. The latter scenario would imply that the mode of traffic, as inactive *cis*-SNARE complexes, might represent a general mode for the delivery of newly synthesised SNARE proteins to their destination. An analogous experimental setup could address this conundrum and additionally exclude the precipitation of plasma membrane- or TGN-derived Qa-SNAREs:

RFP-tagged PEN1/SYP132 under the control of the estradiol-inducible promoter could be co-expressed with either YFP-NPSN11 or GFP-SNAP33 in *gnl1 GNL1*$^{BFAsens.}$ transgenic lines. Thus, following the experimental procedure presented here, seedlings would be pre-treated with BFA and transgene expression induced by estradiol after the membrane blocks are established. Newly synthesised RFP-PEN1 or SYP132 would accumulate together with SNAP33/NPSN11 at blocked sites at ER or TGN membranes. RFP-PEN1 or RFP-SYP132 could be precipitated from these seedlings and tested for the presence of the Qb-, Qc-, Qbc- and R-SNAREs, which would conclusively demonstrate fully assembled SNARE complexes at the ER membrane and thus resolve the specificity of the trafficking mode of SNAREs in *cis*-SNARE complexes.

5. Functional diversification of *Arabidopsis* SEC1-related SM proteins in cytokinetic and secretory membrane fusion

5.1 Introduction

Sec1/Munc18 (SM) proteins and cognate SNARE proteins are essential components of the membrane-fusion machinery (Rizo and Sudhof 2012). Four members of the SM protein family are conserved among eukaryotes and act at different subcellular locations, with SLY1 acting at the ER-Golgi interface, VPS45 at TGN/early endosomes, VPS33 at late endosomes, lysosomes, the vacuole, and SEC1 at the plasma membrane (Koumandou et al. 2007). Studies on VPS45 and VPS33 in *Arabidopsis* suggest the conservation of compartment-specific functions in the different trafficking pathways of plants. VPS33 was detected in membrane fractions of the tonoplast and MVBs. It co-precipitates together with tonoplast-associated Qa-SNAREs SYP21 and SYP22 in precipitates of VCL1, a subunit of the tonoplast tethering (HOPS) complex (Rojo et al. 2003). The TGN-localized SM protein VPS45 is involved in vacuolar trafficking and positively regulates the activity of TGN-localized SNARE complexes, involving Qa-SNAREs SYP42 (aka TLG2b) and SYP43 (aka TLG2a) (Bassham et al. 2000, Zouhar et al. 2009). The SEC1 subfamily (further referred to as SEC1-related or SEC1 isoform), preferentially acts at the plasma membrane and contains several isoforms in different eukaryotic species that perform specialized tasks in distinct tissues and processes. For instance, mammalian Munc18-1 acts exclusively during synaptic neurotransmitter release. In contrast, its close homologue Munc18c is involved in several exocytic trafficking pathways in different mammalian tissues, like for example neutrophil secretion, platelet exocytosis and

GLUT4 secretion from adipocytes and skeletal muscles upon insulin stimulation (Yu et al. 2013).

In *Arabidopsis*, the SEC1 subfamily of SM proteins comprises three members, KEULE, SEC1A and SEC1B (Figure 12). KEULE is an essential component of the vesicle-fusion machinery during plant cytokinesis (Assaad et al. 1996, Waizenegger et al. 2000, Assaad et al. 2001). It was further suggested to be involved in the secretory trafficking pathway of interphase cells, together with the Qa-SNARE SYP121 (Karnik et al. 2013, Karnik et al. 2015). KEULE was also proposed to coordinate microtubule dynamics of the phragmoplast that guides the expanding cell plate (Steiner et al. 2016). However, the other two SEC1 isoforms SEC1A and SEC1B have not been studied and it is unknown whether they perform distinct or overlapping functions with KEULE. From an evolutionary perspective, gymnosperms like Norway spruce *(Picea abies*), the basal angiosperm *Amborella*, the basal dicot *Aquilegia* and the secondarily simplified monocot *Spirodela* all encode only a single SEC1 isoform (Figure 12). In contrast, most dicot and monocot angiosperms encode three isoforms of which *KEULE* and *SEC1B* appear to have arisen by gene duplication independently in the two angiosperm lineages, whereas the gene duplication giving rise to *SEC1A* may have occurred before the monocot-dicot split some 80 myr ago*. KEULE* and *SEC1B* diverged in sequence most strongly in the *Brassicaceae* and closely related species.

In line with the essential function of KEULE during cytokinesis, *keule* mutants are impaired in cell division, which results in the arrests at an early seedling stage and becomes evident on a subcellular level through cell wall stubs, unfused vesicles in the plane of cell division and multinucleate cells. However, its development past an embryonic stage suggests functionally overlapping SM proteins that contribute to cytokinesis during early stages of development. From the SEC1-subfamily in *Arabidopsis,* SEC1B is the closest homologue of KEULE and they share 70% amino acid sequence identity. It thus represented the obvious candidate for an overlapping role during cell division and was functionally analysed. SEC1B was assessed for its subcellular localization, the ability to complement the *keule* mutant phenotype, as well as its ability to physically and genetically interact with putative cognate Qa-SNARE partners KNOLLE and SYP132, and the *sec1b keule* double mutant was phenotypically analysed.

5.2 Results

5.2.1 SEC1B is not essential during plant development because of functional overlap with KEULE

SEC1B localizes at the cell plate of dividing cells and at the plasma membrane of interphase cells

SM proteins positively regulate membrane fusion at distinct membrane subpopulations. To identify putative sites of activity, the subcellular localization of SEC1B was determined in *Arabidopsis* root cells by indirect and direct fluorescence analysis. RFP-SEC1B localization was compared to that of HA-tagged KEULE, both being expressed from the cytokinesis-specific *KNOLLE* promoter; endogenous KNOLLE; and endosomal markers VHA-a1 and GFP-SYP132, expressed from the *35S* promoter. KEULE was detected in the cytosol of interphase cells (not shown) and at the forming cell plate of dividing cells upon immunostaining with antiserum against HA (Figure 13D, arrowhead).

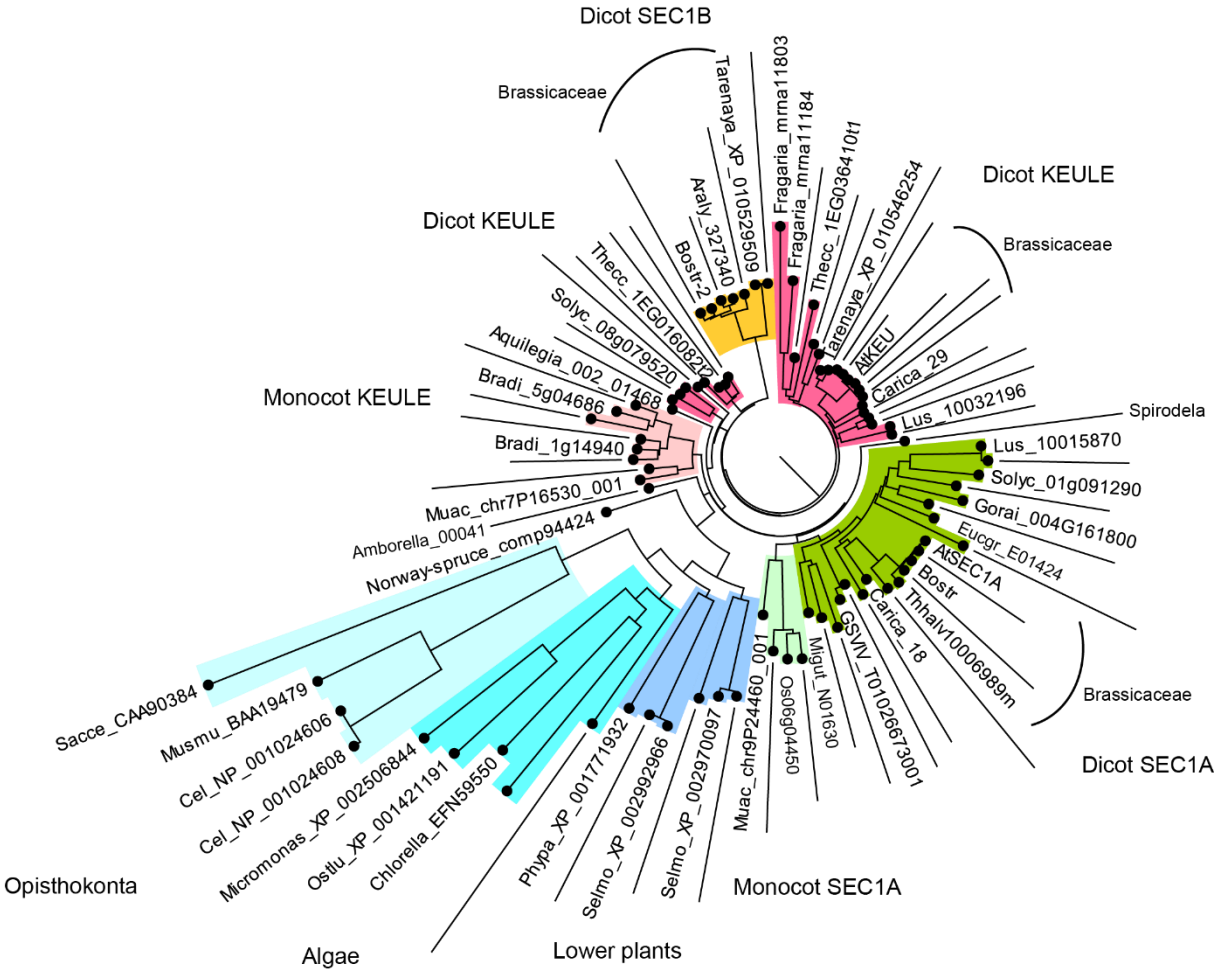

Figure 12 Phylogenetic analysis of SEC1-like SM proteins
(provided by Dr. M. Park)

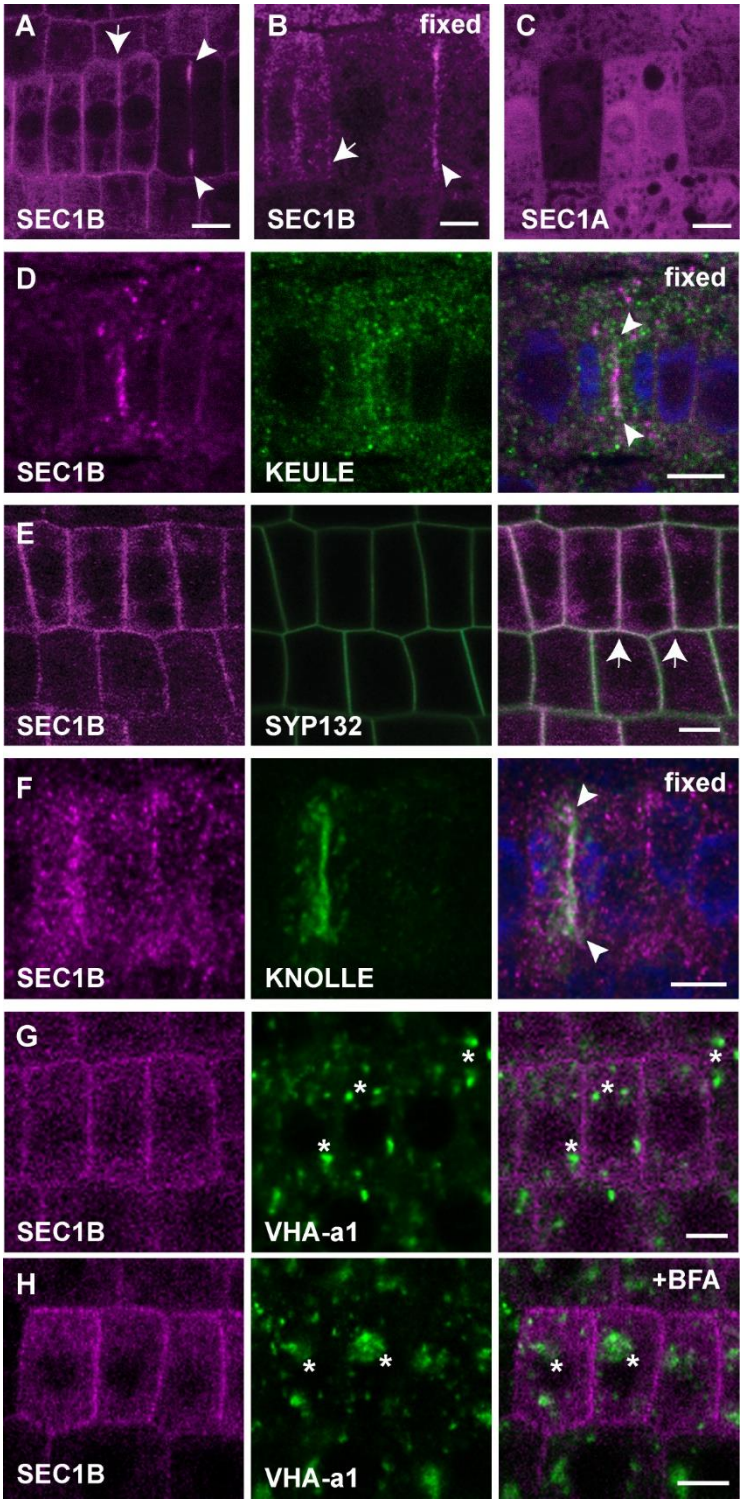

Figure 13 Subcellular localization of SM protein SEC1B.

RFP-SEC1B expressed from the *KNOLLE* promoter was observed in Arabidopsis root cells in live seedlings (**A,E,G,H**) and after fixation (**B,D,F**). RFP-SEC1A (**C**) analogously expressed did not associate with any membrane and localized cytosolic. SEC1B localization in co-expression lines together with HA-KEULE (**C**), GFP-SYP132 (**E**), or VHA-a1-GFP (**G,H**). Note the strong accumulation of SEC1B at the plasma membrane together with SYP132 (**E**, arrow), at the cell plate of dividing cells with KNOLLE (**F**, arrowhead), which was preferentially observed at the cell plate margin (**A,B**, arrowhead) and its absence from BFA-sensitive, VHA-a1-GFP marked endosomes (**G,H**, asterisk). arrow, plasma membrane; arrowhead, cell plate; asterisk, VHA-a1-containing endosome; +BFA, 1h BFA treatment (50 µM); scale bar, 5 µm.

This pattern of KEULE was consistent with its previously observed localization (Park et al. 2012). Live imaging of N-terminally tagged RFP-SEC1B revealed its localization at the cell plate of dividing cells (Figure 13A,B, arrowhead) and its strong accumulation at the plasma membrane of interphase cells (Figure 13A,B, arrow), where it overlapped with plasma membrane Qa-SNARE SYP132 (Figure 13E, arrow). Upon immunostaining, SEC1B colocalized together with either KEULE (Figure 13D, arrowhead), or cytokinesis-specific Qa-SNARE KNOLLE, at the cell plate of dividing cells (Figure 13F, arrowhead). SEC1B signal did neither overlap with MVB-marker ARA7-GFP (not shown) nor TGN-marker VHA-a1-GFP (Figure 13G, asterisk) and it did not accumulate in BFA compartments (Figure 13H, asterisk), indicating no association with endosomes (Ueda et al. 2004, Dettmer et al. 2006). In contrast to SEC1B, the more distantly related SEC1 isoform SEC1A accumulated in the cytosol and revealed no association with any membrane compartment (Figure 13C) in interphase, as well as cytokinetic cells. N-terminally GFP-tagged SEC1A, expressed from the estradiol-inducible promoter, displayed a similar localization in the cytosol, excluding an ectopic localization due to tagging or expression (data not shown).

These data suggest a dual role of SEC1B. At the cell plate, it overlapped with KEULE and KNOLLE and might be involved in vesicle fusion during cytokinesis. SEC1B additionally accumulated at the plasma membrane of interphase cells, where it strongly overlapped with SYP132, suggesting a possible involvement of SEC1B in the secretory pathway at the plasma membrane. In contrast, the evolutionary more ancient SEC1A did not accumulate at any specific endomembrane compartment and thus seems not to exert compartment-specific function during normal development of *Arabidopsis* root cells.

SEC1B functionally overlaps with KEULE and complements the keule mutant phenotype

Putative functional overlap of SEC1A or SEC1B with KEULE was explored by testing their ability to complement the KEULE-deficient mutant *keule*^{mm125}*.* RFP-SEC1B and RFP-SEC1A were expressed from the *KNOLLE* cassette (*pKN*), in analogy to the previously observed complementation of the *keule* mutant by *pKN::HA-KEULE* (Park et al. 2012). To assess for phenotypic complementation, the progenies of transgenic and non-transgenic *keule* heterozygous mutant lines were phenotypically analysed. Only wild-type-like and *keule* mutant phenotypes were observed, but in case of the *pKN::RFP-SEC1B* transgene the occurrence of the *keule* mutant phenotypes was strongly reduced, indicating phenotypic rescue of the absent *keule* mutant plants. The frequency of *keule* mutant seedlings was quantified in different progenies and revealed a comparable occurrence in non-transgenic *keule* mutant lines (18%, Figure 14A) and lines overexpressing *SEC1A* in *keule* mutants (16-19%, Figure 14A). In contrast, the frequency was significantly reduced in lines overexpressing *SEC1B* in these

mutants (2-6%, Figure 14A), further suggesting complementation of the *keule* mutant phenotype by SEC1B. Wild-type-like seedlings from different seedling progenies were genotyped (n=30; in >5 independent lines for SEC1A and SEC1B) and *keule* homozygous alleles were verified in the presence of *pKN::RFP-SEC1B*, whereas no homozygous seedlings were found in the progeny of lines expressing *pKN::RFP-SEC1A* (Figure 14C).

A Frequency of *keule* mutant seedling phenotypes in transgenic SEC1A or SEC1B lines

T1 plants		T2 plants				
Transgene	allele	PPTres	PPTsens	WT	*keule*	N
-	*keule*/+	-	-	82% (339)	18% (72)	411
pKN::RFP-SEC1B #1	*keule*/+	73% (153)	25% (52)	98% (205)	2% (5)	210
pKN::RFP-SEC1B #2	*keule*/+	74% (276)	19% (71)	94% (347)	6% (24)	371
pKN::RFP-SEC1B #3	*keule*/+	76% (376)	20% (100)	96% (476)	4% (20)	496
pKN::RFP-SEC1A #1	*keule*/+	62% (216)	23% (79)	85% (295)	16% (54)	349
pKN::RFP-SEC1A #2	*keule*/+	58% (629)	23% (253)	81% (882)	19% (206)	1088
pKN::RFP-SEC1A #3	*keule*/+	67% (228)	15% (50)	82% (278)	18% (62)	340

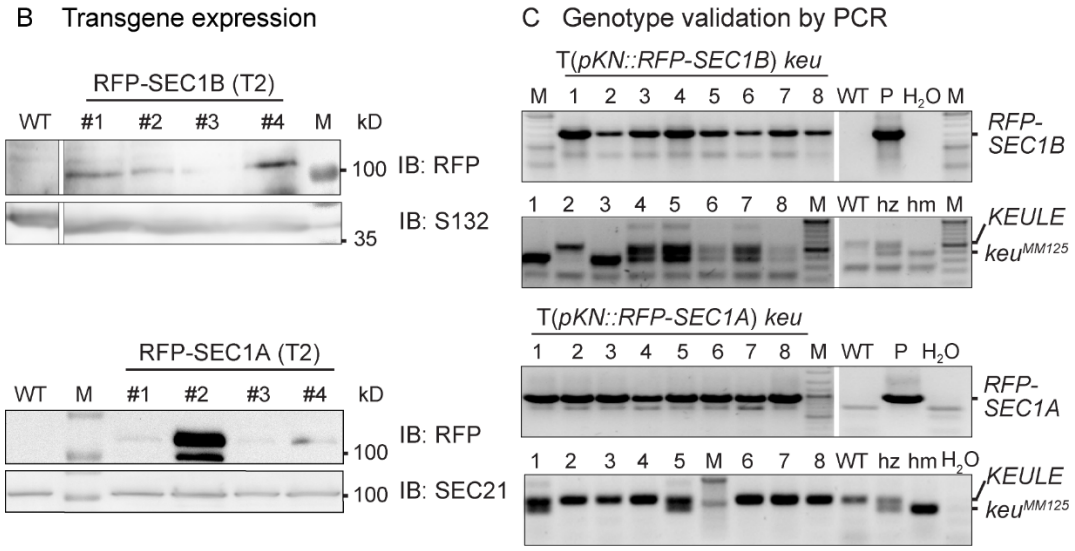

Figure 14 Test for functional complementaion of the *keule* mutant phenotype by N-terminally RFP-tagged SEC1B or SEC1A expressed from the *KNOLLE* promoter.

(**A**) Segregation of the *keule* mutant seedling phenotype was quantified in the presence of RFP-tagged SEC1B or SEC1A, expressed from the *KNOLLE* promoter. Presence of SEC1B reduced *keule* mutant transmission (**A**, about 4%), in contrast to SEC1A (**A**, about 18%) or transgene free lines (**A**, -, 18%). (**B**) Immunoblot analysis of RFP-SEC1B (**B**, upper panel) or RFP-SEC1A (**B**, lower panel) transgene expression in putative complementation lines, compared to SYP132 or SEC21 loading controls, used antisera are indicated (IB): RFP, anti-RFP; S132, anti-SYP132; SEC21, anti-SEC21. kD, molecular weight in kilodalton. (**C**) The seedling progeny of lines heterozygous for the transgene and the *keule* mutant allele were genotyped for the presence of the transgene and the *KEULE* wild-type or mutant (**C,** *keu*^{mm125}) allele. 30 seedlings from five independent transgenic lines for each *SEC1B* and *SEC1A* were analysed and revealed several homozygous *keule* mutants in the presence of *SEC1B*, but none in the presence of *SEC1A.* WT, wild-type; hz, or hm, heterozygous or homozygous *keule* mutant seedlings; H2O, water control; P, positive control (plasmid containing ORF). M, DNA size marker.

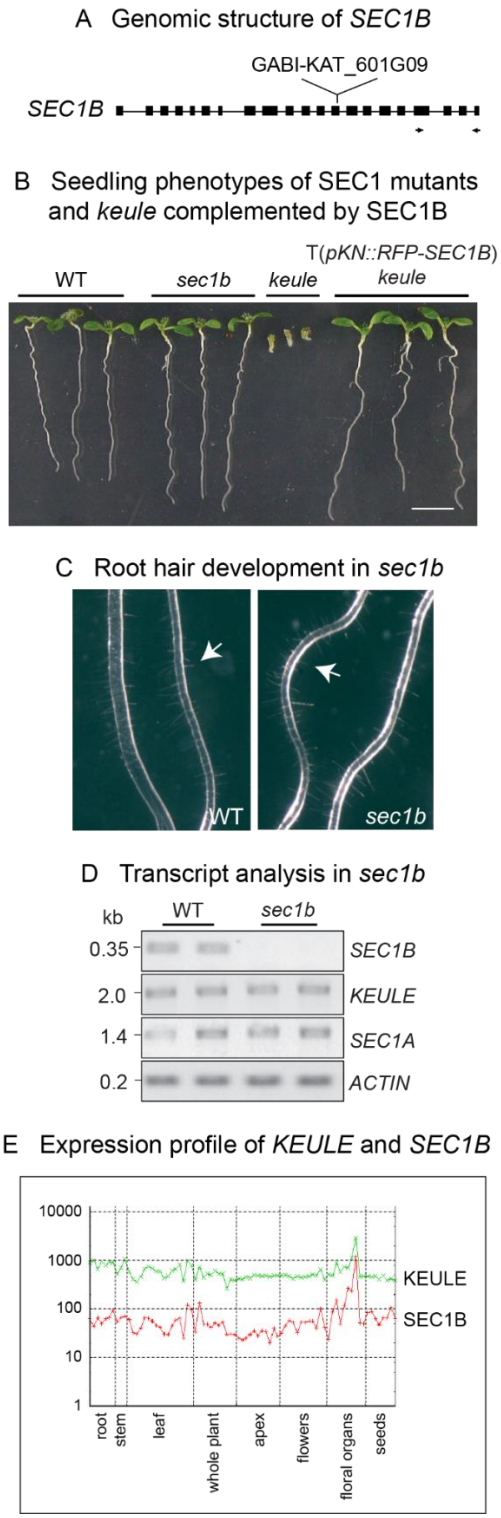

Figure 15 Phenotypic and transcriptional analysis of the *sec1b*$^{GK\_601G09}$ mutant T-DNA insertion line.

(**A**) Genomic structure of SEC1B with T-DNA insertion, Exon (**A**, thick bars) and RT-PCR primer annealing positions (**A**, arrows) indicated. (**B**) Seedling phenotypes of *sec1b* or *keule* single mutants, in comparison to wild-type (**B**, WT; Col-0) and *keule* mutants, carrying *pKN::RFP-SEC1B*. Note that the *sec1b* mutant and *keule* mutants complemented by SEC1B were indistinguishable from wild-type, throughout plant development and transmitted unaffected to the next generation (**C**) Root hair development in *sec1b* mutants and wild-type. (**D**) Transciptional analysis of *SEC1B, KEULE* and *SEC1A*, in the *sec1b* mutant T-DNA line by RT-PCR, in comparison to wild-type (**D**, WT) and in relation to *ACTIN*. (**E**) Transcript levels of *KEULE* and *SEC1B* during plant development (adopted graph from AtGenExpress-Visualization Tool (Schmid et al. 2005))

SEC1B is not essential for plant growth, but genetically interacts with KEULE

To evaluate the functional requirement of SEC1B, a T-DNA knockout allele named *SEC1B*^{GK601G09} was isolated (Figure 15D; for GABI-KAT_601G09 insertion position, see Figure 15A). Homozygous *sec1b* mutant plants were viable, fertile and indistinguishable from wild-type plants (Figure 15B). Notably, *sec1b* mutant seedlings displayed normal root hair

development (Figure 15C, kindly provided by Dr. M. Park), in contrast to previous observation of the *keule* mutant phenotype (Assaad et al. 2001). Transcript levels of the close homologues *SEC1A* and *KEULE* were analysed by RT-PCR analysis and revealed no compensatory upregulation in *sec1b* mutants (Figure 15D), thus SEC1B appears non-essential during regular *Arabidopsis* development. However, on a transcriptional level, KEULE is 10-fold more abundant than SEC1B throughout development (Figure 15E). Considering the close functional relatedness of KEULE and SEC1B that was observed during the complementation analysis, the loss of SEC1B in the *sec1b* mutants might have easily been compensated by the abundant endogenous KEULE, consistent with the reverse scenario during the complementation analysis (see above), in which overexpression of SEC1B compensated for the loss of KEULE.

The substantial functional overlap between these two SM proteins supports the hypothesis that SEC1B could be involved in early stages of development in the *keule* mutant, but only their genetic interaction could confirm or discard this assumption. Thus, the *sec1b keule* double mutant was generated by crossing the two mutant alleles *sec1b*^{601G09} and *keule*^{mm125}. Among the progeny of selfed doubly-heterozygous plants, no doubly-homozygous seedlings were detected. Furthermore, reciprocal crosses between doubly-heterozygous plants with wild-type revealed the strong reduction of allele transmission through both pollen (2%) and embryo sacs (6%), which indicates severe defects in male and female gametophytes of *sec1b keule* double mutant plants (Figure 16C, 25% expected if viable; data included in Figure 16 was kindly provided by Dr. M. Park). Moreover, observing the pollen phenotype of doubly-heterozygous plants revealed that approximately 25% pollen were collapsed (Figure 16E), suggesting defects during the developmental phase of the tricellular pollen grain, rather than during the initial cytokinetic process of the unicellular microspore. These data indicate the genetic interaction of *SEC1B* and *KEULE* and imply that SEC1B compensates for the absence of KEULE during early stages of development *keule* mutants.

To summarize, in the absence of SEC1B, KEULE can fully provide for the function of both SM proteins, whereas in *keule* mutants, endogenous SEC1B is too low abundant to compensate for the loss of KEULE, which results in the early seedling arrest. However, in the absence of both SM proteins in *sec1b keule* double mutants, transmission through both the male and female side is impaired, which reveals the essential role of the two SEC1 isoforms combined in early developmental stages.

Genetic interaction between SEC1-related SM proteins *KEULE* and *SEC1B*

A Pollen phenotype

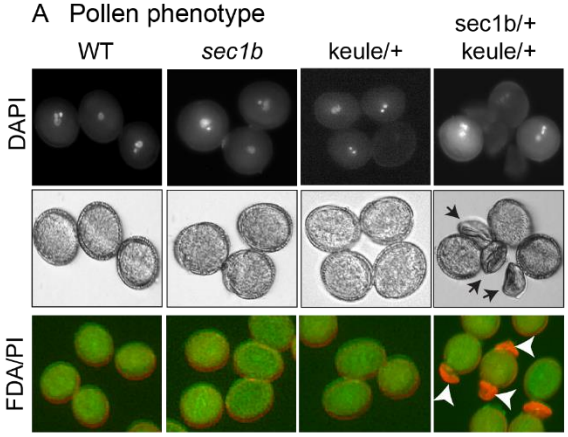

B Frequency of defective pollen in *keule sec1b* double mutants

	Pollen frequency viable	dead	N
WT (Col-0)	100 % (145)	0% (0)	145
sec1b/+	100 % (271)	0% (0)	271
keule/+	100 % (60)	0% (0)	60
F1(*sec1b/+ keu/+*)	75% (295)	25% (99)	394

C Transmission analysis of *sec1b keule* double mutants

Parental genotype (female X male)	*SEC1B/+ KEU/+*	*sec1b/+ KEU/+*	*SEC1B/+ keu/+*	*sec1b/+ keu/+*	N
sec1b/+ keu/+ X *WT*	31% (39)	25% (31)	38% (48)	6% (8)	126
WT X *sec1b/+ keu/+*	34% (36)	32% (34)	33% (35)	2% (2)	107

Figure 16 Pollen development in doulbly heterozygous *sec1b keule* mutant plants and analysis of the doulbe mutant allele transmission to a seedling stage

Double mutants for *sec1b* and *keule* were generated by crossing. Genotyping analysis revealed the absence of doubly homozygous mutants from the F2 generation, indicating synthetic lethality. (**A**) Among the pollen of doubly heterozygous *sec1b keule* mutant plants, an abnormal shrivelled pollen phenotype was observed (**A**, arrow) that was not found in wild-type (**A**, WT; Col-0), *sec1b* or *keule/+* single mutant plants. Pollen viability was visualised through nuclei-staining by DAPI and co-staining with FDA/PI, in which dead pollen is marked by PI (**A**, red, arrowhead) and viable pollen by FDA/fluorescin (A, green fluorescence). (**B**) The frequency of viable and dead pollen was quantified in doubly heterozygous mutant plants (25% double mutant alleles expected in *sec1b/+ keule/+*), compared to wild-type (**B**, WT) and single mutants. (**C**) Reciprocal crosses between doubly heterozygous mutants with wild-type (Col-0) were performed, F1 seedlings genotyped and genotypes quantified (**C**). When the male donor was doubly heterozygous for *keule* and *sec1b*, only 1% double mutant alleles were transmitted to the seedling stage (6.25% expected), indicating near-male-gametophytic lethality.
(Data provided by Dr. M. Park).

5.2.2 Specificity between SEC1-like SM proteins and SYP1 Qa-SNAREs

SEC1B preferentially interacts with Qa-SNARE SYP132

To analyse, whether SEC1B and KEULE exert their overlapping function through the regulation of similar or distinct Qa-SNARE partners, they were tested for their interaction with Qa-SNAREs KNOLLE and SYP132, in quantitative yeast-two-hybrid and co-immunoprecipitation experiments. Cytokinesis-specific Qa-SNARE KNOLLE is a known target of KEULE regulation and Qa-SNARE SYP132 associates with the plasma membrane of interphase cells. It was additionally recently functionally implicated in vesicle fusion during cytokinesis beside KNOLLE

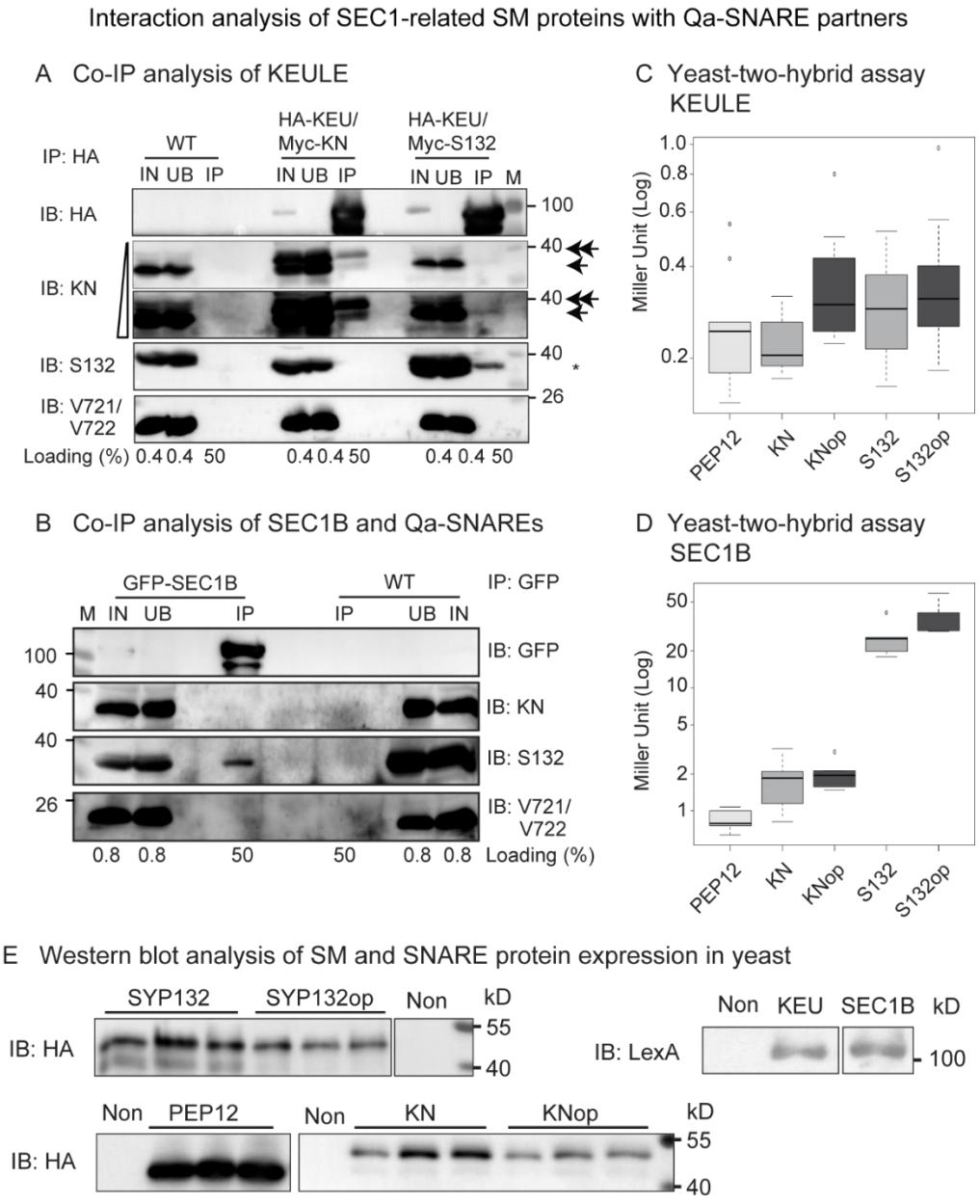

Figure 17 *In vitro* and *in vivo* analysis of physical interactions between SM proteins SEC1B and KEULE with Qa-SNAREs KNOLLE and SYP132.

(**A,B**) Coimmunoprecipitation analysis of HA-KEULE and GFP-SEC1B in Arabidopsis seedlings. (**A**) Wild-type (WT) and transgenic seedlings, co-expressing *HA-KEULE* (HA-KEU) with *MYC-KNOLLE* (Myc-KN) or *MYC-SYP132* (Myc-S132) under control of the *KNOLLE* promoter were subjected to immunoprecipitation with anti-HA beads. (**B**) In *EST::GFP-SEC1B* transgenic seedlings, transgene expression was induced by 20 µM EST for 6h and protein extracts in parallel with non-transformed seedlings (WT) subjected to immunoprecipitation with anti-GFP beads. (**A-B**) Equal amounts of total protein extract (T) and unbound supernatant (UB), together with 33% washed precipitate (IP) were loaded in SDS-PAGE gels and immunoblots stained with anti-HA (**A**), or anti-GFP (**B**) and anti-KNOLLE (KN), anti-SYP132 (S132) or anti-VAMP721/VAMP722 (V721/V722), antisera are indicated beside the blots (IB). Note that in KEULE precipitates, Myc-KNOLLE (**A**, double arrow) and endogenous KNOLLE (**A**, single arrow) were detected, while in anti-SYP132 only one band was present, representing Myc-SYP132 which is implied in its absence from the HA-KEULE/Myc-KNOLLE IP (**A**, asterisk). (**B**) GFP-SEC1B coprecipitated endogenous SYP132, but neither KNOLLE, nor VAMP721/VAMP722. (**C,D**) Quantitative yeast-two-hybrid interaction analysis of SM proteins KEULE (**C**) and SEC1B (**D**) with Qa-SNAREs PEP12 (= SYP21), KNOLLE, SYP132 and constitutive open KNOLLE (KNop) or SYP132

(S132op), containing relevant point mutations (Park 2012). (**C,D**) The relative enzyme activity (β-galactosidase) in Miller units was blotted in a logarithmic scale in box plots (Miller 1972). Note, that for KEULE (**C**) only weak interactions were observed with SYP132 and the open forms of KNOLLE and SYP132, compared to PEP12, in contrast to SEC1B that showed much stronger enzyme activity and interacted preferentially with SYP132 or SYP132 open, over KNOLLE or KNOLLE open in a 10-fold difference. Experiments were technically repeated more than three times and include 5-8 individual colonies. (**E**) Equal protein expression in EGY 48 cells was analysed by immunoblots, stained with anti-HA for the Qa-SNARE variants (**E**, IB: HA), expressed from the pJG4-5 vector (N-terminal HA tag) and anti-lexA for relevant SM proteins (**E**, IB: LexA), expressed from pEG202. Non, non-transformed yeast; KN, KNOLLE; Knop, KNOLLE open; KEU, KEULE; M, protein size marker; kda, protein size in kilodalton.

(Park et al. *in submission*). In a different aspect, eukaryotic SM proteins regulate SNARE proteins through different modes of interaction, either with cognate Qa-SNAREs and/or pre-assembled SNARE complexes (Rizo and Sudhof 2012). KEULE was shown to interact specifically with the open form of monomeric KNOLLE through binding to the linker domain that separates the N-terminal helices from the SNARE domain (Park et al. 2012). To test whether SEC1B interacts through a similar mechanism, the constitutively open protein variants were included for both Qa-SNAREs in the yeast-two hybrid analyses. In the Qa-SNAREs, the open conformation was stabilized by point mutations in two amino acids inside this linker region, as previously described (Dulubova et al. 1999, Park et al. 2012).

As negative control for the quantitative yeast-two-hybrid approach, the MVB-resident Qa-SNARE PEP12 (aka SYP21) was included to the analysis (Muller et al. 2003). The assay revealed a weak interaction of KEULE with both Qa-SNAREs KNOLLE and SYP132, in comparison to PEP12 and showed increased enzyme activity in combination with the two constitutive open forms (Figure 17C). SEC1B interacted with both, KNOLLE and SYP132, much stronger than KEULE and displayed a clear preference for interacting with SYP132, which resembled a 10-fold stronger interaction with SYP132, compared to that with KNOLLE (Figure 17D). Like KEULE, SEC1B showed a higher affinity for the constitutively open forms of the Qa-SNARES, suggesting a comparable mode of interacting with Qa-SNAREs to that of KEULE

To test for consistent interactions *in planta*, co-immunoprecipitation analyses were performed. In the initial experiments, the functional fusion protein RFP-SEC1B was attempted to precipitate from complemented lines, harbouring *pKN::RFP-SEC1B* in the *keule* mutant background. However, several different approaches failed to accumulate any RFP protein, neither RFP-SEC1B, nor monomeric RFP, which should be detectable after protein degradation. The attempts included the use of RFP-beads (Sigma-Aldrich), RFP-trap (Chromotek) and two different polyclonal antisera against RFP that were bound to Agarose beads. Other RFP-tagged proteins were precipitated during the experiments, which was validated by, eg. RFP-SEC1B or RFP-SYP132 controls. Thus, the failure to enrich proteins by these approaches could indicate that relevant antigens were masked in the RFP-SEC1B fusion

protein. Therefore, co-immunoprecipitation experiments were performed on extracts from transgenic estradiol-inducible *EST::GFP-SEC1B* or *pKN::6xHA-KEULE* lines, with the latter co-expressing either *pKN::Myc-KNOLLE* or *pKN::Myc-SYP132*, analogously to published co-immunoprecipitation experiments that originally showed the HA-KEULE/Myc-KNOLLE interaction (Park et al. 2012). Precipitates from both, anti-HA beads for KEULE and anti-GFP beads for GFP-SEC1B were analysed for the presence of Qa-SNAREs KNOLLE and SYP132. Additionally, precipitates were tested for the presence of R-SNAREs VAMP721/VAMP722 to evaluate whether the SM proteins would interact with monomeric Qa-SNAREs or assembled SNARE complexes.

In HA-KEULE precipitates KNOLLE was detected in both its endogenous form (Figure 17B, arrow) and its transgenically overexpressed fusion protein Myc-KNOLLE (Figure 17B, double arrow). In contrast, only overexpressed Myc-SYP132 was detected (Figure 17B, asterisk), while notably, endogenous SYP132 was not precipitated, as indicated by the absence of SYP132 from the HA-KEULE/Myc-KNOLLE precipitate (Figure 17B, asterisk). *HA-KEULE*, *Myc-KNOLLE* and *Myc-SYP132* were overexpressed from the cytokinesis-specific *KNOLLE* promoter, suggesting high levels of co-accumulated interaction partners in dividing cells, together with the endogenous KNOLLE (Lauber et al. 1997). In contrast, endogenous *SYP132* is ubiquitously expressed throughout the different tissues, suggesting a lower co-accumulation with HA-KEULE in dividing cells, which might explain the failure to detect their interaction (Enami et al. 2009). The interaction analysis of SEC1B revealed the presence of SYP132 and the absence of KNOLLE in anti-GFP precipitates (Figure 17B). The converse protein accumulation applies for the interpretation of the SEC1B analysis. Its expression was induced by estradiol, which usually results in rather ubiquitous protein accumulation mainly in peripheral tissues, but no specific enrichment and comparably low levels in dividing cells. The R-SNAREs VAMP721 and VAMP722 were not detected in either of the SM protein precipitates (Figure 17A,B), indicating the interaction of SM proteins with monomeric Qa-SNAREs.

To summarize, in yeast-two-hybrid and co-immunoprecipitation analyses, KEULE interacted with Qa-SNAREs SYP132 and KNOLLE, presumably equally. SEC1B showed a clear preference for interacting with SYP132, which was evident by high enzyme activity during quantitative yeast-two-hybrid experiments and the absence of KNOLLE from the immunoprecipitate. Both, KEULE and SEC1B displayed a higher affinity for open protein variants of both Qa-SNAREs KNOLLE or SYP132. The R-SNAREs VAMP721 and VAMP722, representing SNARE complex partners of SYP132 and KNOLLE, were absent from KEULE and SEC1B precipitates, suggesting the interaction of analysed SM proteins with monomeric Qa-SNAREs rather than assembled complexes.

SEC1B genetically interacts with SYP132 rather than KNOLLE

To evaluate, whether detected interactions between the two SM proteins and KNOLLE or SYP132, are functionally relevant during plant development, their genetic interaction was analysed by generating respective double mutants and their phenotypic analysis. Blocking plant cytokinesis from an early zygotic stage onward, results in an embryo-lethal phenotype that is characterized by a single, enlarged embryonic cell, which accumulates nuclei over time, as was described for the *knolle keule* double mutant phenotype (Figure 18G, data in this figure was kindly provided by Dr. M. Park) (Waizenegger et al. 2000). Notably, the accumulation of multiple nuclei in enlarged cells, implies defective cytokinesis, but partially intact secretory traffic that promotes cell expansion. This phenotype contrasts with the single *knolle* and *keule* mutant phenotypes that can both develop to a seedling stage, undergoing several rounds of cell division, which suggests functional cytokinesis during earlier stages and the involvement of other fusion factors from both protein families. In the *keule* mutant, either KNOLLE is regulated by an alternative SM protein beside KEULE or another Qa-SNARE-SM protein pair contributes cytokinetic activity. Conversely, in the *knolle* mutant, KEULE could promote the activity of (an) alternative SYP1 Qa-SNARE(s) or again a further Qa-SNARE-SM protein pair is involved in cytokinesis. During later developmental stages, the relevant fusion factors become too low abundant to sustain plant growth, which causes the seedlings to arrest and results in the described seedling phenotype of both mutants. Recently, SYP132 was identified as the Qa-SNARE, acting beside KNOLLE during cytokinesis (Park et al. *in submission*). The authors demonstrated the assembly of SYP132 in SNARE complexes with similar SNARE partners as KNOLLE, including either NPSN11, SYP71 and VAMP721/VAMP722, or SNAP33 and VAMP721/VAMP722. They also showed that the *syp132 knolle* double mutant arrests as single, multinucleated-cell at an embryo stage, with a phenotype strongly resembling that of the *knolle keule* double mutant (Figure 18G). *syp132* mutants were generated by introducing an artificial microRNA construct targeting *SYP132* (*syp132*^{amiR}) into a *syp132* T-DNA insertion line (*syp132*^{T}) harbouring the insertion in the promoter region of *SYP132* (Park et al. *in submission*). This *syp132* mutant line was also employed in experiments presented in the current chapter.

The analysis of *keule syp132* double mutants revealed a strong embryonic phenotype (Figure 18H), approaching the *knolle keule* (Figure 18G) and the *knolle syp132* double mutant phenotype (Park et al. *in submission*). This observation indicates that the activity of the remaining KNOLLE together with SEC1B is insufficient for cell division during embryo development. A very similar embryo lethal phenotype was also observed for the *sec1b knolle* double mutant (Figure 18I), revealing that also the combination of KEULE with SYP132 is insufficient during cytokinesis in early stages of embryo development. However, the *sec1b syp132* double mutant (Figure 18K), phenotypically resembled the *syp132* single mutant

(Figure 18F) and developed to an early seedling stage until growth arrested. This indicates that among the fusion components relevant to cytokinesis (KEULE, SEC1B, KNOLLE and SYP132), only the SM-Qa-SNARE combination of KEULE and KNOLLE can sustain cytokinesis during early embryo development in the absence of the other two fusion components. Hence, beside the established cytokinesis-specific function of KNOLLE, also KEULE seems to have acquired some level of specificity to vesicle fusion, and to the regulation of KNOLLE, during *Arabidopsis* cell division, in strong contrast to SEC1B. Still, the *keule* single mutant phenotype and its enhancement in *sec1b keule* double mutant described above, also functionally implicated SEC1B in cytokinesis, but suggests a less important role during cell division. A similar non-specialized function during cytokinesis was described for SYP132, the preferential interaction partner of SEC1B (Park et al. *in submission*).

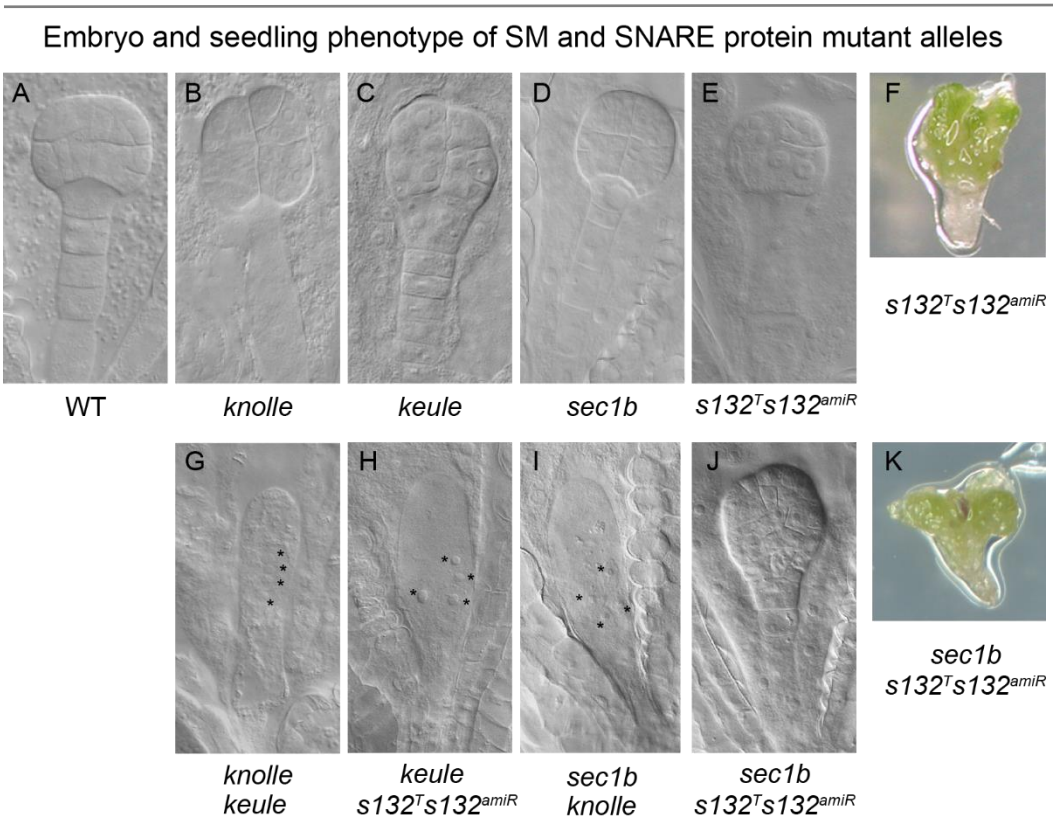

Figure 18 Analysis of the genetic interaction of *KEULE*, *SEC1B*, *KNOLLE* and *SYP132* and respective embryo or seedling mutant phenotypes.

Embryo (**A-E, G-I**) and seedling phenotypes (**F,J**) of different SM protein or Qa-SNARE single and double mutants: wild-type (**A**, WT), *knolle* (**B**), *keule* (**C**), *sec1b* (**D**) and *syp132* (**E,F**) single mutants and *sec1b knolle* (**G**), keule syp132 (**H**), sec1b syp132 (**I,J**) double mutants are shown. Note the strong embryonic phenotype of *knolle sec1b* and *keule syp132* double mutants that forms only a single, multi-nucleated and bloated embryo (**G,H,** nuclei indicated by asterisk), in contrast to the sec1b syp132 double mutant (**I,J**). *s132^{T}syp132^{amiR}*, referred to as syp132 single mutant, represents a transgenic line with a T-DNA insertion in the promoter region of SYP132 and expresses an artificial microRNA against *SYP132*, resulting in SYP132 knock-down **(Data provided by Dr. M. Park)**.

5.3 Discussion

5.3.1 SEC1-isoforms KEULE and SEC1B are both functional during cytokinesis

The experiments provided in this study, imply a substantial functional overlap between KEULE and SEC1B, two closely related members of the SEC1-subfamily in *Arabidopsis* and suggest a rather distinct function of the third member of this clade, SEC1A. The *keule* mutant phenotype displays cytokinetic defects at a seedling stage, whereas embryos could develop without obvious defects (compare Figure 18C). SEC1B fully complemented the *keule* mutant phenotype and thus must be involved in cytokinesis and thus displayed a closely related function to KEULE. In such complemented lines, the overexpression of SEC1B fully restored plant development and allowed the inheritance of the doubly-homozygous *keule* alleles to the next generation. This full complementation is somewhat surprising, considering the presence of endogenous SEC1B in *keule* mutants without transgene. However, in the complemented lines, SEC1B was overexpressed from the cytokinesis-specific *KNOLLE* promoter, suggesting that this cell-cycle specific expression led to a high accumulation of SEC1B in dividing cells, which appears to be essential to compensate for the absence of KEULE. This allows following conclusions: (i) *keule* arrest due to inefficient cytokinetic activity, (ii) endogenous levels of SEC1B are insufficient to sustain cytokinesis in later developmental stages, in which the *keule* mutant arrests, and (iii) SEC1B is clearly functionally involved in cytokinesis during the development of *keule* mutants. Considering that endogenous *SEC1B* is much lower expressed than *KEULE*, which results in about 10-fold less accumulation of *SEC1B* transcripts (Figure 14E), the arrest of *keule* mutants can be dedicated to the low protein accumulation of SEC1B.

The absence of both SM proteins in *keule sec1b* double mutants strongly impaired early developmental stages in both male and female gametophytes, evident by the analysis of reciprocal crosses of doubly-heterozygous plants with wild-type. This early gametophytic defects contrasts with the phenotype of *sec1b* single mutants, which develop entirely unaffected, and the seedling-lethal *keule* single mutant. Thus, the genetic interaction of *SEC1B* and *KEULE* further supports their overlapping function in cytokinesis already during early developmental stages and marks them as single SM proteins involved in this process. Furthermore, the diverging phenotypes of respective single mutants suggest different contributions during regular plant growth.

Doubly-homozygous mutant pollen from *keule/+ sec1b/+* double mutant plants displayed defects during their growth phase, implying intact asymmetric cell division of microspores. The accumulation of KEULE and SEC1B (compare Figure 12A) in interphase cells, upon expression from the cytokinesis-specific *KNOLLE* promoter, indicates slow protein turn-over

and rather stable proteins. Thus, SM protein carry-over from heterozygous meiocytes to microspores might explain the late pollen abortion.

5.3.2 Evaluation of the functional specialisation of SM proteins and SNARE proteins during evolution

Roles of KEULE beside cell division

In addition to obvious cytokinesis defects, *keule* mutant seedings are impaired in root hair development (Assaad et al. 2001), which suggests a cytokinesis-independent function of KEULE in non-dividing root hairs. Seedlings, in which *SYP132* was knocked-down by the expression of an artificial microRNA revealed similarly impaired root hair growth. Together, this could indicate a combined role of KEULE and SYP132 in *Arabidopsis* root hair development (Ichikawa et al. 2014). Another line of evidence implicates KEULE in the regulation of Qa-SNARE PEN1. They were shown to interact in rBIFC or pull-down experiments, and the authors suggested KEULE to act together with PEN1 in the secretory pathway at the plasma membrane (Karnik et al. 2013, Karnik et al. 2015). Further evidence involved the overexpression of truncated or mutated variants of KEULE in plants, which resulted in a dominant negative effect on the secretion of secYFP and a mild decrease in leaf size that was linked to the specific interaction with PEN1 (Karnik et al. 2015). However, these effects were observed for strongly overexpressed KEULE protein and, without disputing the ability of KEULE to interact with PEN1, direct evidence for the biological relevance of this specific Qa-SNARE-SM protein pair, remains to be elucidated. Thus, it is still unclear whether the putative function of KEULE in the secretory trafficking pathway that could also promote cell expansion during root hair development, is exerted through the regulation of PEN1, SYP132 or a so far unknown Qa-SNARE. Moreover, the KEULE signal in interphase cells of *Arabidopsis* roots was observed in the cytosol and did not label specific membranes, indicating no major contribution of KEULE at the plasma membrane in seedling root cells (Steiner et al. 2016).

Distinct contributions of SM proteins and Qa-SNAREs in the secretory pathway of interphase and dividing cells

In contrast to KEULE, SEC1B strongly accumulated at the plasma membrane, where it overlapped with Qa-SNARE SYP132. SEC1B also strongly interacted with SYP132 in the yeast-two-hybrid assay and co-precipitated SYP132 in co-immunoprecipitation analyses. These results, strongly suggest a role of SEC1B in the regulation of SYP132 that might be involved in the secretory trafficking pathway at the plasma membrane. SEC1B interacted additionally with KNOLLE in the yeast-two-hybrid experiment, whereas KNOLLE was absent

from the immunoprecipitates of SEC1B. However, SEC1B was expressed from the estradiol-inducible promoter during the co-immunoprecipitation experiment, which results in a ubiquitous accumulation in peripheral tissues and rather low protein abundance in diving cells. Thus, SEC1B was low abundant in cells, in which endogenous KNOLLE was exclusively present and the low fraction of overlapping proteins that could have interacted might not have been detectable during the experiment. Furthermore, in analysed seedlings, endogenous KEULE was present, which might have removed KNOLLE from a possible interaction with SEC1B. Thus, the interaction between SEC1B and KNOLLE in plants cannot fully be excluded. In contrast, the yeast-two-hybrid assay revealed an interaction between SEC1B and KNOLLE that was, however, significantly weaker than the interaction detected of SEC1B with SYP132. KEULE on the other hand, interacted with both Qa-SNAREs in yeast-two-hybrid experiments and precipitated both transgenically expressed Qa-SNAREs, but not endogenous SYP132. Transgenic seedlings that were used for the experiment, specifically accumulated HA-KEULE in dividing cells together with either Myc-KNOLLE or Myc-SYP132 and endogenous KNOLLE. In contrast, non-detected, endogenous *SYP132* that is expressed ubiquitously in all tissues, did likely rarely overlap with HA-KEULE, which might explain the failure to detect it in KEULE precipitates.

Consistent with the physical interaction data, the analysis of several SM-Qa-SNARE double mutants revealed promiscuous functional SM-Qa-SNARE partners during early stages of plant development. The phenotypes of the *knolle keule*, the *keule syp132* and the *sec1b knolle* double mutants were all strongly enhanced in comparison to respective single mutants. While the single mutants show no defects during embryo development (compare Figure 18B-E) and arrested only at a seedling stage, these three double mutants (dm.) displayed a strong embryonic phenotype that was characterized by an enlarged multinucleate cell (compare Figure 18G-I). This indicates that following combinations of SM proteins and SNARE proteins cannot sustain cytokinesis during embryo development: (i) SEC1B together with KNOLLE (keule syp132 dm.), (ii) SEC1B together with SYP132 (*keule knolle* dm.), (ii) and KEULE together with SYP132 (*sec1b syp132* dm.). In contrast, the *sec1b syp132* double mutant resembled phenotypically the *syp132* single mutant, implying that KEULE together with KNOLLE can sustain cytokinesis during embryo development, without other fusion components. This suggests a rather specialized function of SM protein KEULE in the regulation of Qa-SNARE KNOLLE in *Arabidopsis* cell division. In contrast, the regulation of KNOLLE and SYP132 by SEC1B, or SYP132 by KEULE might contribute to cytokinesis, but the function exerted through these combinations is not as specialized as the one by KNOLLE and KEULE combined.

The R-SNAREs VAMP721/VAMP722 were not detected in immunoprecipitates from SEC1B or KEULE, suggesting the precipitation of monomeric Qa-SNAREs. Furthermore, during yeast-

two-hybrid experiments, the two Qa-SNAREs preferentially interacted with constitutively open Qa-SNAREs. Together, this suggests a comparable mechanism for KEULE and SEC1B to interact with the monomeric Qa-SNARE in its active, open form.

The phylogenetic analysis of SEC1-related SM proteins suggests that the functional diversification of KEULE and SEC1B only started in early angiosperm evolution. Considering the predominant interaction between SEC1B and the ancient Qa-SNARE SYP132, the precursor of KEULE might have specialized in its current form after KNOLLE had arisen in early angiosperms. This specialization might have occurred before or after the duplication into SEC1B and KEULE. The secondarily simplified duckweed *Spirodela polyrhiza* has retained *KNOLLE* and encodes a single remaining SM protein in the SEC1 clade, which could indicate similar interacting SM-SNARE protein partners, like in *Arabidopsis*. Thus, cytokinetic efficiency might have improved through the co-evolution of a cytokinesis-specific Q-SNARE KNOLLE together with the regulatory SM protein KEULE, opposed to the non-specialized progenitor SYP132, and the SM protein SEC1B that can contribute to cytokinesis, but supposedly mainly acts in the secretory pathway at the plasma membrane.

6. Complexity of *Arabidopsis* R-SNAREs in vesicle fusion during cytokinesis

6.1 Introduction

6.1.1 R-SNARE protein structure and function

SNAREs can be classified as Q- and R-SNAREs, according to one conserved amino acid in the central region of the SNARE domain, which is either a glutamine (Q) or an arginine (R) (Fasshauer et al. 1998). It was anticipated that the R-SNARE arrives on the incoming membrane vesicle at the fusion site and binds cognate Q-SNARE partners located at the target membrane to form *trans*-SNARE complexes, which are essential to initiate membrane fusion (Sollner et al. 1993). The domain structure of R-SNAREs led to the further sub-classification in brevins and longins (Filippini et al. 2001). Brevins (lat. *brevis*, short) contain a non-conserved N-terminal domain, followed by the R-SNARE domain and a transmembrane domain, in contrast to longins (lat. *longus*, long), which comprise a large, conserved coiled-coil domain of 120-140 amino acids, called longin domain (Rossi et al. 2004). This domain raises particular interest, because it promotes multiple intra- and intermolecular interactions that allow for functional regulation, as well as protein sorting (Daste et al. 2015). The longin domain of R-

SNAREs promotes the interaction with coat proteins, which is important for correct protein sorting and targeting, as was shown for the mammalian R-SNARE VAMP7, which interacts with the δ-adaptin subunit of the AP-3 complex (Daste et al. 2015). Domain swap experiments among different clades of *Arabidopsis* R-SNAREs indicated a similar dependency of their subcellular localization on their longin domain in plants (Uemura et al. 2005). After *trans*-SNARE complex formation and membrane fusion, the resulting *cis*-SNARE complexes are confined to the target compartment (Baker and Hughson 2016). These *cis*-SNARE complexes are dissociated by α-SNAP/NSF and the vesicle-associated R-SNARE must be selectively sorted into recycling vesicles, in order to cycle back to the donor compartment, and engage in another round of fusion. This model was supported by data on yeast, mammalian and nematode R-SNAREs that indicated overlapping mechanisms for the active sorting of R-SNAREs into recycling vesicles. During sorting, these R-SNAREs interact *via* their longin domain with coat subunits or coat interacting proteins, which simultaneously chaperoned their monomeric form during transport (Maritzen et al. 2012).

6.1.2 Functional overlap of Arabidopsis R-SNAREs during cytokinesis

The two R-SNAREs VAMP721 and VAMP722 perform an essential, overlapping function in vesicle fusion during cell plate formation in dividing cells. They can both be part of two distinct so-far identified KNOLLE-containing, cytokinesis-specific complexes. The phenotype of the *vamp721 vamp722* double mutant displays cytokinetic defects on a subcellular level that include cell wall stubs and multinucleate cells. However, double mutant plants develop to a seedling stage until they arrest growth, suggesting the involvement of further R-SNAREs during earlier developmental stages that can act in similar pathways, beside VAMP721 and VAMP722 (Zhang et al. 2011). Hence, closely-related members from the VAMP72 clade, that contains VAMP721 and VAMP722, were evaluated for putative candidates for an overlapping function during cytokinesis, beside VAMP721 and VAMP722 (Figure 19) (Sanderfoot 2007).

6.1.3 Functional evaluation of R-SNARE from the *Arabidopsis* VAMP72 clade

Unlike other eukaryotes, plants lack the brevin type of R-SNAREs, but contain an abundant and highly diverse protein family of fifteen longin-like members in *Arabidopsis* (Figure 19) (Sanderfoot 2007) of which the VAMP72 clade, contains seven members that are part of three subfamilies (Figure 19). The first diversification within this clade occurred in embryophytes, during which the VAMP727 emerged and a second diversification in angiosperms evolved

VAMP724 and the VAMP721 branch that includes five members: VAMP721, VAMP722, VAMP723, VAMP725 and VAMP726 (Sanderfoot 2007).

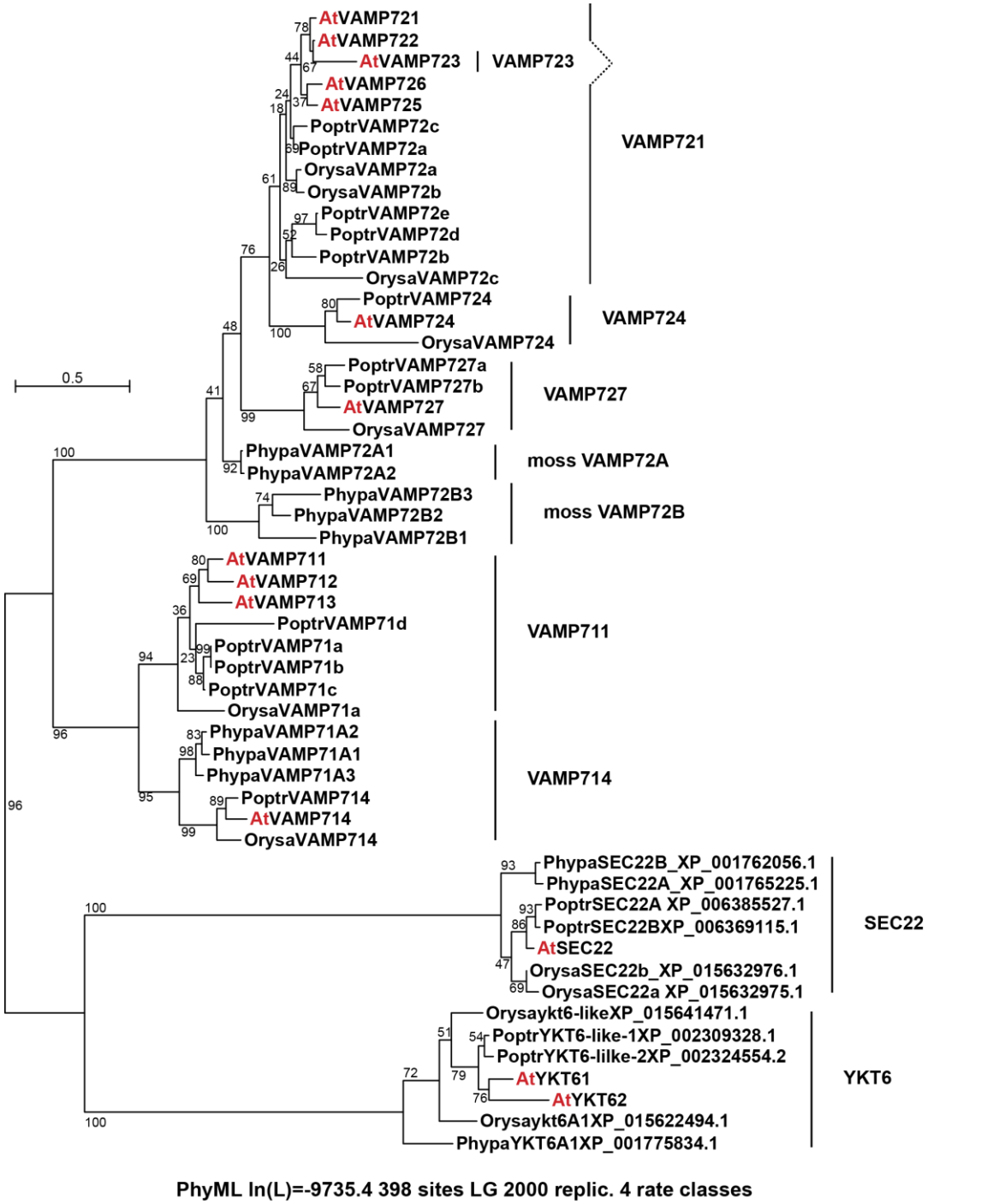

Figure 19 Phylogenetic tree of the plant R-SNARE family.

Amino acid sequences of R-SNARE orhologs from the moss ***Physcomitrella patens*** (Bryophyta), rize (***Oryza sativa****;* monocot: commelinids: Poales), ***Populus trichocarpa*** (eudicot: eurosid: fabids: Malpighiales) *and* ***Arabidopsis thaliana*** (eudicot: eurosids: malvids: Brassicales; red) were aligned (Seaview software) and a phylogenetic tree generated (maximum likelihood – LG model, 2000 bootstraps, PhyLM) (Galtier 1996). Sequences for *A.thaliana* were obtained from TAIR (www.arabidopsis.org), for other species sequences of the VAMP72 and VAMP71 clade were extracted from a previous publication (Sanderfoot 2007) and for the SEC22 and YKT6 clade obtained from the NCBI database, after protein and species search.

VAMP727

VAMP727 was detected at MVBs, where it colocalized with MVB-marker RHA1 and the Qa-SNAREs SYP21/SYP22. It was detected in SNARE complexes, including Qa-SNARE SYP22, Qb-SNARE VTI11 and Qc-SNARE SYP51 (Ebine et al. 2008). Mutant *vamp727* plants develop normally and show no obvious phenotype, whereas *syp22* mutants are severely delayed in development and display alterations in their leaf shape. The *syp22 vamp727* double mutant is embryo lethal, suggesting their involvement in a similar trafficking pathway. Analysis of the double mutant embryo phenotype revealed impaired protein storage vacuole (PSV) morphology and the mislocalization of PSV-markers to the apoplast (Ebine et al. 2008). Together these data suggest that the Qa-Qb-Qc-R-SNARE complex SYP22-VTI11-SYP51-VAMP727 is involved in the vesicle trafficking to PSVs via MVBs. Furthermore, Qa-SNAREs SYP21, SYP22 and SYP23 act redundantly during vacuolar trafficking, in complexes with Qb-SNARE VTI11 and several members of the SYP5 Qc-SNARE family, suggesting further SNARE interaction partners for VAMP727 (Shirakawa et al. 2010, Uemura et al. 2010). An additional function for VAMP727 in a novel trafficking pathway from the pre-vacuolar compartment towards the plasma membrane was suggested (Ebine et al. 2011). In this study, VAMP727 co-localised and interacted *in vivo* with the Qa-SNARE SYP121 (aka PEN1) at foci adjacent to the plasma membrane. This interaction was severely reduced in *ara6* mutants, and increased upon overexpression of the constitutively active ARA6^{Q93L}, indicating that ARA6 regulates the formation of SYP121-VAMP727-containing SNARE complexes. The biological relevance of this pathway has yet to be established, but a role in environmental stress responses was suggested (Ebine et al. 2011). Clonstistent with this idea, VAMP727 was implicated in brassinosteroid signalling, because VAMP727 overexpression induced partial hyposensitivity to brassinosteroids. Furthermore, VAMP727 was shown to interact with the brassinosteroid receptor-like-kinase BRI1, and this interaction was suggested to modulate steady-state levels of BRI1 (Jones et al. 2014).

VAMP724

Angiosperms evolved the VAMP724 clade in a second diversification event within the VAMP72 clade (Sanderfoot 2007). Upon expression in *Arabidopsis* protoplasts, VAMP724 localized to endosomes and the plasma membrane, comparable to the other members of the VAMP721 subfamily (Uemura et al. 2004). In *Arabidopsis* root hairs, VAMP724 localized at the tip region of emerging root hairs, in a similarly overlapping localization with VAMP721 and VAM722 (Ichikawa et al. 2014). Furthermore, it can interact with Qa-SNARE SY123 in vitro and was found to assemble in SNARE complexes with Qbc-SNARE SNAP33 and either Qa-SNARE SYP121 or SYP132 (Kwon et al. 2008b, Ichikawa et al. 2014), suggesting an involvement in the secretory pathway at the plasma membrane together with these plasma-membrane-

localized Qa-SNAREs. Yet, the functional relevance of these VAMP724-containing SNARE complexes remains to be elucidated.

VAMP723

In the most recent duplication within the VAMP72 clade, VAMP723 diverged from VAMP722 (Figure 19), after the separation of the *Arabidopsis* from the *Eutrema* lineage (Liu et al. 2014). VAMP723 localizes to ER membranes, in contrast to its progenitors, which localize to endosomes, the plasma membrane and the cell plate of dividing cells. Causal to this dramatic change in localization appears to be a single amino acid change in the longin domain (Zhang et al. 2015a). Recently available transcriptional data shows the ubiquitous expression of VAMP723 and together with a differential upregulation during biotic stress responses (bar.u.toronto.org, (Schmid et al. 2005, Winter et al. 2007)).

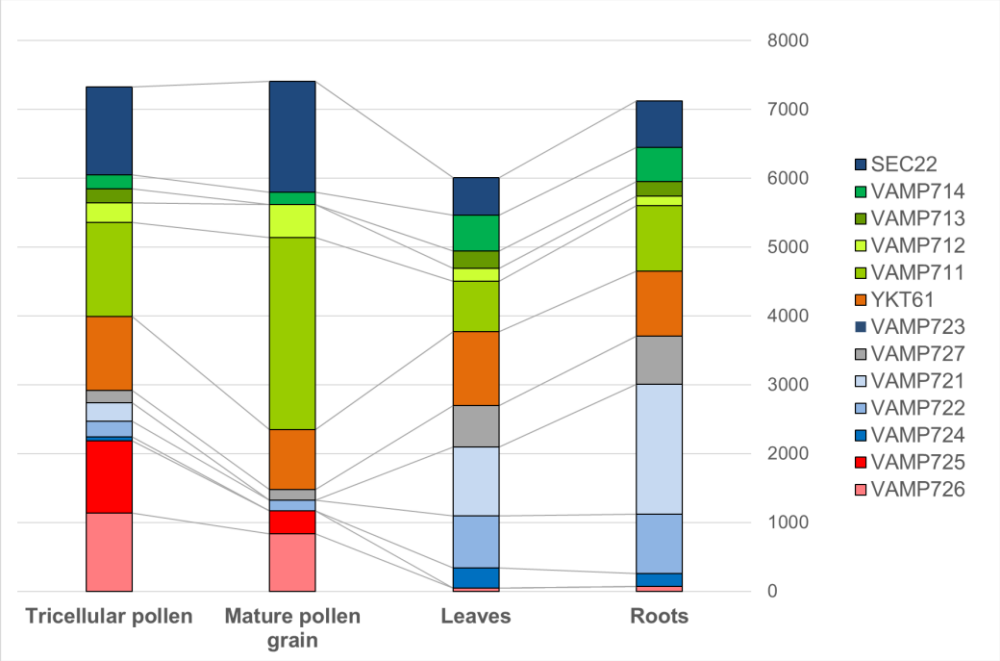

Figure 20 Transcriptional profile of the *Arabidopsis* R-SNARE family.

Analysis of transcriptional databases reveal ubiquitous *VAMP721/ VAMP722/VAMP724* expression during vegetative growth and pollen specific expression of *VAMP725/VAMP726*. Note the lower expression of *VAMP724*, compared to *VAMP721/VAMP722*. Samples include tricellular pollen, mature pollen grain, root and leaf tissue. The median expression values were obtained from the original publication to generate the graph (Honys Twell 2007). *VAMP723* was not available in this dataset and *YKT62* excluded, due to marginal expression levels.

The VAMP721 subfamily

The VAMP721 subfamily in *Arabidopsis* comprises four members, VAMP721, VAMP722, VAMP725 and VAMP726 (Figure 19). The transcript of *VAMP725* and *VAMP726* is highly abundant during pollen development, but widely absent during vegetative growth (Figure 20,

see below). Functional data on VAMP725 and VAMP726 in *Arabidopsis* is rather limited, but a homolog of VAMP726 in *Petunia inflata* showed a tip-focused localization in the growing pollen tube (Guo and McCubbin 2012). VAMP725 and VAMP726 were found at the plasma membrane and in endosomal puncta upon ectopic expression in *Arabidopsis* protoplasts (Uemura et al. 2004). Considering that during pollen tube tip growth, *de novo* synthesized and recycled material from the periphery is delivered into the tip region, which requires the secretory pathway and is likely the most active site of membrane fusion, a function of VAMP725 and VAMP726 in this process can be assumed (Samaj et al. 2006). The other two members of the VAMP721 branch, VAMP721 and VAMP722, share 96% amino-acid sequence identity. They can equally contribute to most processes that they are involved in, which include secretory traffic during cytokinesis, during several pathogen defence responses and during regular plant development, as further described below.

VAMP721 and VAMP722 in the default secretory trafficking of interphase cells

VAMP721 and VAMP722 localize to the TGN together with TGN-localized ATPase VHA-a1 and were detected at the plasma membrane, in case of strong cellular accumulation, whereas they were not detected in RabF2b-marked MVBs (Zhang et al. 2011, El Kasmi and Krause et al. 2013). (Zhang et al. 2011). Further co-localization studies specified their TGN localization to the *trans* side of the TGN through the subsequent localization of *trans*-Golgi marker ST (sialyl transferase), TGN marker SYP43 and VAMP722 localized in close spatial order to each other (Uemura et al. 2012). This subcellular localization is consistent with their combined role in the secretory trafficking pathway to the plasma membrane, during which they reside, as vesicle-associated SNARE component, at transport vesicles and continuously cycle between plasma membrane and the *trans*-side of the TGN. In in *vamp721 vamp722* double mutants secretory trafficking is impaired, which was evident by the mislocalization of plasma-membrane-markers Lti6 and PIP2A (Zhang et al. 2011). Consistently, VAMP721 and VAMP722 were found in SNARE complexes together with plasma-membrane-residing SNAREs, including Qa-SNAREs SYP132, SYP121 (aka PEN1) and SYP122, and the Qbc-SNARE SNAP33 (Kwon et al. 2008b, Yun et al. 2013, Zhang et al. 2015a). Interestingly, during normal plant growth the function of both R-SNAREs VAMP721 and VAMP722 can be fully sustained by a single functional allele, which was evident in the phenotypes of *vamp721-/+ vamp722-/-* or *vamp721-/- vamp722+/-* double mutant lines that developed like wild-type (Kwon et al. 2008b). In summary, the R-SNAREs VAMP721 and VAMP722 act redundantly in the secretory trafficking pathway to the plasma membrane, likely through the formation of SNARE complexes with the Qa-SNAREs SYP121, SYP122 or SYP132 and the Qbc-SNARE SNAP33 (among others).

VAMP721 and VAMP722 during plant pathogen response

During pathogen attacks, the machinery of the secretory trafficking pathway is reorganized for the directional transport of antifungal and antimicrobial compounds to infection sites. It was shown for several classes of powdery mildew fungi that upon infection, SNARE complexes, containing PEN1-SNAP33-VAMP721 or VAMP722 accumulate in foci close to the infection site. Double mutant *vamp721-/+ vamp722-/-* or *vamp721-/- vamp722+/-* lines showed increased susceptibility to *Hyaloperanospora parasitica, Erysiphe pisi* and *Golovinomyces orontii* infection, indicating their essential role during the defence reaction towards fungi (Kwon et al. 2008b). The reorganisation of the secretory trafficking machinery is import for the delivery of cell wall material for haustorium formation and antifungal components, like the resistance protein RPW8.2 to the infection site (Kim et al. 2014).

The immune response against bacterial pathogens similarly involves SNARE-dependent trafficking of antimicrobial compounds. For instance, in tobacco (*N.benthamiana*), silencing of *NbSYP132* resulted in increased susceptibility to several classes of bacterial pathogens and enhanced bacterial growth on these plants (Kalde et al. 2007). In *Arabidopsis*, VAMP721/VAMP722 protein stability is specifically modulated upon bacterial infection. Under normal growth conditions, VAMP721/VAMP722 protein abundance is constitutively regulated by the 26S-proteasome pathway (Yun et al. 2013). In contrast, simulating bacterial infection by treating plants with the bacterial-elicitor flg22, led to the accumulation of these two R-SNAREs through the inhibition of this degradative pathway, accompanied by their transcriptional upregulation (Yun et al. 2013). The specific stabilization of VAMP721 and VAMP722 upon elicitor treatment strongly indicates an essential physiological role of these two R-SNAREs also during bacterial pathogen infection.

VAMP721/VAMP722 are essential to Arabidopsis cytokinesis

A third essential function that VAMP721 and VAMP722 contribute in plants is during homotypic vesicle fusion during cytokinesis (Zhang et al. 2011, El Kasmi and Krause et al. 2013). The double mutant phenotype of *vamp721 vamp722* exhibits a variety of abnormalities, including partial gametophytic lethality, abnormal cotyledon development, rudimentary roots and early arrest at the seedling stage. On a subcellular level, these mutants are characterized by clear signs of impaired cytokinesis, including multinucleate cells and cell wall stubs (Zhang et al. 2011, Zhang et al. 2015b). Both, VAMP721 and VAMP722 localize at the cell plate of dividing cells and are part of cytokinesis-specific, KNOLLE-containing SNARE complexes (El Kasmi and Krause et al. 2013).

The SNARE-dependent fusion machinery during cytokinesis

Vesicle fusion during cytokinesis requires the activity of two distinct SNARE complexes, KNOLLE-SNAP33-VAMP721/VAMP722 (Qa-Qbc-R-SNARE) and KNOLLE-NPSN11-SYP71-VAMP721/VAMP722 (Qa-Qb-Qc-R-SNARE). Plants lacking both complexes in *knolle, snap33 npsn11* or *syp71 snap33* double mutants, present clear cytokinesis defects, including cell wall stubs, multinucleate cells and incomplete cell walls. However, like the *vamp721 vamp722* double mutant, the phenotype is relatively mild, considering supposedly complete termination of cell division (El Kasmi and Krause et al. 2013). In the absence of the SNARE machinery, vesicle fusion in the plane of cell division should be fully terminated, and the double mutant phenotype would be much more severe than reported. Mitosis per se would not be affected, genetic material further duplicated, while no separating membrane would be formed, resulting in a single multinucleate cell. This phenotype was observed for the *knolle keule* double mutant (Waizenegger et al. 2000), in which both KNOLLE, and its alternative Qa-SNARE SYP132 are not available for vesicle fusion, because KNOLLE is absent and SYP132 function is no longer positively regulated by the SM protein KEULE (see chapter 5). Hence, vesicle fusion in the fusion plane is obliterated, resulting in a large, bulging single-celled embryo (Waizenegger et al. 2000). In contrast, the phenotype of the *vamp721 vamp722* double mutant develops to a seedling stage, strongly suggesting a compensatory R-SNARE that promotes vesicle fusion in the plane of cell division during the absence of VAMP721 and VAMP722 in the double mutant.

6.1.4 Evaluating the VAMP72 clade reveals VAMP724 as the best candidate for a functional overlap with VAMP721/VAMP722 in vesicle fusion

In summary, VAMP723 localizes to the ER and likely performs a yet unknown function in ER-Golgi trafficking steps. VAMP725 and VAMP726 are preferentially expressed during pollen development and absent in vegetative seedling growth (Figure 20), excluding their involvement in cytokinesis during later stages of plant development. VAMP727 is essential for trafficking towards the vacuole (Ebine et al. 2008). Additionally, VAMP727 was observed at the plasma membrane and was suggested to be part of an ARA6-regulated pathway that includes the Qa-SNARE PEN1 and might be important for specific stress responses (Ebine et al. 2011). In the absence of VAMP721/VAMP722, this pathway could be reoriented towards the cell plate and contribute to cytokinesis, however several points argue against this hypothesis: Firstly, PEN1 fails to complement the *knolle* mutant phenotype, excluding its involvement in cytokinesis (Reichardt et al. 2011). Secondly, the putative trafficking pathway towards the plasma membrane, originates in (or passes through) MVBs (Ebine et al. 2011), in contrast to the secretory vesicles that contain *de novo* synthesised material and are essential during cytokinesis (Reichardt et al. 2007). Thirdly, markers that are delivered to the plasma membrane

in wild-type plants, fail to accumulate in *vamp721 vamp722* double mutants, excluding the possibility that the secretory pathway could be by-passed through an MVB- and VAMP727-dependent step (Zhang et al. 2011). Thus, the R-SNARE VAMP724 represents the only remaining candidate among the members of the VAMP72 clade (compare Figure 19) to functionally replace VAMP721 and VAMP722 in their absence and contribute to vesicle fusion during cytokinesis. On an amino-acid level, VAMP724 is 70% identical to VAMP721 and VAMP722. Hence, *Arabidopsis* VAMP724 was functionally characterised and evaluated for putative overlapping and distinct roles together or apart from the R-SNAREs VAMP721 and VAMP722, particularly in respect to plant cell division.

6.2 Results

6.2.1 VAMP724 is functionally related to VAMP721 and VAMP722

VAMP724 partially complements the vamp721 vamp722 double mutant phenotype

To first evaluate the functional similarity between VAMP724, VAMP721 and VAMP722, N-terminally Myc-tagged VAMP724 under the control of the cytokinesis-specific *KNOLLE* promoter (*pKN::*) was tested for the functional complementation of the *vamp721 vamp722* double mutant. The progenies of *vamp721 vamp722/+* mutant plants carrying the *VAMP724* transgene were phenotypically analysed and wild-type-like, *vamp721 vamp722* double mutants, and an intermediate phenotype were observed (Figure 21A). This intermediate phenotype was characterised by a delayed development and varying root lengths, in comparison to wild-type. After transfer to soil these seedlings survived for a maximum of 12 days (Figure 21A). These candidate seedlings were subjected to genotyping analysis and a doubly-homozygous genotype for *vamp721* and *vamp722*, as well as the presence of *pKNOLLE::MYC-VAMP724* was confirmed (Figure 21C; further referred to “complemented seedlings”). To quantitatively link the *VAMP724* containing transgene to the complemented phenotype, the frequency of *vamp721 vamp722* double mutant phenotypes in the progeny *vamp721 vamp722/+* double mutants with and without hemizygous transgene was compared. In the progeny of transgene-free double mutant lines, 5% double mutant phenotypes were observed (Figure 21D). In contrast, the progeny of double mutant lines carrying *pKN::MYC-VAMP724* only 1% of the seedlings displayed the mutant phenotype, suggesting that the *vamp721 vamp722* double mutant indeed was complemented by the expression of *VAMP724* (Figure 21D). In a previous study, similarly VAMP721 was expressed from the *KNOLLE* promoter in a *vamp721 vamp722* double mutant line. These seedlings displayed a comparable phenotype and developmental arrested at a similar developmental stage, when compared to

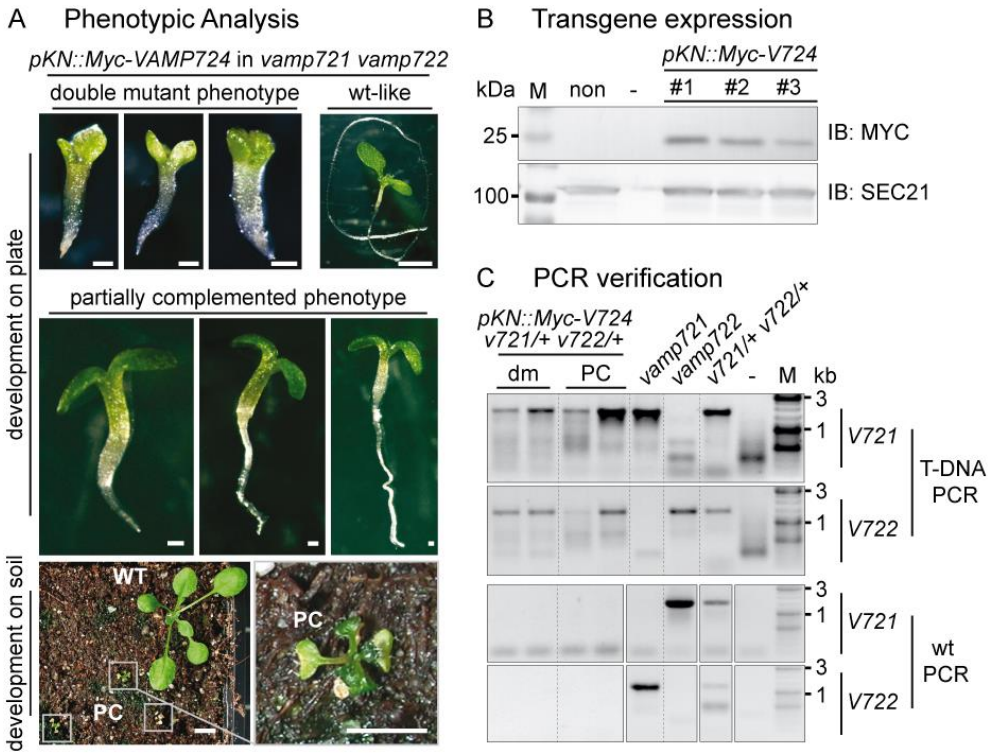

D Segregation analysis of the *vamp721 vamp722* double mutant phenotype

Transgene	genetic background	WT	double mutant phenotype	N
-	*vamp721/- vamp722/+*	95% (1851)	5% (93)	1944
pKN::MYC-VAMP724	*vamp721/- vamp722/+*	99% (1854)	1% (15)	1869

Figure 21 Test for functional complementation the *vamp721 vamp722* double mutant phenotype by *pKN::Myc-VAMP724*.

Seedlings expressing N-terminally tagged *VAMP724,* under control of the *KNOLLE* promoter in *vamp721/+ vamp722* double mutants from a heterozygous transgene were phenotypically analysed. (**A**) Representative seedling phenotypes are shown on plate or after transfer to soil and were classified as: *vamp721 vamp722* double-mutant-like, wild-type-like and partially complemented seedlings, characterized by partially recovered root (**A**, asterisk) and cotyledon development (**A**, arrohead).. (**B**) Transgene expression of independent, *pKN::MYC-VAMP724* single insertion lines (**B**, *pKN::MYC-V724*) in immunoblots probed with anti-Myc (**B**, MYC) and anti-SEC21 antisera (loading control). (**C**) Genotyping analysis of partially complemented seedlings, confirmed homozygous *vamp721 vamp722* alleles; water (-), *vamp721, vamp722* single mutant and *vamp721/+ vamp722/+* doubly heterozygous seedling samples were included as control. (**D**) Frequency double mutant phenotypes in the progeny of *vamp721 vamp722* double mutants, without or with *pKN::Myc-VAMP724* transgene. PC, partially complemented phenotype; M, Protein size marker (**B**); kDa, molecular weight in kilodalton; -, no loading (**B**); non, non-transformed plants; M, DNA size marker (**C**); -, water control (**C**), *v721/+ v722/+, vamp721/+ vamp722/+*; V721, *VAMP721* specific primers*;* V722, *VAMP722* specific primers; kb, DNA size in kilobase. Scale Bar, 1 mm (**A**, double mutant phenotype), 5 mm (**A**, wild-type-like), 10mm (**A**, development on soil).

the complementation with VAMP724 (El Kasmi and Krause et al. 2013). Together these data suggest that VAMP724 is functionally related to VAMP721 and VAMP722 and that it is involved in cytokinesis. However, considering the ability of plants to develop entirely normal with only

one intact allele of either VAMP721 or VAMP722, these partially complemented phenotypes for both, VAMP721 and VAMP724, expressed during cytokinesis, imply that the seedling arrest was not due to low R-SNARE abundance during cytokinesis and thus not related to cell division. It rather suggests that during later stages of development VAMP721, or VAMP724 respectively, were too low abundant in non-dividing cells, because of the dilution through the cell-lineages after cell division. This in turn suggests, together with the established role of VAMP721 in the secretory trafficking pathway in interphase cells, that likely a collapse of this trafficking pathway caused the seedlings to arrest their further development.

VAMP724 is not essential to plant development

To test the functional requirement of VAMP724, a mutant T-DNA line (SAIL569_E12) with a single insertion in the first intron of *VAMP724* was analysed (Figure 22A). RT-PCR analyses revealed a severe knock-down of *VAMP724* transcript accumulation (Figure 22B). Despite the near-absence of VAMP724, *vamp724* mutant and wild-type plants were phenotypically indistinguishable at any developmental stage and the *vamp724* mutant was inherited unaffected to the next generation (Figure 22C). It was previously shown that the loss of one R-SNARE in *vamp721* mutants was compensated by transcriptional upregulation of another R-SNARE, *VAMP722* (Kwon et al. 2008b). Thus, the transcript levels of *VAMP721* and *VAMP722* were analysed in *vamp724* mutant seedlings and tested for upregulation, but no detectable change in expression was observed for both R-SNAREs (Figure 22B). This data indicates that VAMP724 either performs no essential function in *Arabidopsis* and might represent an evolutionary relic, or that endogenous levels closely related R-SNAREs, like VAMP721 or VAMP722 suffice to compensate for the loss of VAMP724 function in this mutant.

The vamp721 vamp722 vamp724 triple mutant is synthetic lethal

Abolishing cytokinesis in the *knolle keule* double mutant results in the arrest at an early embryo stage as single, multinucleate cell. In contrast, the *vamp721 vamp722* double mutant phenotype displays a comparably mild phenotype and develops to an early seedling stage (Zhang et al. 2011). The complementation analysis suggests functional relatedness between VAMP721, VAMP722 and VAMP724, while the *vamp724* mutant suggests no essential function for VAMP724. To assess, whether endogenous VAMP724 performs an essential function in *Arabidopsis* in similar pathways as VAMP721 and VAMP722, triple mutant lines were generated by crossing the *vamp724*$^{SAIL\_569E12}$ T-DNA insertion line with the *vamp721*$^{SALK\_037273}$ *vamp722*$^{SALK\_119149}$ double mutant (see Figure 22A for insertion positions).

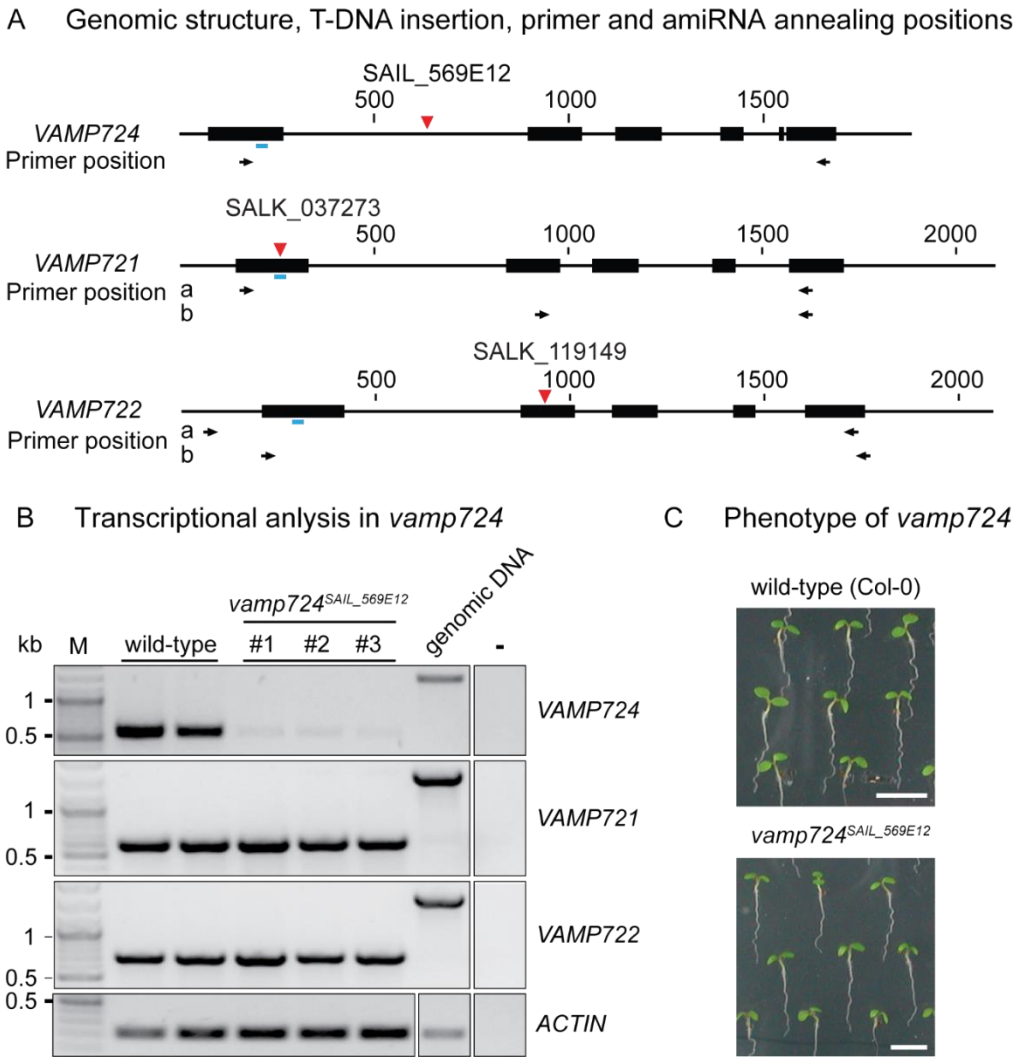

Figure 22 Analysis of the genetic interaction of *VAMP721*, *VAMP722* and *VAMP724* in *vamp721 vamp722 vamp724* triple mutants.

The *vamp721 vamp722 vamp724* triple mutant was generated by crossing the *vamp724* single mutant with *vamp721 vamp722* double mutant lines. (**A-D**) The effect of the mutant *vamp724* mutant allele was assessed in the progeny from different triple mutant mother lines, carrying either wild-type *VAMP724*, heterozygous or homozygous *vamp724* mutant alleles. Note that triple homozygous mutant seedlings could not be obtained. Therefore, the transmission of the *vamp721 vamp722* double mutant allele either to the seedling (**A**), or the embryo stage (**D**) was quantified, in the different lines. Seedling phenotypes, resembling *vamp721 vamp722* phenotype from the triple mutant progeny in **A**, were genotyped (**B**, dm). In over 40 seedlings, a doubly homozygous *vamp721 vamp722* genotype was confirmed, while the *vamp724* allele was either heterozygous or wild-type, but notably never homozygous. Two samples are shown (dm), together with wild-type (**B**, WT), water (**B**, -) and respective homozygous single mutants controls. (**C**) Siliques from different triple mutant lines, carrying *vamp721*/+ *vamp722* and either *vamp724* homozygous, heterozygous or wild-type alleles and wild-type were opened and ovule phenotypes observed. Phenotypes could be classified as: green-coloured ovules, indicating normal development (**C**, wild-type); whitish, translucent ovules, indicative of *vamp721 vamp722* double mutants (**C**, arrowhead; double mutant) (Zhang 2015) and shrivelled, brownish ovules, indicating aborted embryos (**C**, asterisk; aborted). (**D**) The frequency of the occurring ovule phenotypes was quantified, applying these classes as the ratio of phenotype per ovule. The quantification is represented in a Boxblot (**D**), generated using R statistical software; median values are indicated beside individual boxes; absolute number of observations in brackets. WT, wild-type like phenotypes; N, total number of seedlings counted; kb, DNA size in kilobase; M, DNA size marker;

A Transmission of the *vamp721 vamp722* double mutant seedling phenotype

Parental genotype		WT	*vamp721 vamp722* phenotype (dm)	N
vamp721/+ vamp722/-	*VAMP724*	95% (1403)	5% (72)	1475
vamp721/+ vamp722/-	*vamp724/+*	98% (826)	2% (15)	841
vamp721/+ vamp722/-	*vamp724/-*	100% (2001)	-	2001
vamp721/- vamp722/+	*VAMP724*	95% (1851)	5% (93)	1944
vamp721/- vamp722/+	*vamp724/+*	99% (1601)	1% (23)	1624
vamp721/- vamp722/+	*vamp724/-*	100% (1999)	-	1999

B Genetic analysis of *vamp721 vamp722* double-mutant-like phenotypes in the *vamp721/+ vamp722 vamp724/+* triple mutant progeny

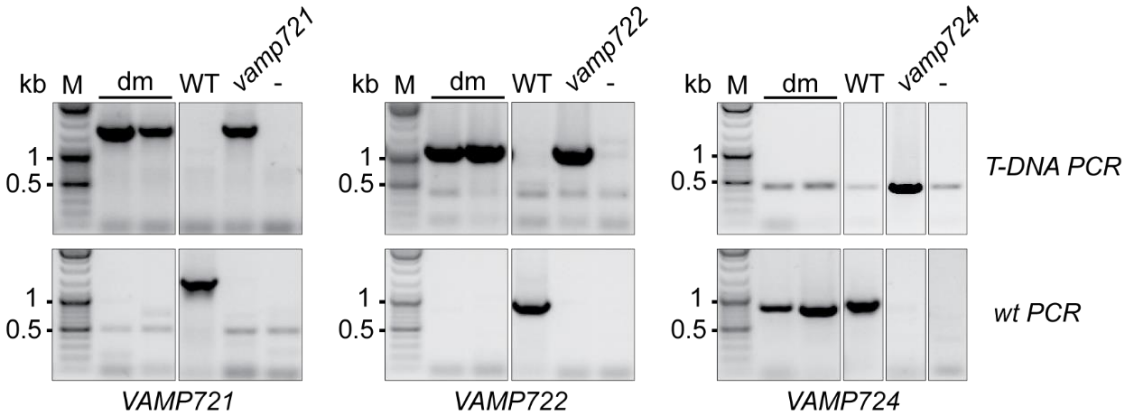

C Ovule phenotype

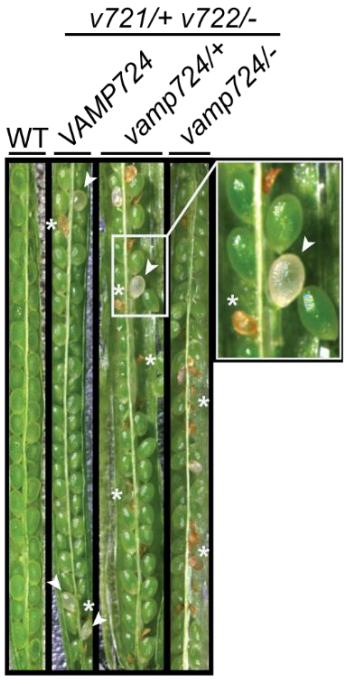

D Ovule phenotype transmission in the different triple mutant allele variants of *vamp721 vamp722 vamp724*

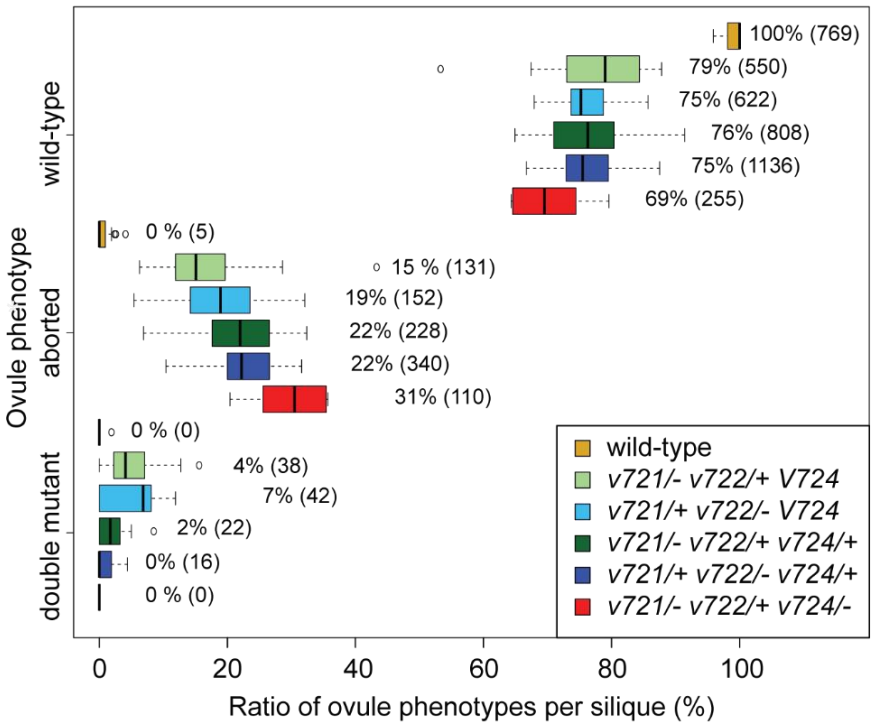

Figure 23 Analysis of the genetic interaction of *VAMP721*, *VAMP722* and *VAMP724* in *vamp721 vamp722 vamp724* triple mutants.

The *vamp721 vamp722 vamp724* triple mutant was generated by crossing and phenotypically analysed. (**A-D**) The effect of the mutant *vamp724* allele was assessed in the progeny of different triple mutant lines, carrying either wild-type *VAMP724*, heterozygous or homozygous *vamp724* mutant alleles. Note that triple homozygous mutant seedlings were not detected at a seedling stage. The frequency of double mutant phenotypes was quantified in progenies of different triple mutant allele combinations, either at a seedling (**A**), or an embryo stage as ovule phenotype (**D**). Seedling phenotypes, resembling *vamp721 vamp722* phenotype from the triple mutant progeny in **A**, were genotyped (**B**, dm). In over 40 seedlings, a doubly homozygous *vamp721 vamp722* genotype was confirmed, the *vamp724* allele was heterozygous or wild-type, but never homozygous. Two of these samples (dm), wild-type (**B**, WT), water (**B**, -) and respective homozygous single mutant controls were tested by PCR. (**C**) Siliques from different triple mutant lines, carrying *vamp721/+ vamp722* and either *vamp724* homozygous, heterozygous or wild-type alleles and wild-type were opened and ovule phenotypes observed. Phenotypes could be classified as: green-coloured ovules, (**C**, wild-type); whitish, translucent ovules, (**C**, arrowhead; double mutant) (zhang 2015) and shrivelled, brownish ovules (**C**, asterisk; aborted). (**D**) The frequency of the occurring ovule phenotypes was quantified and presented in a Boxblot (**D**), using R statistical software; median values are indicated beside individual boxes; absolute number of observations in brackets. WT, wild-type like phenotypes; N, total number of seedlings counted; kb, DNA size in kilobase; M, DNA size marker.

First, the segregating progenies of either *vamp721+/- vamp722-/- vamp724+/- or vamp721-/- vamp722+/- vamp724+/-* were phenotypically analysed at a seedling stage. Among those progenies, exclusively wild-type-like and *vamp721 vamp722* double mutant seedling phenotypes were observed, indicating that either homozygous triple mutants are not transmitted to the seedling progeny or that they must phenotypically resemble the *vamp721 vamp722* double mutant, which would imply that VAMP724 function is not essential to plant development. To evaluate these possibilities, individual seedlings exhibiting the double mutant phenotype were genotyped. This revealed that exclusively wild-type or the heterozygous *vamp724* mutant allele, but importantly, no *vamp724* homozygous allele was present in 40 tested seedlings that were also homozygous for the *vamp721 vamp722* alleles (Figure 23B). This suggests that triple-homozygous mutants were not transmitted to a seedling stage and that they arrested at earlier stages. The frequency of *vamp721 vamp722* double mutant phenotypes was determined in several different double or triple mutant heterozygous progenies (Figure 23A). As described by Zhang et al. 2015b, the transmission of *vamp721 vamp722* double mutants to a seedling stage deviates from a Mendelian distribution, which was also observed in our experiment. 5% seedlings displayed the double mutant phenotype among the progenies of either *vamp721-/+ vamp722-/-* or *vamp721-/- vamp722-/+* (Figure 23A; 25% expected). The Frequency of the mutant phenotype was reduced in lines that contained the heterozygous *vamp724* allele to either 2% in the *vamp721 vamp722-/+* background, or 1% in *vamp721-/+ vamp722-/-* background (Figure 23A). Consistently, no mutant phenotypes were observed in the triple mutant, when *vamp724* was homozygous in

the parental line (Figure 23A), clearly indicating the arrest of the triple-homozygous mutant before reaching the seedlings stage.

To evaluate this putative phenotype during earlier stages, siliques were harvested from abovementioned triple mutant lines, embryos were mounted and cleared by chloralhydrate for several hours. The embryo phenotype of vamp721 vamp722 double mutants was previously described to display variable defects, including abnormal cotyledon development, increased proliferation and arrest at the globular stage. The authors also extracted DNA from these embryos and confirmed them as the doubly-homozygous mutants (Zhang et al. 2015b). Similar embryos were detected in the triple-heterozygous mutants that were analysed here. However, a phenotype reflecting the triple-homozygous mutant embryo was not detected among the progeny. For the analysis, it must be considered, that among the progenies of triple mutants, with two alleles being heterozygous and one being homozygous, only 6% of the progeny is expected to carry the triple-homozygous alleles. Furthermore, this low number might have been further decreased by the described reduced transmission efficiency of *vamp721 vamp722* doubly-homozygous mutants (Zhang et al. 2015b).

In the same publication, the ovules of doubly-homozygous mutants were described to exhibit a “yellowish” appearance, which could clearly distinguish them from the ovules containing wild-type embryos (Zhang et al. 2015b). We observed a comparable ovule phenotype, displaying a translucent and pale appearance, in siliques from double or triple mutant lines, which was not observed in siliques from wild-type controls (Fig. 23C, arrowheads). Beside this phenotype and wild-type like ovules, a shrivelled, brownish ovule phenotype was detected (Fig. 23C, asterisks), representing ovules likely containing early aborted embryos (Andreuzza et al. 2010). Since, an early triple-homozygous mutant phenotype was thus far missing these ovule phenotypes were quantified to substantiate the genetic interaction between *vamp721 vamp722* and *vamp724* (Fig. 23D). For this quantification, very small, likely unfertilized ovules (not shown) that were present in variable numbers - also in wild-type - were excluded. Hence ovules were classified into three groups: green-coloured ovules representing wild-type, paler almost translucent ovules representing the “double mutant”, and shrivelled, brown ovules representing “aborted” embryos. In *vamp721+/- vamp722-/-* siliques, 19% aborted, 7% double mutant and 75% wild-type ovules were observed (Fig. 23, D). In case of normal transmission, progeny from this genetic background should carry 25% of doubly-homozygous alleles, which correlates with the sum of ovules, classified as aborted and double mutant (19% +7%). Consistently, in *vamp721-/- vamp722+/-* a comparable distribution was observed. Therefore, *vamp721 vamp722* homozygous alleles resulted in two different ovule phenotypes either “aborted” (aborted embryo) or “double mutant”, which likely was the one that usually develops to a seedling stage. In the presence of the heterozygous *vamp724* mutant allele, the abundance of double mutant ovules decreased (2-7%; Figure 23D), while that of the aborted

ovules significantly increased (22%; Figure 23D). In lines carrying the homozygous *vamp724* mutant allele in the vamp721 vamp722 doubly-homozygous mutant background, 31% “aborted” and no “double mutant” phenotypes were observed. This clearly indicates that the triple-homozygous mutant must have been synthetically lethal and arrested in, or before, an early embryonic stage, supporting an overlapping function of VAMP724 with VAMP721 and VAMp722 in related pathways that were important during these early stages of development.

Artificial microRNA decreases VAMP721 VAMP722 and VAMP724 transcript levels and causes severe defects in already during embryo seedling development

In the attempt to evaluate the *vamp721 vamp722 vamp724* triple mutant for an interpretable phenotype, an artificial microRNA (amiRNA) was designed to specifically target *VAMP721*, *VAMP722* and *VAMP724* transcripts. (see Fig. 22A, for annealing position; blue bars). This amiRNA was cloned under the control of the UAS promoter (*UAS::amiRNA_vamp721_ vamp722_vamp724*), which can be activated by the transcriptional regulator GAL4 (Weijers et al. 2003). After establishing stable transgenic, single insertion lines, they were crossed with an RPS5a::GAL4 inducer line and the F1 generation was analysed. Expression from the *RPS5a* promoter leads to the accumulation of GAL4 at early embryonic stages. Thus, lines were analysed for their embryonic phenotype, which revealed a consistent, aberrant embryo phenotype among twelve independent lines. These embryos displayed abnormal cotyledon development and bloated, multinucleate cells (Fig. 24D). Secondly, the F1 seeds were harvested and germinated on MS medium. The mutant seedling in these progenies displayed a strong phenotype and died at different time points after germination. Later aborting seedlings displayed defects in several tissues, including abnormal cotyledon and vegetative leaf structures, with bloated, pale cells, as well as bulged primary and secondary root tips (Fig. 24 C, middle/right panel). In contrast, progenies of some lines (n=2 out of 8) arrested at a very early seedling stage, resembling the *knolle* mutant phenotype, and exhibiting stronger defects than the *vamp721 vamp722* double mutant phenotype (Fig. 3.6 C, left panel, asterisk). The phenotypic differences among the independent lines could be due to a variable accumulation of the amiRNA among the different lines, which would have led to the variable regulation of target transcript levels. To test, whether these phenotypes are linked to the knock-down in *VAMP721, VAMP722* and *VAMP724* transcript, aberrant phenotypes were analysed by RT-PCR, in comparison to an *ACTIN* loading control (Fig. 24A). While the expression of *VAMP721 VAMP722* was strongly downregulated, obvious from the PCR gels, differences in *VAMP724* were harder to distinguish. Since the loading control in the *ACTIN* PCR was less abundant in wild-type compared to the other samples, signal intensities were quantified to visualize possible transcriptional differences that were not obvious before (Fig. 3.6B). Intensities were normalised to sample-specific *ACTIN* loading control and to PCR-specific wild-type samples,

thereby indicating the relative abundance of the individual transcript in the pool of total RNA extract. Because RT-PCR represents merely a semi-quantitative method, results must be interpreted carefully. Still, two independent samples for the amiRNA phenotype were analysed and showed about 35% transcript level each for *VAMP721* and *VAMP722* and about 68% transcript level for *VAMP724*, compared to wild-type (Fig. 24B). This indicates that the observed phenotype could be indeed linked to the amiRNA induced knock-down of *VAMP721*, *VAMP722* and *VAMP724.* Yet, in artificial microRNA approaches, off-targets can only be excluded by complementing the amiRNA lines with the expression of a resistant version of one of the target genes. Since this test was not performed, care in the interpretation of the data is required. Still, clear is that a cytokinesis defective mutant phenotype was observed, which was evident by multinucleate cells. Transcript levels of cytokinesis relevant R-SNAREs *VAMP721* and *VAMP722* were knocked-down, as well as the *VAMP724* transcript, which are strong indicators that desired genes were knocked-down and that this knock-down was causal for the phenotype. However, an enhanced phenotype in the triple mutant that could clarify the role of VAMP724 was not obtained from this set of experiment.

VAMP724 localizes at the plasma membrane and co-localizes with KNOLLE in the plane of cell division

The subcellular localization of VAMP724 in *Arabidopsis* root cells was analysed by indirect immunofluorescence analysis and compared to that of VAMP721. The same lines were used as for the complementation analysis, expressing N-terminally tagged VAMP724 or VAMP721. In dividing cells, VAMP721 co-localized with KNOLLE at the cell plate (Fig. 25 A,B; CP). In later stages of cell plate formation, both, KNOLLE and VAMP721 were preferentially observed at the margins of the cell plate, indicative of the active site of vesicle fusion, in which the majority of secretory vesicles accumulate (Fig. 25 A, arrowheads). VAMP721 further localized in endosomes (Fig. 25 A) that relocated to BFA bodies upon BFA treatment (Fig. 25 B; arrow). These VAMP721-containing endosomes were previously identified as VHA-a1 containing TGN and are distinct from Rab2F2b-stained MVBs (Zhang et al. 2011, Uemura et al. 2012). This pattern overlaps with previously reported observations, when antiserum, specific for VAMP721/VAMP722, was applied (El Kasmi and Krause et al. 2013). The most abundant signal for VAMP721 was detected in dividing cells, consistent with the expression from the *KNOLLE* promoter, but signal intensity decreased gradually in post-cytokinetic cells.

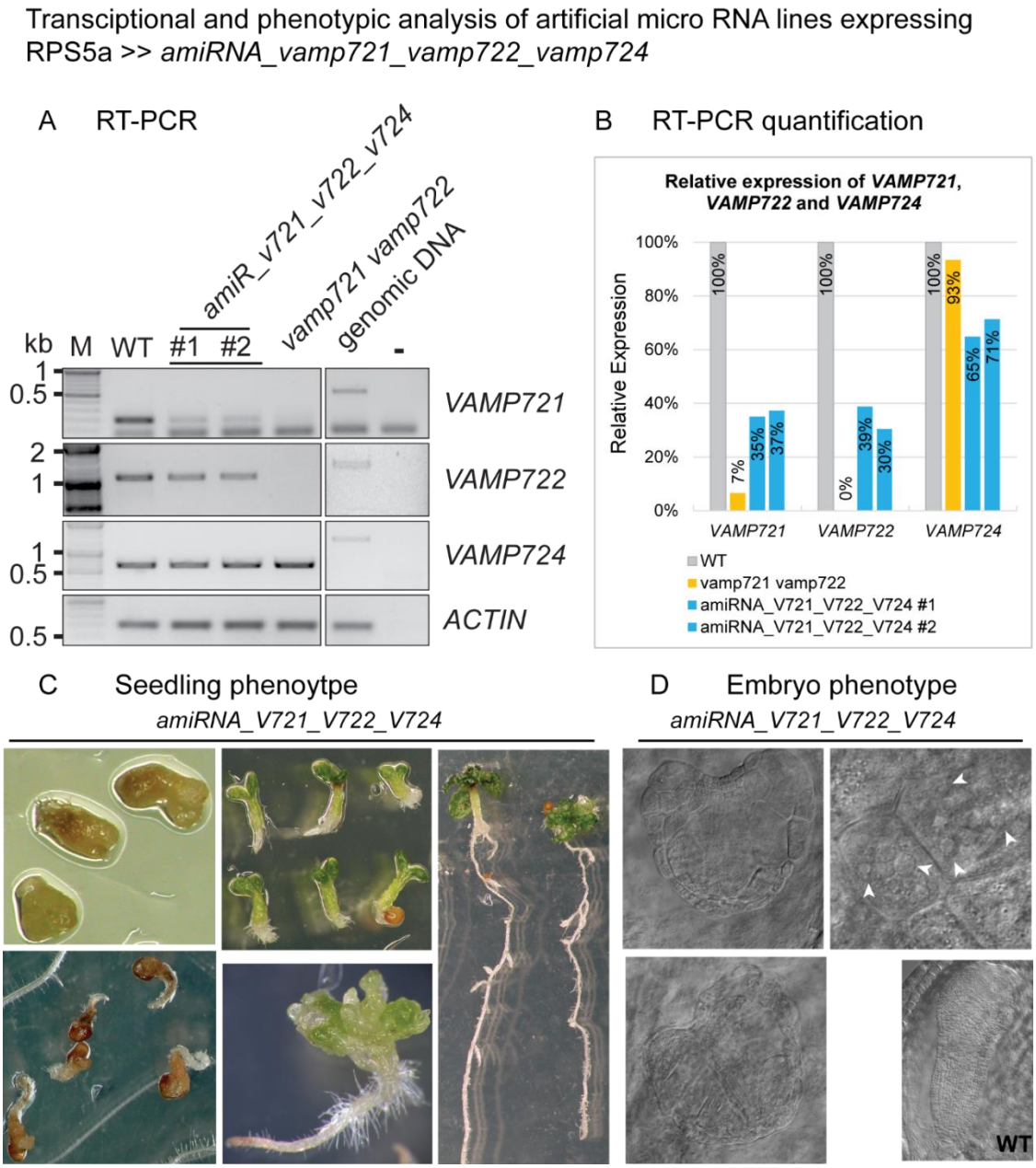

Figure 24 Phenotypic and transcriptional analysis of artificial microRNA (amiRNA) knock-down mutants for *VAMP721 VAMP722* and *VAMP724*.

Artificial microRNAs *amiR_v721_v722_v724* was designed to target the first exon of *VAMP721, VAMP722* and *VAMP724* (see Fig.21, A), genomic structure) and cloned under the control of the GAL4 inducible *UAS* promoter. Transgenic lines carrying *UAS::amiR_v721_v722_v724* were crossed with *RPS5a::GAL4* inducer lines, expressing GAL4 during early embryogenesis. In the F1 progeny, transcript levels of relevant R-SNAREs were assessed by RT-PCR in seedling samples (**A,B**) and phenotypes analysed at the seedling (**C**) and embryo stage (**D**). Note, progeny affected by the amiRNA was significantly delayed in development, contained multi-nucleated cells (**D**, nuclei indicated by arrowheads) and arrested in different stages of seedling development. (**A**) RT-PCR based transcriptional analysis of *VAMP721, VAMP722* and *VAMP724* levels, compared to an *ACTIN* loading control, in aberrant seedlings from two independent amiRNA lines, wild-type (**A**, WT) and *vamp721 vamp722* double mutant seedlings, with genomic DNA and water (**A**, -) controls. (**B**) Signal intensities in PCR gels were quantified and normalized to wild-type and *ACTIN*. Note, both analysed amiRNA lines show comparable knock-down of about 36% for *VAMP721*, 35% *VAMP722*, or 68% for *VAMP724.* kb, DNA size in kilobase; M, DNA size marker.

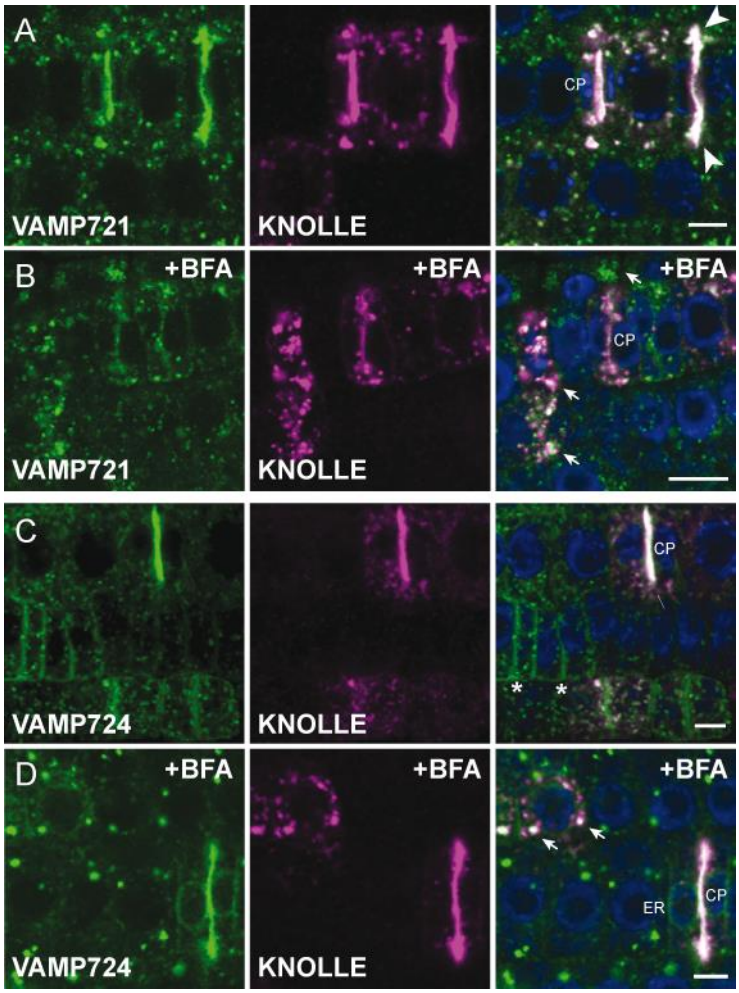

Figure 25 Analysis of the subcellular localization of VAMP724, in comparison to VAMP721 and KNOLLE.

Immunolocalization of Myc-tagged VAMP721 (**A,B**, green) or VAMP724 (**C,D**, green) expressed from the *KNOLLE* promoter and KNOLLE (**A-D**, magenta), after staining seedlings with anti-Myc (**A-D**, green), anti-KNOLLE (**A-D**, magenta) and nuclei with DAPI (**A-D**, right panel, blue). In *Arabidopsis* root cells, VAMP721 (**A**) and VAMP724 (**C**) were detected in endosomes and together with KNOLLE at cell plates of dividing cells (**A-D**, CP). KNOLLE and VAMP721 preferentially accumulated at cell plate margins (**A**, arrowhead). VAMP724 additionally stains the plasma membrane of post-cytokinetic cells (**C**, asterisk) and ER-like structures of cytokinetic cells (**D**, ER). Upon 1h treatment with 50 µM BFA, VAMP721, VAMP724, and KNOLLE relocated to BFA compartments (**B,D**, arrow). +BFA, BFA treatment; scale bars = 5µm.

The pattern of VAMP724 was generally comparable to that of VAMP721. VAMP724 co-localised with KNOLLE in BFA-sensitive endosomes (Fig. 25D; arrow) and at the cell plate of cytokinetic cells (Fig. 25C; arrowhead). In cells directly after cell division, evident by stronger signals, VAMP724 was detected at the plasma membrane (Fig. 25C; asterisks), suggesting its delayed recycling due to a strong protein accumulation, which was previously also observed for VAMP721 (Zhang et al. 2011). Furthermore, in some but not all dividing cells VAMP724 was detected at ER-like structures (Fig. 25D; ER), which might derive from the strong overexpression by the *KNOLLE* promoter (Fig. 25D).

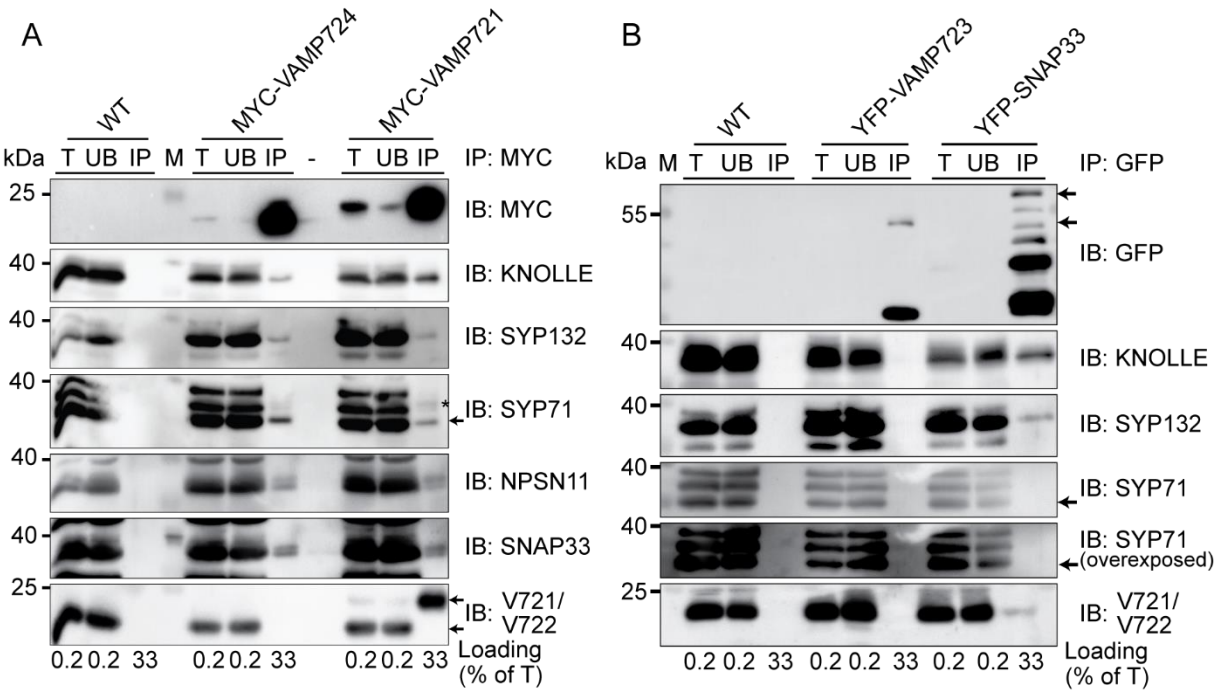

Figure 26 Interaction analysis of VAMP724 with Qa-SNARE KNOLLE, plasma membrane Qa-SNARE SYP132 and SNARE partners.

(**A**) Wild-type seedlings (WT) and seedlings expressing Myc-tagged VAMP721, or VAMP724, under control of the the *KNOLLE* promoter were subjected to immunoprecipitation with anti-Myc beads. (**B**) As control YFP-tagged VAMP723 or SNAP33 analogously expressed were precipitated by anti-YFP beads. Equal amounts of total protein extract (T) and unbound supernatant (UB), together with 33% washed precipitate (IP) were loaded in SDS-PAGE gels. Protein blots were stained with antisera indicated on the right (IB): MYC, anti-Myc; KNOLLE, anti-KNOLLE; SYP132, anti-SYP132; SYP71, anti-SYP71; NPSN11, anti-NPSN11; SNAP33, anti-SNAP33; V721/V722, anti-VAMP721/VAMP722. Note, specific precipitation of Myc-VAMP721 (**A**, upper arrow), in contrast to endogenous VAMP721 (**A**, lower arrow) in anti-VAMP721/VAMP722 and the absence of SYP71 in SNAP33 precipitates, confirming specific precipitation of interacting SNARE partners. M, protein size marker; kda, molecular weight in kilodalton; arrows, protein of interest; *, unstripped protein from previous antiserum incubation.

VAMP724 forms complexes with plasma-membrane Qa-SNARE SYP132 and cytokinesis-specific Qa-SNARE KNOLLE

To evaluate, whether the functional overlap of VAMP724 with VAMP721 and VAMP722 is exerted through SNARE complex formation with similar or distinct SNARE interaction partners, Myc-VAMP721 and Myc-VAMP724 expressed from the *KNOLLE* promoter in transgenic *Arabidopsis* seedlings were precipitated by Myc-beads. To test, whether specific SNARE partners are precipitated, the ER-localized R-SNARE VAMP723 was included to the analysis. VAMP723 was similarly expressed from the *KNOLLE* promoter, but N-terminally YFP-tagged. It was precipitated by anti-GFP beads and YFP-SNAP33 was included as positive control, to ensure appropriate conditions for the co-immunoprecipitation of SNAREs. To test the putative involvement of VAMP724 during cell division, precipitates were tested for the presence of cytokinesis-specific Qa-SNARE KNOLLE and members of both cytokinetic, KNOLLE-

containing SNARE complexes, including Qb-SNARE NPSN11 and Qc-SNARE SYP71 for one complex and Qbc-SNARE SNAP33 for the other. Precipitates were further tested for the Qa-SNARE SYP132, which is involved in the secretory pathway of interphase cells and was recently implicated to act in cytokinesis (Park et al. *in submission*). As further control for the specificity of the assay, precipitates were tested for the presence of VAMP721 and VAMP722, using antiserum that recognizes antigens in both R-SNAREs.

VAMP724 co-precipitated all tested SNARE partners, except for VAMP721 or VAMP722 (Fig. 3.8A), indicating that specific interaction partners were precipitated and that VAMP724. In non-transformed seedlings, no unspecific precipitation was detected, whereas VAMP721 co-precipitated expected, previously published SNARE interactors, as VAMP724 (Fig. 3.8A) (El Kasmi and Krause et al. 2013). Precipitation of the R-SNARE VAMP723 did not co-precipitate the interactors of VAMP724, in contrast to the precipitates of SNAP33, in which VAMP721/VAMP722, KNOLLE and SYP132 but not SYP71 were detected (Fig. 3.8B), further confirming assay specificity. These experiments demonstrate the R-SNARE VAMP724 interact with the analysed, cytokinesis-relevant SNARE proteins and that it can associate in both described KNOLLE-containing SNARE complexes that are relevant during cytokinesis, functionally overlapping with VAMP721 and VAMP722. Additionally, VAMP724 and VAMP721 interacted with Qa-SNARE SYP132, a Qa-SNARE that mainly acts at the plasma membrane of interphase cells, but it also involved during cytokinesis, further suggesting an involvement in the secretory pathway (Reichardt et al. 2011, Park et al. *in submission*).

6.3 Discussion

6.3.1 VAMP724 functionally overlaps with VAMP721 and VAMP722

VAMP724 contributes to cytokinesis and secretory traffic in interphase cells

The two R-SNAREs VAMP721 and VAMP722 contribute equally during, (i) fusion of secretory trafficking vesicles with the plasma membrane in interphase cells and (ii) during vesicle fusion of cytokinetic vesicles in the plane of cell division (El Kasmi and Krause et al. 2013, Yi et al. 2013). While *vamp721 vamp722* double mutants are severely impaired in development and arrest during early seedling development, one wild-type allele of either of these R-SNARE is sufficient to sustain normal plant development (Kwon et al. 2008a, Zhang et al. 2011). Subcellularly, the double mutant shows clear signs of impaired cell division, including bloated multinucleate cells, cell wall stubs and unfused vesicles in the plane of cell division (Zhang et al. 2011, Zhang et al. 2015b). This reveals their essential role during cell division. However,

only a partially complemented phenotype was observed in lines that specifically overexpressed *VAMP721* in dividing cells of the *vamp721 vamp722* double mutant from the cytokinesis-specific KNOLLE promoter (El Kasmi and Krause et al. 2013). The activity of this promoter is restricted to late G2/M-phase of the cell cycle until shortly after cell division is complete (Lauber et al. 1997). This implies, that VAMP721 accumulated in dividing cells to high levels, but was much less abundant in non-cytokinetic cells. Thus, the lack of R-SAREs in their other role beside cytokinesis, that is in secretory pathway, must have been causal to the seedling arrest. Expressing VAMP724 analogously from the *KNOLLE* promoter in these double mutants resulted in a comparable partially complemented phenotype, which implies similar conclusions for VAMP724, that: (i) VAMP724 contributed to cytokinesis, which allowed the complemented plants to grow further and that (ii) VAMP724 must be involved in the secretory trafficking pathway, as indicated by the arrest of the complemented plant at later stages. Notably, both these observed functions were observed in the absence of VAMP721 and VAMP722. Furthermore, in *vamp721 vamp722* double mutants, endogenous VAMP724 is present, but seems insufficient to supply R-SNARE function in the absence of VAMP721/VAMP722. This could be explained by the low transcript levels of *VAMP724*, which are significantly lower than those of the other two R-SNAREs, during normal development (about 10-fold less, Fig. 3.2). This further indicates that substantial amounts of any one of these three R-SNAREs is necessary to sustain normal plant growth and that their activity is important in cytokinetic and non-cytokinetic cells.

VAMP724 subcellularly localizes to the cell plate and transiently associates with the plasma membrane

The subcellular localization of VAMP724 showed a comparable pattern to the one observed for VAMP721/VAMP722. It was detected at BFA-sensitive endosomes, the plasma membrane and the cell plate of dividing cells, where it overlapped with cytokinesis-specific Qa-SNARE KNOLLE. This pattern is supports its involvement in both secretory traffic of interphase cells and a cytokinetic function in dividing cells. Furthermore, expression from the cytokinesis-specific *KNOLLE* promoter led to strong accumulation of VAMP724 in dividing cells, with a gradual decrease in post-cytokinetic cells, in which VAMP724 could be observed at the plasma membrane. Considering its absence from the plasma membrane of older post-cytokinetic cells, a rather transient association with the plasma membrane could be assumed, as would be expected for a recycling, vesicle-associated SNARE protein. This observation overlaps with a similar transient association of VAMP721 with the plasma membrane, when it was tagged and expressed in analogously (El Kasmi and Krause et al. 2013). In contrast, GFP-tagged VAMP721 and VAMP722 expressed from respective native promoters localized more stably to the plasma membrane (Zhang et al. 2011). This difference in localization could be due to

the large (27 kDa) N-terminal GFP-tag that might interfere with the adjacent longin domain and thus protein recycling, because at least in some R-SNAREs the longin domain promotes binding to coat subunits or coat-interacting proteins to mediate SNARE sorting and proper targeting (Maritzen et al. 2012). Hence, the longin domain-dependent sorting of GFP-VAMP721/VAMP722 might be impaired and its localization might not accurately reflect the normal situation.

VAMP724 interacts with Qa-SNAREs KNOLLE and SYP132

VAMP724 interacted with Qa-SNARE KNOLLE and SNARE partners from both described cytokinesis-specific, KNOLLE-containing SNARE complexes, including Qb-SNARE NPSN11, Qc-SNARE SYP71 and Qbc-SNARE SNAP33. Thus, two additional KNOLLE-containing SNARE complexes were identified that contribute to cytokinesis in *Arabidopsis*, (i) the Qa-Qb-Qc-R-complex comprising KNOLLE-NPSN11-SYP71-VAMP724 and (ii) the Qa-Qbc-R-complex containing KNOLLE-SNAP33-VAMP724. Previous studies implicated VAMP724 in a secretion-related function through its interaction with plasma membrane-localised Qa-SNAREs SYP121, SYP123 and SYP132 (Ichikawa et al. 2014). Experimental evidence provided here confirmed the interaction of VAMP724 with SYP132 *in vivo* and further implicates VAMP724 in the secretory pathway. SYP132 was suggested an essential component of the constitutive secretory pathway to the plasma membrane (Enami et al. 2009) for several reasons: First, SYP132 is ubiquitously expressed and shows a uniform distribution along the plasma membrane (Enami et al. 2009). Secondly, SYP132 remains stably associated with the plasma membrane, in contrast to other plasma membrane syntaxins like SYP121 (PEN1), which cycles between the plasma membrane and the TGN (Reichardt et al. 2011). Thirdly, SYP132 belongs to the most ancient branch of SYP1 orthologs in higher plants, which could support the notion of a conserved, ancient function in general secretion (Sanderfoot 2007, Reichardt et al. 2011). However, recently its additional involvement during cytokinesis was described, suggesting that both cytokinetic complexes or complexes derived from the plasma membrane could have been observed, involving VAMP724 and SYP132.

6.3.2 *VAMP724* functionally overlaps with *VAMP721* and *VAMP722 during early plant development*

Strong dependency of plant performance on the abundance of R-SNAREs from the VAMP721 subfamily

Loss of both VAMP721 and VAMP722 caused severe developmental defects that led to the arrest at different developmental stages, as embryos or seedlings. Therefore, there is no clear

phenotype-genotype association and the performance of double-mutant plants most likely depends strongly on environmental conditions. VAMP721 and VAMP722 protein levels are specifically up-regulated, either during abiotic stress shown by treatment with abscisic acid (Yi et al. 2013) or in the absence of either one of the two proteins in respective mutants (Kwon et al. 2008b). During these responses, VAMP721/VAMP722 protein levels are controlled on a transcriptional as well as on a post-translational level through the 26S-proteasome-mediated pathway (Sup Yun et al. 2013). Moreover, the complementation analysis of the *vamp721 vamp722* double mutant with either VAMP724 or VAMP721 (El Kasmi and Krause et al. 2013) confirms the requirement of significant amounts of R-SNARE protein in order to maintain seedling growth. Together, this implies a strong correlation between protein abundance and phenotypic performance during normal plant growth and under the influence of biotic or abiotic stress. Hence, one explanation for the variability in the double-mutant transmission of the same genotype could be the carry-over of different amounts of VAMP721 and/or VAMP722 protein from the meiotic cell to the egg cell, which could be influenced by environmental conditions that the mother plant is exposed to. Considering the functional overlap of VAMP724 with VAMP721/VAMP722 a comparable stringent regulation of VAMP724 and a similar differential regulation upon environmental stimuli could be proposed (see below). Thus, it is likely that the variable double-mutant transmission rate could further depend on varying amounts of endogenous VAMP724.

Synthetic lethality of the vamp721 vamp722 vamp724 triple mutant combination

In the *vamp724* knock-out mutant allele no obvious phenotypic defects in plant development were detected under normal growth conditions. At the same time, neither *VAMP721* nor *VAMP722* transcript levels were elevated to compensate for the loss of *vamp724*, indicating that VAMP724 function is either non-essential or its loss is compensated by the other R-SNAREs without transcriptional upregulation. Furthermore, *vamp721 vamp722 vamp724* triple mutants were viable with only one functional allele of either *VAMP721* or *VAMP722*, suggesting that the loss of VAMP724 can easily be compensated through one of the other R-SNAREs. However, loss of all three R-SNAREs in the homozygous triple mutant allele combination caused synthetic lethality, implying that in *vamp721 vamp722* double mutants, VAMP724 does functionally contribute during early stages of development and that its contribution allows the mutant plant to develop until the embryo or seedling stage, in which it finally aborts.

To conclude, VAMP724 overlaps in localization and analysed interaction partners with VAMP721 and VAMP722. It forms SNARE complexes during cytokinesis, that likely contain either KNOLLE and SNAP33 or KNOLLE, NPSN11 and SYP71. Furthermore, VAMP724 was detected at the plasma membrane and co-precipitated SYP132, suggesting that complexes,

containing these two SNAREs likely contribute during secretory trafficking at the plasma membrane of interphase cells. This dual involvement was directly shown, for its cytokinetic activity, and indirectly for its secretory activity, by the complementation analysis of the vamp721 vamp722 double mutant by VAMP724. Lastly, the synthetic lethality of the triple homozygous mutants showed an essential role of VAMP724 during early developmental stages that can be sustained by either VAMP721 or VAMP722, as evident by the *vamp724* single mutant.

6.3.3 Putative specialized role of VAMP724

Several lines of evidence implicate R-SNAREs in specific responses to environmental conditions, which includes their transcriptional and post-transcriptional regulation. Upon biotic stress, VAMP721 and VAMP722 are transcriptionally upregulated and the 26s-dependant proteasome pathway, that usually keeps them at a steady-state level, is shut down, leading to the rapid accumulation of the two R-SNAREs (Sup Yun et al. 2013, Yun et al. 2013). This upregulation correlates with the plant response mechanism towards pathogens, during which antimicrobial and antifungal components must be delivered to the infection sites and a high rate of secretory traffic is required (Kwon et al. 2008b, Yun et al. 2013, Kim et al. 2014). In contrast, during abiotic stress conditions, *VAMP721* and *VAMP722* protein levels are post-transcriptionally downregulated, supposedly to slow down the growth rate of plants (Sup Yun et al. 2013, Yi et al. 2013). The involvement of such elaborate regulatory mechanisms with opposite outcomes suggest a central role of R-SNAREs during the response to environmental changes.

To evaluate whether also VAMP724 might be subject of such differential regulation and thus to elucidate a putative specialized role of this R-SNARE, transcriptional data in available databases were evaluated. For that the transcriptional levels of *VAMP724*, in comparison to that of *VAMP721* or *VAMP722* were assessed for differences in several different tissues, organs or under specific environmental conditions (bar.u.toronto.org (Winter et al. 2007), AtGenExpress-Visualization Tool (Schmid et al. 2005)). During normal plant growth, *VAMP724* is very low abundant, but ubiquitously expressed. In guard cells, hypocotyl and xylem samples, *VAMP724* transcript appeared more strongly expressed but only accumulated to similar levels as *VAMP721*/*VAMP722*. However, in dry seed samples *VAMP724* was specifically enriched compared to the other two R-SNAREs, which could indicate a role during seed germination (Nakabayashi et al. 2005). Yet, the most significant differential regulation of *VAMP724* was observed in response to biotic or abiotic stress. Among different kinds of abiotic stress stimuli, particularly during heat stress *VAMP724* transcript accumulation was observed. *VAMP724* and

VAMP721 transcripts both strongly accumulated already after 1 h and further increased until after 3 h of heat stress treatment (Fig. 3.9, A).

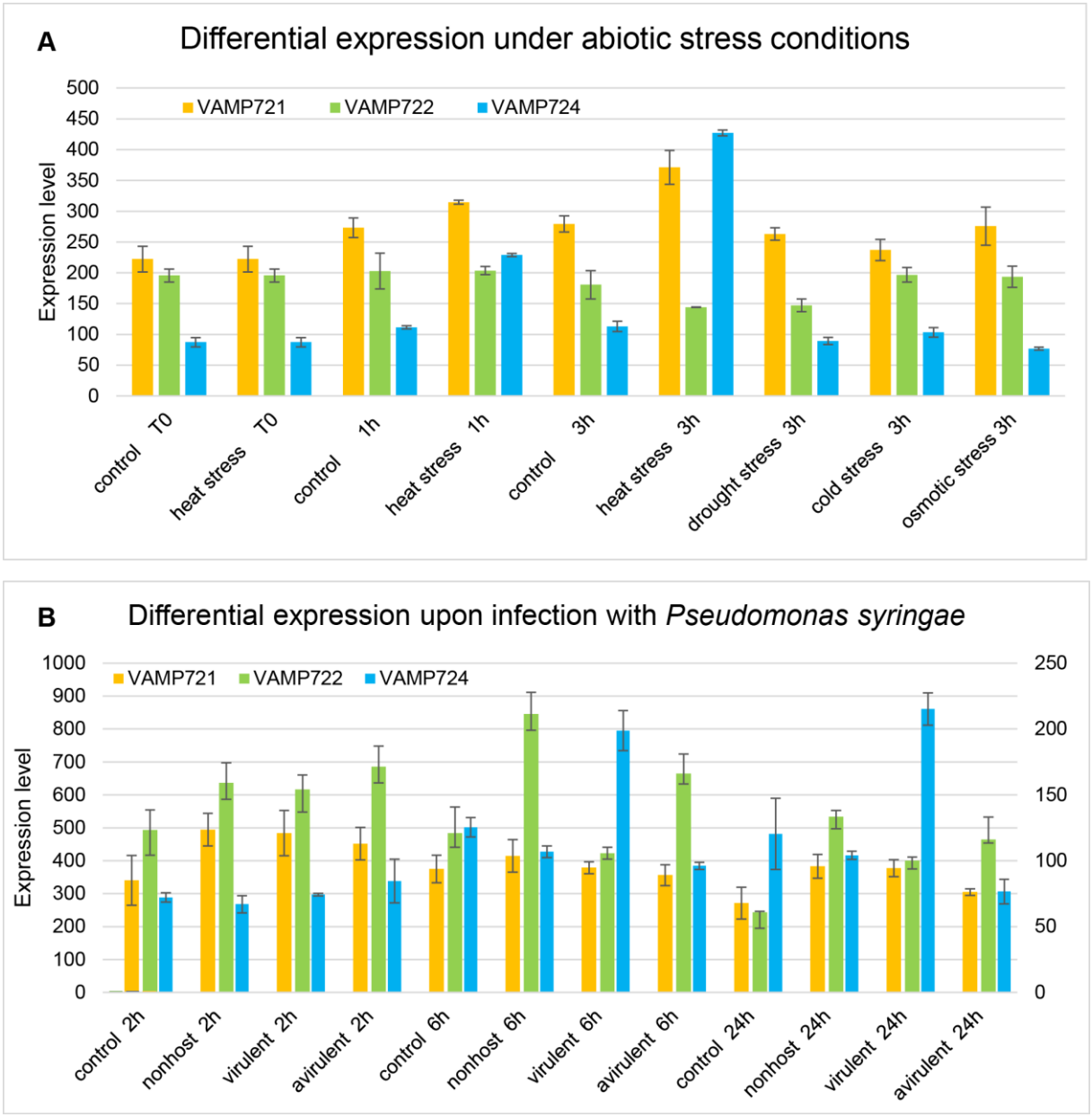

Figure 27 Differential expression of *VAMP721*, *VAMP722* and *VAMP724* during biotic and abiotic stress

Transcriptional data of *VAMP721* (**A,B**, yellow), *VAMP722* (**A,B**, green) and *VAMP724* (**A,B**, blue) was extracted from bar.u.toronto.org. (**A**) For abiotic stress, untreated (**A**, control) and heat stress treated shoot samples are shown, including three time points (**A**, 0h, 1h, 3h). For comparison samples from drought, cold and osmotic stress treatment after 3h are included. (**B**) Transcript levels for biotic stress after *Pseudomonas syringae* infection are visualized, including mock, non-host, virulent and avirulent *P. syringae* treatment for 2h, 6h and 24h post-infection. *VAMP721/VAMP722* expression is blotted at the primary and *VAMP724* at the secondary y-axes.

However, compared to non-treated plants, *VAMP721* expression was only moderately increased (1.2-fold, 1h; 1.3-fold, 3h), in contrast to *VAMP724* transcript, which strongly accumulated over time (2.25-fold, 1h; 4.2-fold, 3h) to an even higher level than *VAMP721.* Another rather specific response was observed for data obtained during virulent *Pseudomonas syringae* infection. While *VAMP721* and *VAMP722* transcript levels increased after two hours and decreased after six hours, upregulation of *VAMP724* was first detected after six hours and then maintained at high levels until 24 h past infection. Thus, it could be speculated about an early response of plants to *Pseudomonas* through the upregulation of VAMP721/VAMP722 and a long-term response through the upregulation of *VAMP724*. These data indicate that plants respond to *P.syrngae* infection and heat stress through the differential upregulation of *VAMP724*, which suggests a specialized function of this R-SNARE under these stress conditions.

R-SNARE involvement in other processes than membrane fusion

During heat stress, stomatal closure is induced through the regulation of calcium and potassium channels (Swarbreck et al. 2013, Hou et al. 2016). KAT1 is one of five potassium channels in *Arabidopsis* and is required for stomatal opening under normal growth conditions. Upon heat or drought stress KAT1 is inactivated, which induces stomatal closure (Sato et al. 2009). The four R-SNAREs VAMP721, VAMP722, VAMP724 and VAMP726 were shown to interact with two plasma membrane-associated potassium channels, KAT1 and KC1. Upon channel binding to VAMP721 and VAMP722, both channels were inactivated and potassium influx was suppressed (Zhang et al. 2015a). Therefore, the specific heat stress-induced expression of VAMP724 could indicate a specific role in stress-signalling pathways through the inactivation of ion channels. The abundance of VAMP724 in guard cells could support such a role specific to stomatal closure upon heat stress. A putative potassium efflux carrier, KEA6, was identified as VAMP724 interactor in a membrane-specific yeast split-ubiquitin interactomic approach (Jones et al. 2014). It could be interesting to validate this potential interaction and test for its biological relevance during stress responses. Furthermore, to assign a specialized function of VAMP724, the phenotypic performance of *vamp724* mutants/ or *vamp721 vamp722* double mutant lines could be analysed for enhanced susceptibility towards different stress treatments, in comparison to wild-type. Additionally, loss or gain of specific interactions between R-SNAREs and selected ion-channels could be observed under differential stress conditions to test for specific signalling responses.

7. Materials and Methods

7.1 General Procedures

* For primer sequences, see table in Chapter 8.3

Growth Condition and Transformation

Arabidopsis thaliana seeds were surface sterilized either by treatment for 1 minute with 70% EtoH or 4 -16 h exposure to chlorine gas and grown on soil, in solid (0.8% agar) or liquid media (1/2 MS medium, 0.1% MES, pH 5.6;) (MS media). After stratification at 4°C in the dark for more than 48 h, seeds were transferred to controlled growth conditions (continuous light and 22°C). *Arabidopsis thaliana* plants from the Columbia (Col-0) ecotype were used as reference (wild type).

*Plant material and transformation**

For experiments in **chapter 4:**, *big3* homozygous plants were transformed with *pMDC7::GFP:SNAP33* or *pMDC7::YFP:NPSN11* using Agrobacterium-mediated floral dipping (Clough and Bent 1998, Richter et al. 2014). T1 seedlings were selected on Hygromycin (20 µg/ml, Duchefa) plates to isolate *big3* mutant plants carrying transgenes *pMDC7::GFP:SNAP33* or *pMDC7::YFP:NPSN11*. The same transgenes were introduced into a BFA-sensitive *GNL1* genetic background by crossing these transgenic plants with *gnl1* homozygous plants bearing a *pGNL1::GNL1*$^{BFA\text{-}sens.}$ transgene (Richter et al. 2007). For interaction analysis of NPSN11 and SNAP33 with MVB-localized Qa-SNARE PEP12 (aka SYP21), *big3* homozygous plants bearing *pMDC7::GFP:SNAP33* or *pMDC7::YFP:NPSN11* were transformed with *pKNOLLE::mRFP:PEP12*. T1 plants were selected by spraying them three times with 1:1000 diluted BASTA (183 g/l glufosinate; AgrEvo, Düsseldorf, Germany). The homozygous background of *big3* or *gnl1 GNL1*$^{BFA\text{-}sens.}$ was confirmed as previously reported (Richter et al. 2007, Richter et al. 2014).

For experiments in **Chapter 5:** SM protein constructs *pKN::RFP-SEC1B* and *pKN::RFP-SEC1A* were transformed into the *keule*^{MM125} mutant background (ecotype LER) and T1 seedlings selected for the BASTA-resistant transgene as described above. The *keule* mutant background was confirmed as previously described (Park et al. 2012). *keule* heterozygous T2 plants bearing *pKN::RFP-SEC1B, pKN::RFP-SEC1A* were tested for complementation of the *keule* mutant phenotype. Segregation of antibiotic resistance and *keule* mutant phenotype was counted on on phosphinothricin-supplemented medium (PPT, 15 mg/l, Duchefa)-. Phenotypic analysis was accompanied by PCR verification of Transgene and *keule* mutant background

(Park et al. 2012). For transgene PCR verification of *pKN::RFP-SEC1B,* primers mRFP-700 and s1b-700-as were used and for *pKN::RFP-SEC1A* primers mRFP-700 and sec1a-800-as.

pKN::MYC-SYP132open was transformed into Col-0 and similarly selected for the BASTA-resistant transgene. *pKN::HA-KEULE* plants (Park et al. 2012) were crossed with *pKN::MYC-SYP132 and pKN::MYC-KN (Reichardt et al. 2011).* For the co-immunoprecipitation analysis transgenes were verified in the F1-F3 generation by PCR, with primers Myc-5' and KN-3'-EcoRI for *pKN::MYC-KN* and s132op-as for *pKN::MYC-SYP132*.

The *sec1b* T-DNA insertion line (AT4G12120; GK-601G09-023443; ecotype Col-0) (Kleinboelting et al. 2012) was isolated from a segregating line and single insertion was verified by germination on sulfadiazine (Sigma-Aldrich) and confirmation of a segregating resistance frequency of 75%. The position of the insertion was tested by sequencing with primer GK-LB-8409 and confirmed in the 13th exon between nt 2559 and 2560 from the start of the coding sequence. Genotyping PCRs were performed using primers 601G09 LP, 601G09 RP and GK-LB-8409.

To test gametophytic viability, reciprocal crosses were performed between heterozygous *keule^{mm125}* and *sec1b^{601G09}* and F1 seedlings genotyped for mutation as described above. For the phenotypic analysis, the *sec1b* mutant was crossed with the *knolle^{X37-2}* mutant (Lauber et al. 1997) or the *sec1b* mutant, carrying the *RPS5a-GAL4* inducer was crossed with transgenic *syp132* T-DNA lines, carrying the artificial microRNA construct against *SYP132*. After crossing siliques were harvested and embryos mounted and cleared by chloralhydrate for several hours.

For experiments in **Chapter 6:** *pKN::YFP-VAMP723* (Col-0) and *pKN::MYC-VAMP724* in the *vamp721* (At1g04750; SALK_037273) *vamp722* (At2g33120; SALK_119149) double mutant background were kindly provided by Dr. F. el-Kasmi. Double mutants for *vamp721* and *vamp722* carrying the *pKN::MYC-VAMP724* transgene were germinated on MS media plates and the segregation of the *vamp721 vamp722* double mutant phenotype was counted. Putative complemented seedlings were transferred to soil after 10 days and transgene presence and respective mutant backgrounds were verified by genotyping PCR using following primers: KN-5'UTR-ss, v724-3'-SmaI for the *pKN::MYC-VAMP724* transgene; v721-ss, v721-as for the *VAMP721* wild-type PCR; SALK-LBA1, v721-as for the *vamp721* T-DNA insertion PCR, v722-3 ss, v722-3-UTR-as for the *VAMP722* wild-type PCR; v722-3-UTR-as, SALK-LBA1 for the *vamp722* T-DNA insertion PCR.

The *vamp724* T-DNA insertion line (AT4G15780; SAIL_569_E12; ecotype Col-0) was isolated from a segregating line and single insertion verified by segregation analysis of resistance towards Basta on phosphinothricin-containing media (PPT, 15 mg/l, Duchefa). For the

generation of R-SNARE triple mutants *vamp724* was crossed with *vamp721/+ vamp722* and genotypes analysed by PCR using abovementioned primers and for the *vamp724* allele V724-ss, SAIL_RP for the wild-type fragment and SAIL_RP, LB3-SAIL to amplify the T-DNA insertion. The transgene *UAS::amiR_v721_v722_v724* was transformed into the Col-0 ecotype and T1 plants selected by BASTA. Transgene positive lines were crossed with lines, carrying homozygous *RPS5a::GAL4* and seedlings and embryos from the F1 generation analysed.

Chemical treatment

To induce trafficking blocks in **chapter 4**, seedlings were transferred to liquid media with or without 50 µM brefeldin A (BFA, 50 mM stock solution in 1:1 DMSO/EtOH, Invitrogen). After 30 minutes, 20 µM EST was added, and seedlings further incubated for 210 minutes until harvest. For the analysis of EST induced seedlings in **chapter 5**, five-day-old seedlings were transferred to liquid media (1/2 MS, 0.1% MES, 1% sucrose pH 5.6) containing 20 µM β-estradiol (EST, 20 mM stock solution in DMSO, Sigma-Aldrich), incubated for 6 h under mild agitation until harvest and freezing for further analysis. BFA treatment in **chapter 6** was performed on five-day-old seedlings that were transferred to liquid media and incubated for 1 h prior to fixation.

Softwares

Sequences were analysed with CLC main workbench 6. Fluorescent images were maximally projected from Z-stack images using the Fiji imageJ program. Images were further processed using Adobe Photoshop CS5 and Adobe Illustrator CS5. For quantifying signal intensities of the immunoblot analysis and the DNA gels of RT-PCRs, the Fiji (imageJ, NIH) program was used. Statistical Analysis were performed using R. Excel was used to generate graphs visualizing R-SNARE expression or the RT-PCR analysis and the seaview software for the phylogenetic analysis of R-SNAREs. The Mega software was used to align and generate the phylogenetic tree for SEC1 proteins.

7.1.1 Molecular Biology

* For primer sequences, see table in Chapter 8.3

*RT-PCR analysis**

Seedlings were grown on MS plates for 7 days until harvest and immediate transfer into nitrogen (N_2). Plant material was ground, total RNA extracted using Trizol reagent (1ml/g plant material, TRI Reagent®, Sigma Aldrich) and transcribed into cDNA using RevertAid H Minus Reverse Transcriptase (Thermo Fischer Scientific, USA), following the manufacturer

instructions. PCRs in chapter 5 were performed using following primers: s1b-RT-ss, s1b-RT-as for *SEC1B*; keu-ss, keu-as for *KEULE*; s1a-RT-ss, s1a-RT-as for *SEC1A* and act-ss, act-as for *Actin* transcripts. PCRs for the analysis of the *vamp724* mutant transcript to generate Figure 22 in chapter 6 included primers: v724-RT-ss, v724-RT-as for *VAMP724*, v721-RT-ss-B, v721-RT-as-AB for *VAMP721*; v722-RT-ss-B, v722RT-ss-B for *VAMP722* and for RT-PCR analysis of the amiRNA displayed in Figure24 of chapter 6, primers: v724-RT-ss, v724-RT-as for *VAMP724;* v721-RT-ss-A, v721-RT-as-AB, for *VAMP721*; and v722-RT-ss-B, v722-RT-as-B for *VAMP722* were used.

*Molecular cloning**

For Chapter4: For generating *pMDC7::GFP-SNAP33, GFP-SNAP33* was amplified with GFP-AttB1-5 and SNAP33-AttB2-3 primers from *35S::GFP-SNAP33* (Park et al. 2012). According to the manufacturer's instruction (Invitrogen, Molecular Probes), the PCR product was cloned into a modified β-estradiol inducible *pMDC7* vector (Zuo et al. 2000), in which *Ubiquitin 10* promoter replaced the original promoter (pMDC7_EST; kindly provided by Niko Geldner, Univ. Lausanne). For generating *pMDC7::YFP-NPSN11*, *YFP-NPSN11* was amplified by PCR with YFP-AttB1-5 and NPSN11-AttB2-3 primers from *KN::YFP-NPSN11* (El Kasmi and Krause et al. 2013) and further cloned into the same *pMDC7* vector as described above. For generating *pKNOLLE::mRFP-PEP12*, *PEP12* coding sequence was amplified by PCR with PEP12-XbaI-5 and PEP12-EcoRI-3 primers. The PCR products were digested with *Xba*I and *Eco*RI (Thermo Fischer Scientific) and cloned in-frame downstream of *mRFP* in the *KNOLLE* expression cassette (Muller et al. 2003).

For Chapter 5: *SEC1B* was amplified by PCR from cDNA derived from Col-0 seedlings, using sec1b-5'-AvrII and sec1b-3'-NotI. The PCR product was digested with AvrII and NotI (Thermo Fischer Scientific, USA), whereas pBLUE-SK+_6xHA was digested with XbaI and NotI. The fragmented was ligated in-frame, downstream of 6xHA, resulting in *pBLUE-SK+_6xHA-SEC1B*. Cloning of *SEC1A*, followed a similar procedure, using primers sec1a-5'-AvrII and sec1a-3'-NotI. For generating *pKN::mRFP-SEC1B,* the *SEC1B* CDS was amplified by PCR from *pBLUE-SK+_6xHA-SEC1B* using primers sec1b-5'-SmaI and sec1b-3'-EcorI. The PCR product was digested with XmaI and EcoRI (Thermo Fischer Scientific, USA) and cloned in-frame downstream of *mRFP* in the *KNOLLE* expression cassette (Muller et al. 2003). SEC1a was amplified from *pBLUE-SK+_6xHA-SEC1A* by PCR with primers sec1a-5'SmaI and sec1a-3'-XbaI. The PCR product was digested with XmaI and XbaI, and cloned into *pKN::mRFP-SEC1B* plasmid that was digested with XmaI and AvrII. For generating *pMDC7::GFP-SEC1B*, *GFP-SEC1B* was amplified using GFP-AttB1-5 and pSK-3'-AttBI primers and the PCR product

cloned into pMDC7_EST (see above) according to the manufacturer's instruction for gateway cloning (Invitrogen, Molecular Probes).

For generating the constitutive open form of SYP132, two fragments were amplified including the mutation sites, using primers containing respective point mutations. One PCR was performed using Primers s132-5'-SmaI and s132op-as amplifying the N-terminal part, another with s132-3'-EcoRI and s132op-ss amplifying the C-terminal part. On these templates, a subsequent PCR was performed, amplifying the complete CDS of *SYP132 open*, using the primers s132-5'-SmaI and s132-3'-EcoRI. The product was digested with SmaI and EcoRI and cloned in-frame downstream of MYC into the KN cassette (Reichardt et al. 2011). From there it was amplified by PCR depleting the C-terminal membrane anchor using primers s132-5'-EcoRI and s132-dTM-3'-SalI. The PCR product was digested with EcoRI and SalI and sub-cloned into the pJG4-5 vector, which was digested with EcoRI and XhoI. To generate the SM constructs used for the yeast experiments, SEC1B was amplified from the plasmid containing *pKN::RFP-SEC1B* with primers sec1b-5'-EcoRI and sec1b-3'-NotI, digested with EcoRI and NotI and cloned in-frame downstream of *lexA* into the vector pEG202.

For **Chapter 6**: An artificial microRNA (amiRNA) against *VAMP721, VAMP722* and *VAMP724,* was designed and selected according to information provided from the *WMD3* webtool and personal communication with Dr. R. Schwab. The sequence of the artificial microRNA was chosen to target all three genes with the lowest likelihood for off-targets (wmd3.weigelworld.org/cgi-bin/webapp.cgi). Primers were designed harbouring respective amiRNA or the corresponding amiRNA* sequence, together with a partial sequence of the miR319a backbone. In a first amplification step on the plasmid pRS300 template, which harbours the miR319a backbone, three fragments were amplified: (i) the 5' region of the backbone, including the amiRNA* sequence, using miR319a_bb_ss and amiR*_triple_as, (ii) the middle region of the miR319a backbone, introducing the amiRNA* at the 5' end and the amiRNA at the 3' end, using amiR*_triple_ss and amiR_triple_as, and (iii) the 3' region of the miR319a backbone including the amiRNA at the 5' end, using amiR_triple_ss and miR319a_bb_as. In a subsequent PCR reaction, these three fragments were combined using primers miR319a_bb_ss and miR319a_bb_as. The PCR product was digested with EcoRI and BamHI and cloned under the control of the UAS-inducible promoter into the pGIIB_UAS plasmid.

Yeast Analysis

The yeast strain EGY48 was transformed with three plasmids using a polyethylene glycol (PEG) transformation method (33.3% [w/v] PEG3500,100 mM LiAc, 0.3 mg/ml ssDNA). These plasmids were the lacZ reporter pSH18-34, pEG202 carrying the SM protein *KEULE*, (Park et

al. 2012), or *SEC1B* and pJG4-5 carrying truncated SNARE protein inserts that lack C-terminal the transmembrane domain, including *PEP12*, *KNOLLE*, *KNOLLE open*, *SYP132* (Park et al. 2012) and *SYP132 open*. Quantitative β-galactosidase analysis was performed as follows. In brief, cell mass was suspended in reaction solution (Buffer H [100 mM HEPES pH 7, 150 mM NaCl, 2 mM MgCl2, 1% [w/v] BSA, 0.008% [w/v] SDS) followed by addition of ortho-nitrophenyl-β -galactoside (ONPG, 4 mg/ml in buffer H, Sigma-Aldrich). The reaction was stopped by addition of 0,32 M NA2CO3 and OD was measured at 420 nm. The Miller Unit of each sample was calculated [1,000 * OD420/ culture volume/ time / OD600] (Miller, 1972). Each measurement was done with eight independent colonies and repeated three times.

Co-immunoprecipitation and immunoblot analysis

Co-immunoprecipitation was slightly modified from a published protocol (Park et al. 2012). In brief, 1-2 g of seedlings were frozen in liquid nitrogen (N_2) immediately after chemical treatment. The seedlings were thoroughly ground and the powder suspended in ice-cold buffer (50 mM Tris pH 7.5, 150 mM NaCl, 1 mM EDTA, 0.5% Triton X-100) supplemented with EDTA-free complete protease inhibitors cocktail (Roche Diagnostics). Cleared protein lysate was incubated with anti-GFP beads (GFP-Trap®, Chromotek) [**Chapter 4**; incubation time, 2h; **Chs. 5,6;** 3h], anti-HA beads (Sigma-Aldrich) [**Ch.5**, 3hr], or anti-Myc beads (Myc-Trap®, Chromotek) [**Ch.6**; 3h] in the cold room with mild rotation. The beads were washed six times with ice-cold buffer (50 mM Tris pH 7.5, 150 mM NaCl, 1 mM EDTA, 0.2% Triton X-100) supplemented with EDTA-free complete protease inhibitors cocktail and resuspended with 2x Laemmli buffer.

For immunoblot analysis, primary antisera anti-GFP (1:1000, mouse, Roche), anti-KNOLLE (KN) (1:6000, rabbit) (Lauber et al. 1997), anti-SYP132 (1:3,000, rabbit) [Schulze-Lefer lab, MPI Köln], anti-VAMP721/VAMP722 (V721/V722) (1:5000, rabbit) (Kwon et al. 2008b), anti-SNAP33 (1:5000, rabbit) (Heese et al. 2001), anti-SYP71 (1:4000, rabbit) (El Kasmi and Krause et al. 2013), anti-RFP (1:700, rat, Chromotek), anti-γCOP (aka SEC21) (1:5000, rabbit, Agrisera, Vännäs, SWEDEN), anti-LexA (1:1,000, mouse, Santa Cruz Biotechnologies) and POD-conjugated secondary antibodies (1:5000 for anti-rabbit-POD, 1:2000 for anti-rat-POD, Sigma-Aldrich) or POD-conjugated anti-HA antibodies (1:1,000, Roche Diagnostics) were used. Membranes were developed using a chemiluminescence detection system (Fusion Fx7 Imager, PEQlab, Germany).

Immunofluorescence analysis

Seedlings were grown on MS plates (see above) for 5-6 days, chemically treated in respective experiments (**Ch.4**) and immediately fixed in 4% (w/v) paraformaldehyde for 1 hr and stored

at -20°C until use. For immunostaining, primary antisera anti-KN (1:4000, rabbit, **Chs.4-6**) (Lauber et al. 1997), anti-γCOP (1:2000, rabbit, Agrisera, **Ch.4**), anti-alpha-tubulin (1:600, rat, Abcam Cambridge, UK, **Ch.1**), anti-HA (1:1000, mouse, BAbCO, Richmond, CA, **Ch.2**), anti-Myc (1:600, mouse, Santa Cruz Biotechnologies, **Ch.3**) and secondary antibodies anti-rabbit Cy3™ (1:600, Dianova, Hamburg, Germany **Ch.4,6**), anti-rat FITC (1:600, Dianova, **Ch.4**), anti-rabbit Alexa488 (1:600, Invitrogen, **Ch.5**), anti-mouse Cy3 (1:600, Dianova, **Ch.5**) and anti-mouse Alexa488 (1:600, Invitrogen, **Ch.6**) were applied. Nuclei were stained with 1 µg/ml DAPI (1 mg/ml stock solution in H2O). Samples were prepared manually or with an immunohistochemistry system (InsituPro VSi, Intavis, Germany). Fluorescent images were taken using a confocal laser scanning microscope (Leica SP8 or Zeiss LSM880).

8. Appendix

8.1 Oligonucleotide and primer sequences

Nr.	Name of primer	Sequence 5'-3'	Application
1	mRFP-700	CAAGACCGACATCAAGCTGGA	genotyping
2	sec1b-700-as	TCCATACACTAGCAGCAAGC	genotyping
3	sec1a-800-as	CGTGTATGATAGGAGCGATC	genotyping
4	Myc-5'	AAAAAGCAGGCTGTATGGAGCAAAAGCTTATTTCTGAGG	genotyping
5	KN-3'-EcoRI	GAATTCTCAAGAAGAGCTGAAACTGGTAAT	genotyping
6	s132-op-ss	GAAGATACTGCTGCTGAATTGATTGAAACTGGAAACAGCG	cloning, genotyping
7	GK-LB-8409	ATATTGACCATCATACTCATTGC	genotyping, sequencing
8	601G09 LP	GTTGTGCTCTTTTTGCACTCC	genotyping
9	601G09 RP	CACACACGAGGTGACATTTTG	genotyping
10	KN-5'UTR-ss	CTTTACTTCACACTACTCTCTCACTTTCTGGGCA	genotyping
11	V724-3'-SmaI	CATCCCGGGTCAATCCGTGCAATTAAATC	genotyping
12	v721-ss	GACGGTCGATTGGATCGGAGATTTAAGG	genotyping
13	v721-as	CCATTTTCTGCTAAGCCACATCTTTCTTCTCATCTGCG	genotyping
14	SALK-LBA1	TGGTTCACGTAGTGGGCCATCG	genotyping
15	v722-3 ss	CTTATCAGCGATATATTGATGAATC	genotyping
16	v722-3-UTR-as	GCCAAGAACAAGTATCGTCC	genotyping
17	SAIL_RP	CTTGAAATCAGCTTTCACACGCTCC	genotyping
18	V724-ss	CGTCTATTGCTGCTCAGTGTCTCCAGAAGC	genotyping
19	LB3-SAIL	TAGCATCTGAATTTCATAACCAATCTCGATACAC	genotyping
20	s1b-RT-ss	GCCAACCTTTTATTCTGGCTC	RT-PCR
21	s1b-RT-as	GATTCTCAAATGACAATATCATCAAGTGAGATCTCCTC	RT-PCR
22	s1a-RT-ss	AGAAAGCTGGGTCGAATTCCGTGAAAGGCGATCTATC	RT-PCR
23	s1a-RT-as	AACTCGAGTCACCAGTATTGTGGTTTGAAGGG	RT-PCR
24	act-ss	ATTCAGATGCCCAGAAGTCTT	RT-PCR
25	act-as	GCAAGTGCTGTGATTTCTTTG	RT-PCR
26	keu-ss	AAAAAAGGATCCAAATGTCGTACTCTGACTCC	RT-PCR
27	keu-as	TTTTTTGTCGACTCATATTTGGAGATCGTCTAA	RT-PCR
28	v721-RT-ss-A	GATCTGTAGTTTTTTTCCGCGACCG	RT-PCR

29	v721-RT-ss-B	GGTCTTGGAAACTAAGCTTGCTAAGGTGAAGGCG	RT-PCR
30	v721-RT-as-AB	CCATTTTCTGCTAAGCCACATCTTTCTTCTCATCTGCG	RT-PCR
31	v722-RT-ss-A	CACCGTATTCTCTTTTAGTCCTCGATTCTCTAC	RT-PCR
32	v722-RT-as-A	GCCAAGAACAAGTATCGTCC	RT-PCR
33	v722-RT-ss-B	GATTCTAGAATGGCGCAACAATCGTTGAT	RT-PCR
34	v722-RT-as-B	CGAGAATTCTTATTTACCGCAGTTGAATC	RT-PCR
35	v724-RT-ss	CTCTTTCTCTCTGTCTGAGCCAACTCG	RT-PCR
36	v724-RT-as	GTAGTAGCAAGATCCCAAGAACCACCAG	RT-PCR
37	GFP-AttB1-5	AAAAAGCAGGCTGTATGAGTAAAGGAGAAGAACTTTTCAC	cloning
38	SNAP33_AttB2-3	AGAAAGCTGGGTCCTATTTGCCCAACAAACGTCGGCCTCGTTGGTTTGATTG	cloning
39	YFP-AttB1-5	AAAAAGCAGGCTATATGGTGAGCAAGGGCG	cloning
40	NPSN11-AttB2-3	AGAAAGCTGGGTCTCAGTAATGGTTCCAGAGCAGAC	cloning
41	PEP12-XbaI-5	AAAAAATCTAGAATGAGTTTCCAAGATCTC	cloning
42	PEP12-EcoRI-3	TTTTTTGAATTCTTAGACCAAGACAACGAT	cloning
43	sec1b-5'-AvrII	AAACCTAGGATGTCCTTCTCCGATTCTGG	cloning
44	sec1b-3'-NotI	AAGCGGCCGCTCAAATGACAATATCATCAAGTGAG	cloning
45	sec1a-5'AvrII	AAACCTAGGATGTCGTTCTCCGATTCAGAGTC	cloning
46	sec1a-3'-NotI	AAGCGGCCGCTCACCAGTATTGTGGTTTGAAGGG	cloning
47	sec1b-5'-SmaI	AACCCGGGATGTCCTTCTCCGATTCTGG	cloning
48	sec1b-3'-EcoRI	AAGAATTCTCAAATGACAATATCATCAAGTGAGATCTC	cloning
49	sec1a-5'-SmaI	AACCCGGGATGTCCTTCTCCGATTCTGG	cloning
50	sec1a-3'-XbaI	AATCTAGATCACCAGTATTGTGGTTTGAAGG	cloning
51	pSK-3'-AttBI	AGAAAGCTGGGTCTCCACCGCGGTGGC	cloning
52	s132-5'-SmaI	AAACCCGGGATGAACGATCTTCTGAAGGGTTC	cloning
53	s132-op-as	CAATTCAgCAgcAGTATCTTCATCCGCCC	cloning
54	s132-3'-EcoRI	AAAGAATTCTCAAGCACTCTTGTTTTTCCAA	cloning
55	s132-5'-EcoRI	AAAAAAGAATTCATGAACGATCTTCTGAAGGGT	cloning
56	s132-dTM-3'-SalI	AAGTCGACCTACATCCATTTTCTTGAGTTCTTCTGC	cloning
57	sec1b-5'-EcoRI	aaGAATTCATGTCCTTCTCCGATTCTGGATC	cloning
58	sec1b-3'NcoI	AACCATGGCATGTCCATTTTCGCGTGTTCTTCTGG	cloning
59	sec1a-5'-NcoI	AACCATGGATGTCGTTCTCCGATTCAGAGTC	cloning
60	sec1a-3'-XhoI	AACTCGAGTCACCAGTATTGTGGTTTGAAGGG	cloning
61	sec1a-5'-NcoI	AACCATGGATGTCGTTCTCCGATTCAGAGTC	cloning
62	sec1a-3'-XhoI	AACTCGAGTCACCAGTATTGTGGTTTGAAGGG	cloning
63	amiR_triple_ss	GATCTGGAGGCACTGACCAGCGATCTCTCTTTTGTATTCC	cloning
64	amiR_triple_as	GATCGCTGGTCAGTGCCTCCAGATCAAAGAGAATCAATGA	cloning
65	amiR*_triple_ss	GATCACTGGTCAGTGGCTCCAGTTCACAGGTCGTGATATG	cloning
66	amiR*_triple_as	GAACTGGAGCCACTGACCAGTGATCTACATATATATTCCT	cloning
67	amiR319a_bb_ss	AAACCTAGGGTCGACGGTATCGATAAGCTTG	cloning
68	amiR319a_bb_as	AAACCTAGGGAACAAAAGCTGGAGCTCCAC	cloning

8.2 Construct list

Nr.	Construct Name	Binary vector	Remarks	Resistance in bacteria	Resistance in plants
1	pDONR221_GFP-SNAP33	pDONR221 (entry vector)	GFP5-SNAP33 (CDS) amplified by PCR from 35S::GFP5-SNAP33 and inserted via BP reaction	Kanamycin	-
2	pMDC7_EST::GFP-SNAP33	pMDC7 (estradiol)	GFP5-SNAP33 (CDS) from pDONR221 (plasmid nr.1) via LR reaction into pMDC7 (estradiol inducible promoter)	Spectinomycin	Hygromycin
3	pDONR221_YFP-SNAP33	pDONR221 (entry vector)	vYFP-NPSN11 (CDS) amplified by PCR from pKN::vYFP-NPSN11 and inserted via BP reaction	Kanamycin	-
4	pMDC7_EST::YFP-NPSN11	pMDC7 (estradiol)	vYFP-NPSN22 (CDS) from pDONR221 (plasmid nr.3) via LR reaction into pMDC7 (estradiol inducible promoter)	Spectinomycin	Hygromycin
5	pKNOLLE::mRFP-PEP12	pGIIB (KNOLLE cassette)	PEP12 (CDS) via XbaI/EcoRI into pKNOLLE::mRFP (cloned by Dr. M. Park)	Kanamycin	Basta
6	pBLUE-SK+_6xHA-SEC1B	pBLUE-SK+_6xHA	SEC1B (CDS) amplified by PCR from plant cDNA and cloned AvrII/NotI into pBLUE-SK+_6xHA (XbaI/NotI) (provided by Dr. T. Krupnova)	Ampicillin	-
7	pKNOLLE::mRFP-SEC1B	pGIIB (KNOLLE cassette)	SEC1B (CDS) via *XmaI/EcorI* from construct Nr.6 into pKNOLLE::mRFP	Kanamycin	Basta
8	pBLUE-SK+_6xHA-SEC1A	pBLUE-SK+_6xHA	SEC1A (CDS) amplified by PCR from plant cDNA and cloned via AvrII/NotI into pBLUE-SK+_6xHA (XbaI/NotI)	Ampicillin	-
9	pKNOLLE::mRFP-SEC1A	pGIIB (KNOLLE cassette)	SEC1A (CDS) via *XmaI/XbaI* from construct Nr.8 into pKNOLLE::mRFP	Kanamycin	Basta
10	pDONR221_GFP-SEC1B	pDONR221 (entry vector)	GFP5-SEC1B (CDS) amplified by PCR from plasmid nr. 7 and inserted via BP reaction	Kanamycin	-
11	pMDC7_EST::GFP-SEC1B	pMDC7 (estradiol)	GFP5-SEC1B from pDONR221 (plasmid nr.10) via LR reaction into pMDC7 (estradiol inducible promoter)	Spectinomycin	Hygromycin
12	pKN::Myc-SYP132open	pGIIB (KNOLLE cassette)	SYP132 CDS (LER) mutated by PCR and SYP132 open cloned into pKN::MYC via *SmaI/EcoRI*	Kanamycin	Basta
13	pJG4-5_SYP132open	pJG4-5	SYP132 open (CDS) via *EcoRI/SalI* from construct Nr.12 into pJG4-5 (*EcoRI/XhoI*)	Ampicillin	-
14	pEG202-SEC1B	pEG202	SEC1B (CDS) amplified by PCR from plasmid nr.7 and cloned via *EcoRI/NotI*	Ampicillin	
15	pUAS::amiR_V721_V722_V724	pGIIB_UAS	amiRNA together with miR319a backbone amplified by PCR and cloned via *EcoRI/BamHI*	Kanamycin	Basta

8.3 Transgenic Lines:

Nr.	Transgenic Lines	Mutant background	Resistance
1	*pMDC7::GFP:SNAP33;*	*pGNL1::GNL1$^{BFA\text{-}sens}$ in gnl1*	Hygromycin
2	*pMDC7::GFP:SNAP33*	*big3*	Hygromycin
3	*pMDC7::YFP:NPSN11*	*pGNL1::GNL1$^{BFA\text{-}sens}$ in gnl1*	Hygromycin
4	*pMDC7::YFP:NPSN11*	*big3*	Hygromycin
5	*pMDC7::YFP:NPSN11; pKNOLLE::mRFP-PEP12*	*big3*	Hygromycin, Basta
6	*pKNOLLE::mRFP-SEC1B*	*keule*	Basta
7	*pKNOLLE::mRFP-SEC1A*	*keule*	Basta
8	*pMDC7_EST::GFP-SEC1B*		Hygromycin
9	*pKNOLLE::HA-KEULE*		Basta
10	*pKNOLLE::HA-KEULE; pKNOLLE::MYC-KNOLLE*		Basta
11	*pKNOLLE::HA-KEULE; pKNOLLE::MYC-SYP132*		Basta
12	*sec1b (GK_601G09)*		Sulfadiazine
13	*keule (mm125)*		-
14	*UAS::amiRNA_V721_V722_V724*		Basta
15	*RPS5a::GAL4*		Basta
16	*UAS:amiRNA_syp132, syp132*		Basta
17	*knolle (X37-2)*		-
18	*vamp721 (SALK_037273) vamp722 (SALK_119149)*		Kanamycin
19	*vamp724 (SAIL_569_E12)*		Basta
20	*pKNOLLE::Myc-VAMP724*		Basta
21	*pKNOLLE::Myc-VAMP721*		Basta
22	*pKNOLLE::YFP::VAMP723*		Basta

8.4 Other *Arabidopsis* R-SNAREs beside the VAMP72 subfamily

YKT6-like R-SNAREs are involved in post-Golgi trafficking towards the vacuole and the plasma membrane

Eukaryotic YKT6-like proteins act in multiple transport steps, including ER-Golgi, intra-Golgi, endosome-Golgi and vacuolar transport (Daste et al. 2015). In contrast to other R-SNAREs, they lack the C-terminal transmembrane domain but become anchored upon post-translational modifications during which lipid membrane moieties are attached. Interestingly, these lipid modifications serve as regulatory elements for YKT6-like proteins. Upon farnesylation the longin domain of YKT6 folds back on its SNARE domain, rendering the protein inactive. Upon YKT6 palmitoylation, it becomes attached to the target membrane, where it undergoes a conformational change to become activated for SNARE complex formation and membrane fusion. Thus, this reversible palmitoylation is a regulatory mechanism that allows YKT6 to cycle between an inactive state in the cytosol and an its active conformation at the target membrane (Wen et al. 2010). In *Arabidopsis*, there are two YKT6-like proteins, YKT61 is highly abundant on a transcriptional level, whereas YKT62 is barely expressed (bar.u.toronto.org (Winter et al. 2007), AtGenExpress-Visualization Tool (Schmid et al. 2005)). YKT61 and YKT62 can form SNARE complexes sufficient for vesicle fusion with TGN-localized Qa-SNARE SYP41, Qb-SNARE VTI12 and Qc-SNARE SYP61 during *in vitro* lipid mixing experiments (Chen et al. 2005). Members of the SYP4 Qa-SNARE family were shown to be involved in post-Golgi traffic towards the vacuole and the plasma membrane, which was shown by the mislocalization of markers of both pathways in *syp42 syp43* double mutant (Uemura et al. 2012). Furthermore, plants lacking either the SM protein VPS45 that regulate the SYP41- VTI12-SYP61 SNARE complex or the Qb-SNARE VTI12 showed overlapping defects in the vacuolar pathway, suggesting their activity in involvement in this trafficking pathway (Sanmartin et al. 2007, Zouhar et al. 2009, Uemura et al. 2012). From this data, it can be assumed that YKT6-like proteins in *Arabidopsis* are part of Sp4-containing SNARE complexes that involve Qb-SNARE VTI12, Qc-SNARE SYP61 and act at the TGN to maintain post-Golgi traffic towards the vacuole and the plasma membrane.

SEC22-like R-SNAREs act at the ER-Golgi interface

SEC22-like proteins are present in all eukaryotes and serve a conserved R-SNARE function ER-Golgi trafficking pathways (Hong 2005). There is evidence for a further function in the establishment of non-fusogenic SNARE complexes to bridge membrane contact sites. Mammalian SEC22 was shown in complexes with plasma membrane Qa-SNARE Syntaxin1a that did not include other SNARE partners. Unlike common SNARE complexes, this dual

complex did not promote fusion, but remained in a *trans* conformation between ER and plasma membrane. This contact site was proposed to allow the rapid exchange of membrane material and signals and circumvent the time-consuming process of vesicle trafficking (Petkovic et al. 2014, Daste et al. 2015). In *Arabidopsis* SEC22 is expressed throughout plant development (Figure 20). It was localized to ER and Golgi membranes and in *sec22* mutants a distorted Golgi morphology was observed, suggesting its involvement in anterograde or retrograde ER-Golgi trafficking pathways (Bubeck et al. 2008, El-Kasmi et al. 2011).

VAMP7-like R-SNAREs

The third group of longin R-SNAREs shares homology to mammalian VAMP7 and diverged into the VAMP71 and the VAMP72 subfamilies before the evolution of Chloro- and Charophyta from ancestral algae (Sanderfoot 2007). The VAMP71 clade contains four members in *Arabidopsis*, VAMP711-VAMP714 (Figure 19). VAMP714 localizes to the Golgi apparatus in *Arabidopsis* protoplasts, whereas the other members of this family VAMP711, VAMP712 and VAMP713 were detected at the tonoplast (Uemura et al. 2004). Little data is available about VAMP714. VAMP711-VAMP713 were suggested to promote homotypic vacuolar fusion, based on their homology to their yeast orthologs (Ebine et al. 2008). Consistently, *Araibdopsi*s VAMP711-VAMP713 co-accumulated together with Qa-SNARE SYP22, Qb-SNARE VTI11 and Qc-SNARE SYP51 in *Arabidopsis* vacuoles, suggesting their assembly in SNARE complexes, which could promote fusion at vacuolar membranes (Carter et al. 2004). SNARE complex formation was confirmed for VAMP713 in complexes with SYP22, VTI11 and members of the SYP5 family (Ebine et al. 2011). The downregulation of *VAMP711-VAMP713* in seedlings resulted in their increased susceptibility to salt stress. Under these conditions, they accumulated ROS-containg vesicles inside the cytosol, which fused in wild-type with the vacuole, indicating impaired vesicle fusion at the tonoplast and suggesting a role of the R-SNAREs VAMP711-VAMP713 in the vacuolar trafficking pathway (Leshem et al. 2006, Leshem et al. 2010).

8.5 Protein sequence alignment of SEC1-related SM proteins in Arabidopsis

```
SEC1A      MSFSDSESSSHGGGGGDYKFFRQISRDRLLHEMLGSTKTGDSK-AWKILIMDRVTVKVMS
KEULE      MSYSDSDSSSHG---GEYKNFRQITRERLLYEMLRSAKTGSSKSTWKVLIMDKLTVKIMS
S1B        MSFSDSGSSSYG---GEYKNFRQITRERLLCEMLRPERNGSSKLTWKVLVMDKFTVKIMS
           **:*** ***:*   *:** ****:*:*** ***   :.*.** :**:*:**:.***:**

SEC1A      QSCKMADITDQGISLVEELFKRREPMPGMDAIYFIQPSKENIVMFLSDMSGREPLYRKAF
KEULE      YACKMADITQEGVSLVEDIFRRRQPLPSMDAIYFIQPTKENVIMFLSDMSGKSPLYKKAF
S1B        SACKMSEITQEGISLVEVITKHRQPMTAMEVIYFIQPTEENVTAFLSDMTGKSPLYKKAF
            :***::**::*:**** : ::*:*: .*:.******::**:  *****:*:.***:***

SEC1A      IFFSSTIPKELVNHIKSDSSVLPRIGALREMNMEYFPIDNQGFLTIDHEQALETLYAEDAE
KEULE      VFFSSPVSKELVGHIKKDSSVLPRIGALREMNLEFFAIDSQGFITDHERALEDLFGDE-E
S1B        VFFSSPVSRSLVNLIKKDMRAMKRIGGLKEMNLEYISMDIQGFVINNENALEELFCDD-E
           :**** : :.**. **.*  .: ***.*:***:*:: :* ***:*::*.*** *: :: *

SEC1A      NSRHFHICLNIMATRIATVFASLKELPFVRYRAAKS------TASRDLVPSKLAAAIWDC
KEULE      TSRKGDACLNVMASRIATVFASLREFPAVRYRAAKSLDASTMTTLRDLIPTKLAAGIWNC
S1B        NHQRADACLNVVAKRIATVLASLKEYPFVRYRGAKALDATTMTTYRELIPTKLAASVWNC
           . :: . ***::*.*****:***:* * ****.**:      *: *:*:*:****.:*:*

SEC1A      ISKYK-AIPNFPQTETCELLIVDRSVDQIAPIIHEWTYDAMCHDLLDMEGNKHVIEVPSK
KEULE      LAKHKQSIENFPQTETCELLILDRSIDQIAPVIHEWTYDAMCHDLLNMEGNKYVHVIPSK
S1B        LARYKQTIEDFPQTETCELLILDRSIDQIAPLIHEWTYDAMCHDLLNMEGNKYTHEVPSK
           :::::* :* :***********:***:*****:**************:*****:.  :***

SEC1A      TGGPPEKKEIVLEDHDPVWLELRHTHIADASERLHEKMTNFASKNKAAQMR--SRDGSEL
KEULE      SGGQPEKKDVLLEEHDPIWLELRHAHIADASERLHDKMTNFLSKNKAAQLQGK-RDGAEL
S1B        TGDKPEKKEVLLDEEDSIWVELRDAHIADASERLHEKMTNFVSKNKAAQLKHSSKDFGDL
           :*. ****:::*::.* :*:***.:**********:***** *******::   :* .:*

SEC1A      STRDLQKIVQALPQYGEQVDKLSTHVELAGKINRIIRDTGLRDLGQLEQDLVFGDAGAKD
KEULE      STRDLQKMVQALPQYSEQIDKLSLHVEIARKLNDLIREQGLRELGQLEQDLVFGDAGMKD
S1B        SSKDLQKMVHALPQYSEQIDKLSLHVEIARTINRTIMEQGLRDLGQLEQDLVFGDAGRKD
           *::****:*:*****.**:**** ***:* .:*  * : ***:************** **

SEC1A      VINFLRTNQDTNPENKLRLLMIYATVYPEKFEGDKGVKLMQLARLSPVDMKVISNMQLIA
KEULE      VIKYLSTQEEASREGKLRLLMILATIYPEKFEGEKGQNLMKLAKLSSDDMTAVNNMSLLG
S1B        VIKFLSTNHIISHESKLRLIMIVAAIYPKKFEGEKGRKMMELAKLSGDDVVAVNNMRLLG
           **::* *:.  . *.****:** *::**:****:** ::*:**:**  *: .:.** *:.

SEC1A      GSP--ENKAKSGSFSLKFDAGKTKQANRKDRSGEEETWQLFRFYPMIEELLEKLVKGDLS
KEULE      SAV-DAKKNTPGGFTLKFDLHKKKRAVRKERQ-EEAAWQLSRFYPMIEELIEKLSKGELP
S1B        PVHTECKKSTTGSFPLKFDVLKTKRAARRDRVGETQTWQLSRFYPIVEELVEKLSKGHLP
                 :* . *.* ****  *.*:* *::*  *  :*** ****::***:*** **.*

SEC1A      KSDYLCMNQSSHKEESEARTGSVRKSSAPTAVPERKATPHSMRSRRTATWARPHSSDDGY
KEULE      KEDFPCMNDPSPSFHGSTSL-------SSAASSSQGQAAQSMRSRRTPTWAKPRGSDDGY
S1B        KQDYPCMNEPKPTFYSGSLS-------PS-------ASPVLPHSRRTPTWARRHLSDDGY
           *.*: ***: . .  . :                  :    :**** ***: : *****

SEC1A      SSDSVLKSASTEFKKLGQRIFVFIIGGATRSELRVCHKLTSSLRREVVLGSTSFDDPPQY
KEULE      SSDSVLRHASSDFRKMGQRIFVFIVGGATRSELKVCHKLSTKLKREVILGSTSLDDPPQF
S1B        FSDSVLGRASSGFKRKGQRIFVFIVGGATRSELRVCHKLTEKLDREVILGSSSFLDPLTF
            *****  **: *:: ********:********:*****: .* ***:***:*: **  :

SEC1A      ITKLKLLSEKDIQGAPAQPFKPQYW
KEULE      ITKLKLLTANDDLSLDDLQI-----
S1B        LTKMKQLNEEEEISLDDIVI-----
           :**:* *. ::  .     :
```

8.6 Protein sequence of Arabidopsis R-SNAREs

```
VAMP727     ------------------------------------------------------------
VAMP724     ------------------------------------------------------------
VAMP723     ------------------------------------------------------------
VAMP721     ------------------------------------------------------------
VAMP722     ------------------------------------------------------------
VAMP725     MDRSVVPISLAPFQFLLVFWIFLISVHTNPNKQQKTVVSLSLWWNSKNRIRGCVWFFFLL
VAMP726     ------------------------------------------------------------
VAMP714     ------------------------------------------------------------
VAMP713     ------------------------------------------------------------
VAMP711     ------------------------------------------------------------
VAMP712     ------------------------------------------------------------
SEC22       ------------------------------------------------------------
YKT61       ------------------------------------------------------------
YKT62       ------------------------------------------------------------

VAMP727     -----MSQKGLI----YSFVAKGTVVLAEHTP----------YSGNFSTIAV----Q---
VAMP724     -----MGQESFI----YSFVARGTMILAEYTE----------FTGNFPSIAA----Q---
VAMP723     -----MAQQSLF----YSFIARGTVILVEFTD----------FKGNFTSVAA----Q---
VAMP721     -----MAQQSLI----YSFVARGTVILVEFTD----------FKGNFTSIAA----Q---
VAMP722     -----MAQQSLI----YSFVARGTVILVEFTD----------FKGNFTSIAA----Q---
VAMP725     RVTRTMGQQNLI----YSFVARGTVILVEYTE----------FKGNFTAVAA----Q---
VAMP726     -----MGQQSLI----YSFVARGTVILAEYTE----------FKGNFTSVAA----Q---
VAMP714     --------MAIV----YAVVARGTVVLAEFSA----------VTGNTGAVVR----R---
VAMP713     --------MAII----FALVARGTVVLSEFSA----------TSTNASSISK----Q---
VAMP711     --------MAIL----YALVARGTVVLSEFTA----------TSTNASTIAK----Q---
VAMP712     --------MSIL----YALVARGTVVLAELST----------TSTNASTIAK----Q---
SEC22       -----MVKMTLI------ARVTDGLPLAEGLDDGRDLPDSDMYKQQVKALFK----NLSR
YKT61       ------MKITALLVLKCAPEASDPVILS-NASDVSHFGYF--QRSSVKEFVVFVGRTVAS
YKT62       ------MKITALLVLKCDPETREPVILA-NVSDLSQFGKFSFYRSNFEEFIVFIARTVAR
                        .       .   : *                   .   .

VAMP727     ------------------CLQKLPTN--SSKYTYSCDGHTFNFLVDNGF--------VFL
VAMP724     ------------------CLQKLPSS-SNSKFTYNCDHHTFNFLVEDGY--------AYC
VAMP723     ------------------YLENLPSS--NNKFTYNCDGHTFNDLVENGF--------TYC
VAMP721     ------------------CLQKLPSS--NNKFTYNCDGHTFNYLVEDGF--------TYC
VAMP722     ------------------CLQKLPSS--NNKFTYNCDGHTFNYLVENGFSESKYCSISYC
VAMP725     ------------------CLQKLPSS--NNKFTYNCDGHTFNYLVENGF--------TYC
VAMP726     ------------------CLQKLPSS--NNKFTYNCDGHTFNYLADNGF--------TYC
VAMP714     ------------------ILEKLSPEISDERLCFSQDRYIFHILRSDGL--------TFL
VAMP713     ------------------ILEKLPGNDSDSHMSYSQDRYIFHVKRTDGL--------TVL
VAMP711     ------------------ILEKVPGD-NDSNVSYSQDRYVFHVKRTDGL--------TVL
VAMP712     ------------------ILEKIPGN-GDSHVSYSQDRYVFHVKRTDGL--------TVL
SEC22       GQNDASRMSVETG---PY----------------------VFHYIIEGRV--------CYL
YKT61       RTPPSQRQSVQHEGCAPFLILDLPGL--CPGFNFLRFYLIVHAYNRNGL--------CAV
YKT62       RTPPGQRQSVKHEEY----------------------KVHAYNINGL--------CAV
                                                     .
```

(continued)

```
VAMP727     VVADESTGRSVPFVFLERVKEDFKKRYEASIKNDERHPLADEDEDDDLFGDRFSVAYNLD
VAMP724     VVAKDSLSKQISIAFLERVKADFKKRYGGGKAST------------------AIAKSLN
VAMP723     VVAVDSAGREIPMAFLERVKEDFYKRYGGEKAAT------------------DQANSLN
VAMP721     VVAVDSAGRQIPMSFLERVKEDFNKRYGGGKAAT------------------AQANSLN
VAMP722     VVAVDSAGRQIPMAFLERVKEDFNKRYGGGKAAT------------------AQANSLN
VAMP725     VVAVESVGRQIPMAFLERVKEDFNKRYGGGKATT------------------AQANSLN
VAMP726     VVVIESAGRQIPMAFLERVKEDFNKRYGGGKAST------------------AKANSLN
VAMP714     CMANDTFGRRVPFSYLEEIHMRFMKNYGKVAHN--------------------APAYAMN
VAMP713     CMADETAGRNIPFAFLDDIHQRFVKTYGRAIHS--------------------AQAYSMN
VAMP711     CMAEETAGRRIPFAFLEDIHQRFVRTYGRAVHT--------------------ALAYAMN
VAMP712     CMADEDAGRRIPFSFLEDIHQRFVRTYGRAIHS--------------------AQAYAMN
SEC22       TMCDRSYPKKLAFQYLEDLKNEFERVNGPNI----ETA---------------ARPYAFI
YKT61       GFMDDHYPVRSAFSLLNQVLDEYQKSFGESWRSAKEDS---------------NQPWPYL
YKT62       GFMDDHYPVRSAFSLLNQVLDVYQKDYGDTWRF--ENS---------------SQPWPYL
             .         :  *: :   : :

VAMP727     REFGPILKEHMQYCMSHPEEMSKLSKLKAQITEVKGIMMDNIEKVLDRGEKIELLVDKTE
VAMP724     KEFGPVMKEHMNYIVDHAEEIEKLIKVKAQVSEVKSIMLENIDKAIDRGENLTVLTDKTE
VAMP723     KEFGSNLKEHMQYCMDHPDEISNLAKAKAQVSEVKSLMMENIEKVLARGVICEMLGS---
VAMP721     KEFGSKLKEHMQYCMDHPDEISKLAKVKAQVSEVKGVMMENIEKVLDRGEKIELLVDKTE
VAMP722     KEFGSKLKEHMQYCMDHPDEISKLAKVKAQVSEVKGVMMENIEKVLDRGEKIELLVDKTE
VAMP725     REFGSKLKEHMQYCVDHPDEISKLAKVKAQVTEVKGVMMENIEKVLDRGEKIELLVDKTE
VAMP726     KEFGSKLKEHMQYCADHPEEISKLSKVKAQVTEVKGVMMENIEKVLDRGEKIELLVDKTE
VAMP714     DEFSRVLHQQMEFFSSNPS-VDTLNRVRGEVSEIRSVMVENIEKIMERGDRIELLVDKTA
VAMP713     DEFSRVLSQQMEFYSNDPN-ADRMSRIKGEMSQVRNVMIENIDKVLDRGERLELLVDKTE
VAMP711     EEFSRVLSQQIDYYSNDPN-ADRINRIKGEMNQVRGVMIENIDKVLDRGERLELLVDKTA
VAMP712     DEFSRVLNQQIEYYSNDPN-ADTISRIKGEMNQVRDVMIENIDNILDRGERLELLVDKTA
SEC22       -KFDTFIQKTKKL-YQDTRTQRNIAKLNDELYEVHQIMTRNVQEVLGVGEKLDQVSEMSS
YKT61       -T------EALNK-FQDPAEADKLLKIQRELDETKIILHKTIDSVLARGEKLDSLVEKSS
YKT62       -K------EASDK-FRDPAEADKLLKIQRELDETKIILHKTIDGVLARGEKLDSLVEKSS
                   :  .    .     : : . :: : : ::  .::  :  *    : .

VAMP727     NLQFQADSFQRQGRQLRRKMWLQSLQMKLMVAGAVFSFILIVWVVACGGFKCSS---
VAMP724     NLRSQAREYKKQGTQVRRKLWYQNMKIKLVVLGILLLLVLIIWISVCHGFNCTD---
VAMP723     -SESQPQAFYIKRTQMKRKKWFQNMKIKLIVLAIIIALILIIIILSVCGGFNCGK---
VAMP721     NLRSQAQDFRTTGTQMRRKMWLQNMKIKLIVLAIIIALILIIIVLSVCHGFKC-----
VAMP722     NLRSQAQDFRTQGTQMRRKMWFQNMKIKLIVLAIIIALILIIIILSICGGFNCGK---
VAMP725     NLRSQAQDFRTQGTKIRRKMWFENMKIKLIVLGIIITLILIIIILSVCGGFKCT----
VAMP726     NLRSQAQDFRTQGTKMKRKLWFENMKIKLIVFGIIVALILIIIILSVCHGFKCT----
VAMP714     TMQDSSFHFRKQSKRLRRALWMKNAKLLVLLTCLIVFLLYIIIASFCGGITLPSCRS
VAMP713     NMQGNTFRFRKQARRYRTIMWWRNVKLTIALILVLALVVYIAMAFVCHGPSLPSCFK
VAMP711     NMQGNTFRFRKQARRFRSNVWWRNCKLTVLLILLLLVIIYIAVAFLCHGPTLPSCI-
VAMP712     NMQGNTFRFRKQTRRFNNTVWWRNCKLTLLLILVLLVIIYIGVAFACHGPTLPSCV-
SEC22       RLTSESRIYADKAKDLNRQALIRKWAPVAIVFGVVFLLFWVKNKLW-----------
YKT61       DLSMASQMFYKQAKKTNSCCTIL---------------------------------
YKT62       ELSLASKMFYKQAKKTNSCCTLL---------------------------------
                   :      .
```

9. References

Andreuzza, S., J. Li, A. E. Guitton, J. E. Faure, S. Casanova, J. S. Park, Y. Choi, Z. Chen and F. Berger (2010). "DNA LIGASE I exerts a maternal effect on seed development in Arabidopsis thaliana." Development **137**(1): 73-81.

Assaad, F. F., Y. Huet, U. Mayer and G. Jurgens (2001). "The cytokinesis gene KEULE encodes a Sec1 protein that binds the syntaxin KNOLLE." J Cell Biol **152**(3): 531-543.

Assaad, F. F., U. Mayer, G. Wanner and G. Jurgens (1996). "The KEULE gene is involved in cytokinesis in Arabidopsis." Mol Gen Genet **253**(3): 267-277.

Assaad, F. F., J. L. Qiu, H. Youngs, D. Ehrhardt, L. Zimmerli, M. Kalde, G. Wanner, S. C. Peck, H. Edwards, K. Ramonell, C. R. Somerville and H. Thordal-Christensen (2004). "The PEN1 syntaxin defines a novel cellular compartment upon fungal attack and is required for the timely assembly of papillae." Mol Biol Cell **15**(11): 5118-5129.

Austin, J. R., 2nd, J. M. Segui-Simarro and L. A. Staehelin (2005). "Quantitative analysis of changes in spatial distribution and plus-end geometry of microtubules involved in plant-cell cytokinesis." J Cell Sci **118**(Pt 17): 3895-3903.

Baker, R. W. and F. M. Hughson (2016). "Chaperoning SNARE assembly and disassembly." Nat Rev Mol Cell Biol **17**(8): 465-479.

Bassham, D. C., F. Brandizzi, M. S. Otegui and A. A. Sanderfoot (2008). "The secretory system of Arabidopsis." Arabidopsis Book **6**: e0116.

Bassham, D. C., A. A. Sanderfoot, V. Kovaleva, H. Zheng and N. V. Raikhel (2000). "AtVPS45 complex formation at the trans-Golgi network." Mol Biol Cell **11**(7): 2251-2265.

Bennett, M. K., N. Calakos and R. H. Scheller (1992). "Syntaxin: a synaptic protein implicated in docking of synaptic vesicles at presynaptic active zones." Science **257**(5067): 255-259.

Bock, J. B., H. T. Matern, A. A. Peden and R. H. Scheller (2001). "A genomic perspective on membrane compartment organization." Nature **409**(6822): 839-841.

Boruc, J. and D. Van Damme (2015). "Endomembrane trafficking overarching cell plate formation." Curr Opin Plant Biol **28**: 92-98.

Bubeck, J., D. Scheuring, E. Hummel, M. Langhans, C. Viotti, O. Foresti, J. Denecke, D. K. Banfield and D. G. Robinson (2008). "The syntaxins SYP31 and SYP81 control ER-Golgi trafficking in the plant secretory pathway." Traffic **9**(10): 1629-1652.

Burkhardt, P., D. A. Hattendorf, W. I. Weis and D. Fasshauer (2008). "Munc18a controls SNARE assembly through its interaction with the syntaxin N-peptide." EMBO J **27**(7): 923-933.

Carter, C., S. Pan, J. Zouhar, E. L. Avila, T. Girke and N. V. Raikhel (2004). "The vegetative vacuole proteome of Arabidopsis thaliana reveals predicted and unexpected proteins." Plant Cell **16**(12): 3285-3303.

Chen, X., J. Lu, I. Dulubova and J. Rizo (2008). "NMR analysis of the closed conformation of syntaxin-1." J Biomol NMR **41**(1): 43-54.

Chen, Y., Y. K. Shin and D. C. Bassham (2005). "YKT6 is a core constituent of membrane fusion machineries at the Arabidopsis trans-Golgi network." J Mol Biol **350**(1): 92-101.

Cherfils, J. (2014). "Arf GTPases and their effectors: assembling multivalent membrane-binding platforms." Curr Opin Struct Biol **29**: 67-76.

Chow, C.-M., H. Neto, C. Foucart and I. Moore (2008). "Rab-A2 and Rab-A3 GTPases Define a trans-Golgi Endosomal Membrane Domain in Arabidopsis That Contributes Substantially to the Cell Plate." The Plant Cell **20**(1): 101-123.

Clough, S. J. and A. F. Bent (1998). "Floral dip: a simplified method for Agrobacterium-mediated transformation of Arabidopsis thaliana." Plant J **16**(6): 735-743.

da Silva Conceicao, A., D. Marty-Mazars, D. C. Bassham, A. A. Sanderfoot, F. Marty and N. V. Raikhel (1997). "The syntaxin homolog AtPEP12p resides on a late post-Golgi compartment in plants." Plant Cell **9**(4): 571-582.

Daste, F., T. Galli and D. Tareste (2015). "Structure and function of longin SNAREs." J Cell Sci **128**(23): 4263-4272.

Dettmer, J., A. Hong-Hermesdorf, Y. D. Stierhof and K. Schumacher (2006). "Vacuolar H+-ATPase activity is required for endocytic and secretory trafficking in Arabidopsis." Plant Cell **18**(3): 715-730.

Dulubova, I., M. Khvotchev, S. Liu, I. Huryeva, T. C. Sudhof and J. Rizo (2007). "Munc18-1 binds directly to the neuronal SNARE complex." Proc Natl Acad Sci U S A **104**(8): 2697-2702.

Dulubova, I., S. Sugita, S. Hill, M. Hosaka, I. Fernandez, T. C. Sudhof and J. Rizo (1999). "A conformational switch in syntaxin during exocytosis: role of munc18." EMBO J **18**(16): 4372-4382.

Ebine, K., M. Fujimoto, Y. Okatani, T. Nishiyama, T. Goh, E. Ito, T. Dainobu, A. Nishitani, T. Uemura, M. H. Sato, H. Thordal-Christensen, N. Tsutsumi, A. Nakano and T. Ueda (2011). "A membrane trafficking pathway regulated by the plant-specific RAB GTPase ARA6." Nat Cell Biol **13**(7): 853-859.

Ebine, K., Y. Okatani, T. Uemura, T. Goh, K. Shoda, M. Niihama, M. T. Morita, C. Spitzer, M. S. Otegui, A. Nakano and T. Ueda (2008). "A SNARE complex unique to seed plants is required for protein storage vacuole biogenesis and seed development of Arabidopsis thaliana." Plant Cell **20**(11): 3006-3021.

El-Kasmi, F., T. Pacher, G. Strompen, Y. D. Stierhof, L. M. Muller, C. Koncz, U. Mayer and G. Jurgens (2011). "Arabidopsis SNARE protein SEC22 is essential for gametophyte development and maintenance of Golgi-stack integrity." Plant J **66**(2): 268-279.

El Kasmi, F., C. Krause, U. Hiller, Y. D. Stierhof, U. Mayer, L. Conner, L. Kong, I. Reichardt, A. A. Sanderfoot and G. Jurgens (2013). "SNARE complexes of different composition jointly mediate membrane fusion in Arabidopsis cytokinesis." Mol Biol Cell **24**(10): 1593-1601.

Enami, K., M. Ichikawa, T. Uemura, N. Kutsuna, S. Hasezawa, T. Nakagawa, A. Nakano and M. H. Sato (2009). "Differential expression control and polarized distribution of plasma membrane-resident SYP1 SNAREs in Arabidopsis thaliana." Plant Cell Physiol **50**(2): 280-289.

Fasshauer, D., W. Antonin, V. Subramaniam and R. Jahn (2002). "SNARE assembly and disassembly exhibit a pronounced hysteresis." Nat Struct Biol **9**(2): 144-151.

Fasshauer, D., R. B. Sutton, A. T. Brunger and R. Jahn (1998). "Conserved structural features of the synaptic fusion complex: SNARE proteins reclassified as Q- and R-SNAREs." Proc Natl Acad Sci U S A **95**(26): 15781-15786.

Fendrych, M., L. Synek, T. Pečenková, H. Toupalová, R. Cole, E. Drdová, J. Nebesářová, M. Šedinová, M. Hála, J. E. Fowler and V. Žárský (2010). "The Arabidopsis Exocyst Complex Is Involved in Cytokinesis and Cell Plate Maturation." The Plant Cell **22**(9): 3053-3065.

Fernandez, I., J. Ubach, I. Dulubova, X. Zhang, T. C. Sudhof and J. Rizo (1998). "Three-dimensional structure of an evolutionarily conserved N-terminal domain of syntaxin 1A." Cell **94**(6): 841-849.

Filippini, F., V. Rossi, T. Galli, A. Budillon, M. D'Urso and M. D'Esposito (2001). "Longins: a new evolutionary conserved VAMP family sharing a novel SNARE domain." Trends Biochem Sci **26**(7): 407-409.

Fujiwara, M., T. Uemura, K. Ebine, Y. Nishimori, T. Ueda, A. Nakano, M. H. Sato and Y. Fukao (2014). "Interactomics of Qa-SNARE in Arabidopsis thaliana." Plant Cell Physiol **55**(4): 781-789.

Garcia, E. P., E. Gatti, M. Butler, J. Burton and P. De Camilli (1994). "A rat brain Sec1 homologue related to Rop and UNC18 interacts with syntaxin." Proc Natl Acad Sci U S A **91**(6): 2003-2007.

Granger, C. and R. Cyr (2001). "Use of abnormal preprophase bands to decipher division plane determination." J Cell Sci **114**(Pt 3): 599-607.

Guizetti, J. and D. W. Gerlich (2010). "Cytokinetic abscission in animal cells." Semin Cell Dev Biol **21**(9): 909-916.

Guo, F. and A. G. McCubbin (2012). "The pollen-specific R-SNARE/longin PiVAMP726 mediates fusion of endo- and exocytic compartments in pollen tube tip growth." J Exp Bot **63**(8): 3083-3095.

Heese, M., X. Gansel, L. Sticher, P. Wick, M. Grebe, F. Granier and G. Jurgens (2001). "Functional characterization of the KNOLLE-interacting t-SNARE AtSNAP33 and its role in plant cytokinesis." J Cell Biol **155**(2): 239-249.

Hirst, J. and M. S. Robinson (1998). "Clathrin and adaptors." Biochim Biophys Acta **1404**(1-2): 173-193.

Hong, W. (2005). "SNAREs and traffic." Biochim Biophys Acta **1744**(3): 493-517.

Hou, Q., G. Ufer and D. Bartels (2016). "Lipid signalling in plant responses to abiotic stress." Plant Cell Environ **39**(5): 1029-1048.

Ichikawa, M., T. Hirano, K. Enami, T. Fuselier, N. Kato, C. Kwon, B. Voigt, P. Schulze-Lefert, F. Baluska and M. H. Sato (2014). "Syntaxin of plant proteins SYP123 and SYP132 mediate root hair tip growth in Arabidopsis thaliana." Plant Cell Physiol **55**(4): 790-800.

Ito, E., M. Fujimoto, K. Ebine, T. Uemura, T. Ueda and A. Nakano (2012). "Dynamic behavior of clathrin in Arabidopsis thaliana unveiled by live imaging." Plant J **69**(2): 204-216.

Jahn, R. and R. H. Scheller (2006). "SNAREs--engines for membrane fusion." Nat Rev Mol Cell Biol **7**(9): 631-643.

Jones, A. M., Y. H. Xuan, M. Xu, R. S. Wang, C. H. Ho, S. Lalonde, C. H. You, M. I. Sardi, S. A. Parsa, E. Smith-Valle, T. Y. Su, K. A. Frazer, G. Pilot, R. Pratelli, G. Grossmann, B. R. Acharya, H. C. Hu, C. Engineer, F. Villiers, C. L. Ju, K. Takeda, Z. Su, Q. F. Dong, S. M. Assmann, J. Chen, J. M. Kwak, J. I. Schroeder, R. Albert, S. Y. Rhee and W. B. Frommer (2014). "Border Control-A Membrane-Linked Interactome of Arabidopsis." Science **344**(6185): 711-716.

Kalde, M., T. S. Nuhse, K. Findlay and S. C. Peck (2007). "The syntaxin SYP132 contributes to plant resistance against bacteria and secretion of pathogenesis-related protein 1." Proc Natl Acad Sci U S A **104**(28): 11850-11855.

Karnik, R., C. Grefen, R. Bayne, A. Honsbein, T. Kohler, D. Kioumourtzoglou, M. Williams, N. J. Bryant and M. R. Blatt (2013). "Arabidopsis Sec1/Munc18 Protein SEC11 Is a Competitive and Dynamic Modulator of SNARE Binding and SYP121-Dependent Vesicle Traffic." Plant Cell **25**(4): 1368-1382.

Karnik, R., B. Zhang, S. Waghmare, C. Aderhold, C. Grefen and M. R. Blatt (2015). "Binding of SEC11 indicates its role in SNARE recycling after vesicle fusion and identifies two pathways for vesicular traffic to the plasma membrane." Plant Cell **27**(3): 675-694.

Kim, H., R. O'Connell, M. Maekawa-Yoshikawa, T. Uemura, U. Neumann and P. Schulze-Lefert (2014). "The powdery mildew resistance protein RPW8.2 is carried on VAMP721/722 vesicles to the extrahaustorial membrane of haustorial complexes." Plant J **79**(5): 835-847.

Kleinboelting, N., G. Huep, A. Kloetgen, P. Viehoever and B. Weisshaar (2012). "GABI-Kat SimpleSearch: new features of the Arabidopsis thaliana T-DNA mutant database." Nucleic Acids Res **40**(Database issue): D1211-1215.

Koumandou, V. L., J. B. Dacks, R. M. Coulson and M. C. Field (2007). "Control systems for membrane fusion in the ancestral eukaryote; evolution of tethering complexes and SM proteins." BMC Evol Biol **7**: 29.

Kwon, C., P. Bednarek and P. Schulze-Lefert (2008a). "Secretory pathways in plant immune responses." Plant Physiol **147**(4): 1575-1583.

Kwon, C., C. Neu, S. Pajonk, H. S. Yun, U. Lipka, M. Humphry, S. Bau, M. Straus, M. Kwaaitaal, H. Rampelt, F. El Kasmi, G. Jurgens, J. Parker, R. Panstruga, V. Lipka and P. Schulze-Lefert (2008b). "Co-option of a default secretory pathway for plant immune responses." Nature **451**(7180): 835-840.

Lauber, M. H., I. Waizenegger, T. Steinmann, H. Schwarz, U. Mayer, I. Hwang, W. Lukowitz and G. Jurgens (1997). "The Arabidopsis KNOLLE protein is a cytokinesis-specific syntaxin." J Cell Biol **139**(6): 1485-1493.

Lee, M. C., E. A. Miller, J. Goldberg, L. Orci and R. Schekman (2004). "Bi-directional protein transport between the ER and Golgi." Annu Rev Cell Dev Biol **20**: 87-123.

Lerman, J. C., J. Robblee, R. Fairman and F. M. Hughson (2000). "Structural analysis of the neuronal SNARE protein syntaxin-1A." Biochemistry **39**(29): 8470-8479.

Leshem, Y., Y. Golani, Y. Kaye and A. Levine (2010). "Reduced expression of the v-SNAREs AtVAMP71/AtVAMP7C gene family in Arabidopsis reduces drought tolerance by suppression of abscisic acid-dependent stomatal closure." J Exp Bot **61**(10): 2615-2622.

Leshem, Y., N. Melamed-Book, O. Cagnac, G. Ronen, Y. Nishri, M. Solomon, G. Cohen and A. Levine (2006). "Suppression of Arabidopsis vesicle-SNARE expression inhibited fusion of H2O2-containing vesicles with tonoplast and increased salt tolerance." Proc Natl Acad Sci U S A **103**(47): 18008-18013.

Lipka, E., A. Gadeyne, D. Stockle, S. Zimmermann, G. De Jaeger, D. W. Ehrhardt, V. Kirik, D. Van Damme and S. Muller (2014). "The Phragmoplast-Orienting Kinesin-12 Class Proteins Translate the Positional Information of the Preprophase Band to Establish the Cortical Division Zone in Arabidopsis thaliana." Plant Cell **26**(6): 2617-2632.

Lipka, V., C. Kwon and R. Panstruga (2007). "SNARE-ware: the role of SNARE-domain proteins in plant biology." Annu Rev Cell Dev Biol **23**: 147-174.

Liu, S. L., A. Q. Pan and K. L. Adams (2014). "Protein subcellular relocalization of duplicated genes in Arabidopsis." Genome Biol Evol **6**(9): 2501-2515.

Low, S. H., X. Li, M. Miura, N. Kudo, B. Quinones and T. Weimbs (2003). "Syntaxin 2 and endobrevin are required for the terminal step of cytokinesis in mammalian cells." Dev Cell **4**(5): 753-759.

Lukowitz, W., U. Mayer and G. Jurgens (1996). "Cytokinesis in the Arabidopsis embryo involves the syntaxin-related KNOLLE gene product." Cell **84**(1): 61-71.

Maritzen, T., S. J. Koo and V. Haucke (2012). "Turning CALM into excitement: AP180 and CALM in endocytosis and disease." Biol Cell **104**(10): 588-602.

Medine, C. N., C. Rickman, L. H. Chamberlain and R. R. Duncan (2007). "Munc18-1 prevents the formation of ectopic SNARE complexes in living cells." J Cell Sci **120**(Pt 24): 4407-4415.

Memon, A. R. (2004). "The role of ADP-ribosylation factor and SAR1 in vesicular trafficking in plants." Biochimica et Biophysica Acta (BBA) - Biomembranes **1664**(1): 9-30.

Mossessova, E., R. A. Corpina and J. Goldberg (2003). "Crystal structure of ARF1*Sec7 complexed with Brefeldin A and its implications for the guanine nucleotide exchange mechanism." Mol Cell **12**(6): 1403-1411.

Muller, I., W. Wagner, A. Volker, S. Schellmann, P. Nacry, F. Kuttner, Z. Schwarz-Sommer, U. Mayer and G. Jurgens (2003). "Syntaxin specificity of cytokinesis in Arabidopsis." Nat Cell Biol **5**(6): 531-534.

Muller, S. and G. Jurgens (2016). "Plant cytokinesis-No ring, no constriction but centrifugal construction of the partitioning membrane." Semin Cell Dev Biol **53**: 10-18.

Munson, M., X. Chen, A. E. Cocina, S. M. Schultz and F. M. Hughson (2000). "Interactions within the yeast t-SNARE Sso1p that control SNARE complex assembly." Nat Struct Biol **7**(10): 894-902.

Nakabayashi, K., M. Okamoto, T. Koshiba, Y. Kamiya and E. Nambara (2005). "Genome-wide profiling of stored mRNA in Arabidopsis thaliana seed germination: epigenetic and genetic regulation of transcription in seed." Plant J **41**(5): 697-709.

Pajonk, S., C. Kwon, N. Clemens, R. Panstruga and P. Schulze-Lefert (2008). "Activity determinants and functional specialization of Arabidopsis PEN1 syntaxin in innate immunity." J Biol Chem **283**(40): 26974-26984.

Park, M. and G. Jurgens (2011). "Membrane traffic and fusion at post-Golgi compartments." Front Plant Sci **2**: 111.

Park, M., C. Krause, M. Karnahl, I. Reichardt, F. El Kasmi, U. Mayer, Y. D. Stierhof, U. Hiller, G. Strompen, M. Bayer, M. Kientz, M. H. Sato, M. Nishimura, D. J. L., A. Sanderfoot and G. Jürgens (*in submission*). "Concerted action of ancient and novel SNARE complexes in flowering-plant cytokinesis." submitted to Cell.

Park, M., K. Song, I. Reichardt, H. Kim, U. Mayer, Y. D. Stierhof, I. Hwang and G. Jurgens (2013). "Arabidopsis mu-adaptin subunit AP1M of adaptor protein complex 1 mediates late secretory and vacuolar traffic and is required for growth." Proc Natl Acad Sci U S A **110**(25): 10318-10323.

Park, M., S. Touihri, I. Muller, U. Mayer and G. Jurgens (2012). "Sec1/Munc18 protein stabilizes fusion-competent syntaxin for membrane fusion in Arabidopsis cytokinesis." Dev Cell **22**(5): 989-1000.

Petkovic, M., A. Jemaiel, F. Daste, C. G. Specht, I. Izeddin, D. Vorkel, J. M. Verbavatz, X. Darzacq, A. Triller, K. H. Pfenninger, D. Tareste, C. L. Jackson and T. Galli (2014). "The SNARE Sec22b has a non-fusogenic function in plasma membrane expansion." Nat Cell Biol **16**(5): 434-444.

Pevsner, J., S. C. Hsu, J. E. Braun, N. Calakos, A. E. Ting, M. K. Bennett and R. H. Scheller (1994). "Specificity and regulation of a synaptic vesicle docking complex." Neuron **13**(2): 353-361.

Peyroche, A., B. Antonny, S. Robineau, J. Acker, J. Cherfils and C. L. Jackson (1999). "Brefeldin A acts to stabilize an abortive ARF-GDP-Sec7 domain protein complex: involvement of specific residues of the Sec7 domain." Mol Cell **3**(3): 275-285.

Qi, X., M. Kaneda, J. Chen, A. Geitmann and H. Zheng (2011). "A specific role for Arabidopsis TRAPPII in post-Golgi trafficking that is crucial for cytokinesis and cell polarity." Plant J **68**(2): 234-248.

Reichardt, I., D. Slane, F. El Kasmi, C. Knoll, R. Fuchs, U. Mayer, V. Lipka and G. Jurgens (2011). "Mechanisms of functional specificity among plasma-membrane syntaxins in Arabidopsis." Traffic **12**(9): 1269-1280.

Reichardt, I., Y. D. Stierhof, U. Mayer, S. Richter, H. Schwarz, K. Schumacher and G. Jurgens (2007). "Plant cytokinesis requires de novo secretory trafficking but not endocytosis." Curr Biol **17**(23): 2047-2053.

Renault, L., B. Guibert and J. Cherfils (2003). "Structural snapshots of the mechanism and inhibition of a guanine nucleotide exchange factor." Nature **426**(6966): 525-530.

Richter, S., N. Geldner, J. Schrader, H. Wolters, Y. D. Stierhof, G. Rios, C. Koncz, D. G. Robinson and G. Jurgens (2007). "Functional diversification of closely related ARF-GEFs in protein secretion and recycling." Nature **448**(7152): 488-492.

Richter, S., M. Kientz, S. Brumm, M. E. Nielsen, M. Park, R. Gavidia, C. Krause, U. Voss, H. Beckmann, U. Mayer, Y. D. Stierhof and G. Jurgens (2014). "Delivery of endocytosed proteins to the cell-division plane requires change of pathway from recycling to secretion." Elife **3**: e02131.

Rizo, J. and T. C. Sudhof (2012). "The membrane fusion enigma: SNAREs, Sec1/Munc18 proteins, and their accomplices--guilty as charged?" Annu Rev Cell Dev Biol **28**: 279-308.

Robatzek, S., D. Chinchilla and T. Boller (2006). "Ligand-induced endocytosis of the pattern recognition receptor FLS2 in Arabidopsis." Genes Dev **20**(5): 537-542.

Robinson, M. S. (2015). "Forty Years of Clathrin-coated Vesicles." Traffic **16**(12): 1210-1238.

Rodkey, T. L., S. Liu, M. Barry and J. A. McNew (2008). "Munc18a scaffolds SNARE assembly to promote membrane fusion." Mol Biol Cell **19**(12): 5422-5434.

Rojo, E., J. Zouhar, V. Kovaleva, S. Hong and N. V. Raikhel (2003). "The AtC-VPS protein complex is localized to the tonoplast and the prevacuolar compartment in arabidopsis." Mol Biol Cell **14**(2): 361-369.

Rossi, V., D. K. Banfield, M. Vacca, L. E. Dietrich, C. Ungermann, M. D'Esposito, T. Galli and F. Filippini (2004). "Longins and their longin domains: regulated SNAREs and multifunctional SNARE regulators." Trends Biochem Sci **29**(12): 682-688.

Rothman, J. E. (1994). "Mechanisms of intracellular protein transport." Nature **372**(6501): 55-63.

Rybak, K., A. Steiner, L. Synek, S. Klaeger, I. Kulich, E. Facher, G. Wanner, B. Kuster, V. Zarsky, S. Persson and F. F. Assaad (2014). "Plant cytokinesis is orchestrated by the sequential action of the TRAPPII and exocyst tethering complexes." Dev Cell **29**(5): 607-620.

Samaj, J., J. Muller, M. Beck, N. Bohm and D. Menzel (2006). "Vesicular trafficking, cytoskeleton and signalling in root hairs and pollen tubes." Trends Plant Sci **11**(12): 594-600.

Sanderfoot, A. (2007). "Increases in the number of SNARE genes parallels the rise of multicellularity among the green plants." Plant Physiol **144**(1): 6-17.

Sanmartin, M., A. Ordonez, E. J. Sohn, S. Robert, J. J. Sanchez-Serrano, M. A. Surpin, N. V. Raikhel and E. Rojo (2007). "Divergent functions of VTI12 and VTI11 in trafficking to storage and lytic vacuoles in Arabidopsis." Proc Natl Acad Sci U S A **104**(9): 3645-3650.

Sato, A., Y. Sato, Y. Fukao, M. Fujiwara, T. Umezawa, K. Shinozaki, T. Hibi, M. Taniguchi, H. Miyake, D. B. Goto and N. Uozumi (2009). "Threonine at position 306 of the KAT1 potassium channel is essential for channel activity and is a target site for ABA-activated SnRK2/OST1/SnRK2.6 protein kinase." Biochemical Journal **424**: 439-448.

Schmid, M., T. S. Davison, S. R. Henz, U. J. Pape, M. Demar, M. Vingron, B. Scholkopf, D. Weigel and J. U. Lohmann (2005). "A gene expression map of Arabidopsis thaliana development." Nat Genet **37**(5): 501-506.

Shen, J., D. C. Tareste, F. Paumet, J. E. Rothman and T. J. Melia (2007). "Selective activation of cognate SNAREpins by Sec1/Munc18 proteins." Cell **128**(1): 183-195.

Shirakawa, M., H. Ueda, T. Shimada, Y. Koumoto, T. L. Shimada, M. Kondo, T. Takahashi, Y. Okuyama, M. Nishimura and I. Hara-Nishimura (2010). "Arabidopsis Qa-SNARE SYP2 proteins localized to different subcellular regions function redundantly in vacuolar protein sorting and plant development." Plant J **64**(6): 924-935.

Sollner, T., S. W. Whiteheart, M. Brunner, H. Erdjument-Bromage, S. Geromanos, P. Tempst and J. E. Rothman (1993). "SNAP receptors implicated in vesicle targeting and fusion." Nature **362**(6418): 318-324.

Steiner, A., L. Muller, K. Rybak, V. Vodermaier, E. Facher, M. Thellmann, R. Ravikumar, G. Wanner, M. T. Hauser and F. F. Assaad (2016). "The Membrane-Associated Sec1/Munc18 KEULE is Required for Phragmoplast Microtubule Reorganization During Cytokinesis in Arabidopsis." Mol Plant **9**(4): 528-540.

Steinmann, T., N. Geldner, M. Grebe, S. Mangold, C. L. Jackson, S. Paris, L. Galweiler, K. Palme and G. Jurgens (1999). "Coordinated polar localization of auxin efflux carrier PIN1 by GNOM ARF GEF." Science **286**(5438): 316-318.

Stenmark, H. (2009). "Rab GTPases as coordinators of vesicle traffic." Nat Rev Mol Cell Biol **10**(8): 513-525.

Sup Yun, H., C. Yi, H. Kwon and C. Kwon (2013). "Model for regulation of VAMP721/722-mediated secretion: growth vs. stress responses." Plant Signal Behav **8**(11): e27116.

Swarbreck, S. M., R. Colaco and J. M. Davies (2013). "Plant calcium-permeable channels." Plant Physiol **163**(2): 514-522.

Takano, J., K. Miwa, L. Yuan, N. von Wiren and T. Fujiwara (2005). "Endocytosis and degradation of BOR1, a boron transporter of Arabidopsis thaliana, regulated by boron availability." Proc Natl Acad Sci U S A **102**(34): 12276-12281.

Teh, O.-K., Y. Shimono, M. Shirakawa, Y. Fukao, K. Tamura, T. Shimada and I. Hara-Nishimura (2013). "The AP-1 μ Adaptin is Required for KNOLLE Localization at the Cell Plate to Mediate Cytokinesis in Arabidopsis." Plant and Cell Physiology **54**(6): 838-847.

Togneri, J., Y. S. Cheng, M. Munson, F. M. Hughson and C. M. Carr (2006). "Specific SNARE complex binding mode of the Sec1/Munc-18 protein, Sec1p." Proc Natl Acad Sci U S A **103**(47): 17730-17735.

Touihri, S., C. Knoll, Y. D. Stierhof, I. Muller, U. Mayer and G. Jurgens (2011). "Functional anatomy of the Arabidopsis cytokinesis-specific syntaxin KNOLLE." Plant Journal **68**(5): 755-764.

Ueda, T., T. Uemura, M. H. Sato and A. Nakano (2004). "Functional differentiation of endosomes in Arabidopsis cells." Plant J **40**(5): 783-789.

Uemura, T., H. Kim, C. Saito, K. Ebine, T. Ueda, P. Schulze-Lefert and A. Nakano (2012). "Qa-SNAREs localized to the trans-Golgi network regulate multiple transport pathways and extracellular disease resistance in plants." Proc Natl Acad Sci U S A **109**(5): 1784-1789.

Uemura, T., M. T. Morita, K. Ebine, Y. Okatani, D. Yano, C. Saito, T. Ueda and A. Nakano (2010). "Vacuolar/pre-vacuolar compartment Qa-SNAREs VAM3/SYP22 and PEP12/SYP21 have interchangeable functions in Arabidopsis." Plant J **64**(5): 864-873.

Uemura, T., M. H. Sato and K. Takeyasu (2005). "The longin domain regulates subcellular targeting of VAMP7 in Arabidopsis thaliana." FEBS Lett **579**(13): 2842-2846.

Uemura, T., T. Ueda, R. L. Ohniwa, A. Nakano, K. Takeyasu and M. H. Sato (2004). "Systematic analysis of SNARE molecules in Arabidopsis: dissection of the post-Golgi network in plant cells." Cell Struct Funct **29**(2): 49-65.

Valster, A. H., E. S. Pierson, R. Valenta, P. K. Hepler and A. Emons (1997). "Probing the Plant Actin Cytoskeleton during Cytokinesis and Interphase by Profilin Microinjection." Plant Cell **9**(10): 1815-1824.

Waizenegger, I., W. Lukowitz, F. Assaad, H. Schwarz, G. Jurgens and U. Mayer (2000). "The Arabidopsis KNOLLE and KEULE genes interact to promote vesicle fusion during cytokinesis." Curr Biol **10**(21): 1371-1374.

Walker, K. L., S. Muller, D. Moss, D. W. Ehrhardt and L. G. Smith (2007). "Arabidopsis TANGLED identifies the division plane throughout mitosis and cytokinesis." Curr Biol **17**(21): 1827-1836.

Weijers, D., J. P. Van Hamburg, E. Van Rijn, P. J. Hooykaas and R. Offringa (2003). "Diphtheria toxin-mediated cell ablation reveals interregional communication during Arabidopsis seed development." Plant Physiol **133**(4): 1882-1892.

Wen, W., J. Yu, L. Pan, Z. Wei, J. Weng, W. Wang, Y. S. Ong, T. H. Tran, W. Hong and M. Zhang (2010). "Lipid-Induced conformational switch controls fusion activity of longin domain SNARE Ykt6." Mol Cell **37**(3): 383-395.

Winter, D., B. Vinegar, H. Nahal, R. Ammar, G. V. Wilson and N. J. Provart (2007). "An "Electronic Fluorescent Pictograph" browser for exploring and analyzing large-scale biological data sets." PLoS One **2**(8): e718.

Xu, X. M., Q. Zhao, T. Rodrigo-Peiris, J. Brkljacic, C. S. He, S. Muller and I. Meier (2008). "RanGAP1 is a continuous marker of the Arabidopsis cell division plane." Proc Natl Acad Sci U S A **105**(47): 18637-18642.

Yi, C., S. Park, H. S. Yun and C. Kwon (2013). "Vesicle-associated membrane proteins 721 and 722 are required for unimpeded growth of Arabidopsis under ABA application." J Plant Physiol **170**(5): 529-533.

Yu, H., S. S. Rathore, J. A. Lopez, E. M. Davis, D. E. James, J. L. Martin and J. Shen (2013). "Comparative studies of Munc18c and Munc18-1 reveal conserved and divergent mechanisms of Sec1/Munc18 proteins." Proc Natl Acad Sci U S A **110**(35): E3271-3280.

Yun, H. S., M. Kwaaitaal, N. Kato, C. Yi, S. Park, M. H. Sato, P. Schulze-Lefert and C. Kwon (2013). "Requirement of vesicle-associated membrane protein 721 and 722 for sustained growth during immune responses in Arabidopsis." Mol Cells **35**(6): 481-488.

Zhang, B., R. Karnik, Y. Wang, N. Wallmeroth, M. R. Blatt and C. Grefen (2015a). "The Arabidopsis R-SNARE VAMP721 Interacts with KAT1 and KC1 K+ Channels to Moderate K+ Current at the Plasma Membrane." Plant Cell **27**(6): 1697-1717.

Zhang, L., W. C. Li, T. Q. Wang, F. X. Zheng and J. Y. Li (2015b). "Requirement of R-SNAREs VAMP721 and VAMP722 for the gametophyte activity, embryogenesis and seedling root development in Arabidopsis." Plant Growth Regulation **77**(1): 57-65.

Zhang, L., H. Zhang, P. Liu, H. Hao, J. B. Jin and J. Lin (2011). "Arabidopsis R-SNARE proteins VAMP721 and VAMP722 are required for cell plate formation." PLoS One **6**(10): e26129.

Zouhar, J., E. Rojo and D. C. Bassham (2009). "AtVPS45 is a positive regulator of the SYP41/SYP61/VTI12 SNARE complex involved in trafficking of vacuolar cargo." Plant Physiol **149**(4): 1668-1678.

Zuo, J., Q. W. Niu and N. H. Chua (2000). "Technical advance: An estrogen receptor-based transactivator XVE mediates highly inducible gene expression in transgenic plants." Plant J **24**(2): 265-273.

10. Personal contribution

Chapter 4 - Assembly in the ER of inactive cis-SNARE complexes destined for cell plate formation in plant cytokinesis:

Molecular cloning, generation and selection of transgenic *pMDC7::GFP-SNAP33* and *pMDC7::YFP-NPSN11* lines were executed by me, as well as co-immunoprecipitation analyses, confocal imaging, in part and data analysis. Dr. U. Mayer-Jürgens and Dr. M.Park were involved in the localization analysis by confocal imaging. Dr. M. Park cloned and generated transgenic *pKN::mRFP-PEP12*, whereas co-immunoprecipitation experiments were conducted by me. Dr. M. Park carried out the control experiments, including confocal imaging and determination of cytokinetic frequency in Fig. 4 and co-immunoprecipitation experiments in Fig. 6.

Chapter 5 - Functional diversification of Arabidopsis SEC1-related SM proteins in cytokinetic and secretory membrane fusion

sec1b single mutant analysis, RT-PCR, confocal imaging, molecular cloning, transgenic line generation, yeast-two-hybrid analysis and co-immunoprecipitation analyses were performed by me. Generation by crossing and phenotyping of SM protein/SNARE protein double mutants were conducted by Dr. M. Park and U. Hiller. Phylogenetic analysis, crossing and phenotypic analysis of the *keule sec1b* double mutant, together with reciprocal crosses and its analysis, as well as phenotyping of double mutant pollen were performed by Dr. M. Park.

Chapter 6 - Arabidopsis R-SNARE function in vesicle trafficking

All experiments in this chapter were carried out by me.

11. Danksagung

Zunächst möchte ich mich bei dir, Gerd, herzlich für die Möglichkeit bedanken, diese Projekte in der Entgen, mit einer so ausgereiften Infrastruktur bearbeiten und abschließen zu können. Besonders dankbar bin ich dabei, für die zahlreichen, lehrreichen Diskussionen, die hilfreichen Kommentare zur Dissertation, und dass ich deine kreative, gründliche und geduldige Art Wissenschaft zu betreiben, kennenlernen durfte, die ich sehr zu schätzen weiß.

For all the support and advice, I am also especially grateful to you, Misoon. I learned most of my lab-related skills from you and, within these techniques, the critical interpretation and accuracy in their application. Many thanks also for the countless helpful discussions and advice, when the techniques failed to do, what they were supposed to do.

I would also like to thank Florian, Hauke, Manoj and Christopher for constructive discussions and Jennifer for the great work in the Co-immunoprecipitation experiments, with her being a very interested and pro-active student, with whom it was a pleasure to work.
I would like to acknowledge Farid el Kasmi, for the introduction to the lab and for providing the transgenic lines; pKN::YFP-VAMP723 and pKN::MYC-VAMP724.

Thank you, Kerstin, for an amusing and collaborative time at the bench. The rest of the crew I would like to acknowledge for the nice Thursdays and other extra-laboratorial activities.
Vor allem aber vielen lieben Dank an meine Familie für die bedingungslose und zeitlose Unterstützung. Dieser Dank richtet sich auch an den engen Kreis der NAPS Biologie Gruppe Tübingen.
Finally, I would like to thank a very nice and very special person. Thank you for the tremendous support during the hard times in the lab, early, or late, for helping me through many difficult times, by enduring these together with me, but also enduring me during those.

12. Publications

eLIFE elifesciences.org

SHORT REPORT

ER assembly of SNARE complexes mediating formation of partitioning membrane in *Arabidopsis* cytokinesis

Matthias Karnahl[1†], Misoon Park[1†], Ulrike Mayer[2], Ulrike Hiller[1,2], Gerd Jürgens[1*]

[1]Center for Plant Molecular Biology (ZMBP), Developmental Genetics, University of Tübingen, Tübingen, Germany; [2]Center for Plant Molecular Biology (ZMBP), Microscopy, University of Tübingen, Tübingen, Germany

Abstract Intracellular membrane fusion mediates diverse processes including cell growth, division and communication. Fusion involves complex formation between SNARE proteins anchored to adjacent membranes. How and in what form interacting SNARE proteins reach their sites of action is virtually unknown. We have addressed this problem in the context of plant cell division in which a large number of TGN-derived membrane vesicles fuse with one another to form the partitioning membrane. Blocking vesicle formation at the TGN revealed *cis*-SNARE complexes. These inactive cytokinetic SNARE complexes were already assembled at the endoplasmic reticulum and, after passage through Golgi/TGN to the cell division plane, transformed into fusogenic SNARE complexes. This mode of trafficking might ensure delivery of large stoichiometric quantities of SNARE proteins required for forming the partitioning membrane in the narrow time frame of plant cytokinesis. Such long-distance trafficking of inactive SNARE complexes would also facilitate directional growth processes during cell differentiation.
DOI: 10.7554/eLife.25327.001

***For correspondence:** gerd.juergens@zmbp.uni-tuebingen.de

[†]These authors contributed equally to this work

Competing interests: The authors declare that no competing interests exist.

Funding: See page 9

Received: 20 January 2017
Accepted: 05 May 2017
Published: 19 May 2017

Reviewing editor: Mohan K Balasubramanian, University of Warwick, United Kingdom

Introduction

Cytokinesis partitions the cytoplasm of the dividing cell. In non-plant eukaryotes, a contractile actomyosin ring strongly reduces the area of contact between the forming daughter cells. Consequently, little membrane expansion has to be supported by membrane traffic and fusion, which can largely be afforded by local recycling (***Nakayama, 2016***). In contrast, dividing plant cells lack the contractile actomyosin ring and thus have to make a large partitioning membrane – named cell plate – which is progressively formed from the centre to the periphery of the cell (***Müller and Jürgens, 2016***). The cell plate originates from membrane vesicles that fuse with one another upon delivery to the plane of cell division along the highly dynamic microtubules of the phragmoplast. Membrane fusion during *Arabidopsis* cytokinesis requires a cytokinesis-specific Qa-SNARE (aka syntaxin) named KNOLLE (***Lauber et al., 1997***), which forms two distinct functionally overlapping SNARE complexes by interaction with different sets of promiscuous SNARE partners: (i) QaQbcR-complex containing Qbc-SNARE SNAP33 and R-SNARE VAMP721 or VAMP722, and (ii) QaQbQcR-complex containing Qb-SNARE NPSN11, Qc-SNARE SYP71 and R-SNARE VAMP721 or VAMP722 (***El Kasmi et al., 2013***; ***Heese et al., 2001***; ***Zheng et al., 2002***). The formation of these *trans*-SNARE complexes requires the cytokinesis-specific action of the Sec1/Munc18 (SM) protein KEULE, which interacts with monomeric KNOLLE but not with the assembled KNOLLE-containing SNARE complex at the plane of cell division (***Park et al., 2012***). It is not known in what form the SNARE proteins reside on the vesicles prior to the action of the SM protein. One possibility is that each SNARE protein is trafficked separately and kept in its monomeric form until fusion. Alternatively, one or more SNARE proteins might form inactive complexes. Or there might be a mixture of vesicles, some bearing the R-SNARE and

others a preassembled Q-SNARE complex. Here, we examine in what form – monomers or complexes – SNARE proteins are present on the cytokinetic vesicles and where along the trafficking pathway complexes of cytokinetic SNARE proteins might be formed.

Results and discussion

The cytokinesis-specific Qa-SNARE KNOLLE is made during late G2/M phase and turned over rapidly at the end of cytokinesis (**Lauber et al., 1997**). Newly synthesised KNOLLE protein is inserted into the membrane of the endoplasmic reticulum (ER) and traffics along the secretory pathway via Golgi stack and *trans*-Golgi network (TGN) to the plane of cell division (**Figure 1A**) (**Reichardt et al., 2007**). Upon cell-plate formation, KNOLLE is endocytosed and targeted via multivesicular body (MVB) to the vacuole for degradation (**Figure 1A**) (**Reichardt et al., 2007**). Unlike the situation in mammals, yeast and most flowering plants, secretory traffic in *Arabidopsis* is insensitive to the fungal toxin brefeldin A (BFA). BFA inhibits the ARF-activating guanine-nucleotide exchange reaction of sensitive ARF-GEFs, thus preventing the formation of transport vesicles (**Mossessova et al., 2003**; **Renault et al., 2003**). We have engineered in *Arabidopsis* a BFA-inducible system with which secretory traffic can be blocked at two specific sites along the route, ER and TGN. Relevant BFA-insensitive ARF-GEFs, human GBF1-related GNL1 or human BIG1-related BIG3, were eliminated by mutation, leaving BFA-sensitive GNOM and BIG1,2,4, respectively (**Richter et al., 2007**, **2014**). Consequently, BFA treatment of *gnl1* mutant plants prevents recruitment of COPI coat complexes to the *cis*-Golgi membrane, causing collapse of the ER-Golgi traffic. Qa-SNARE KNOLLE is thus retained in the ER and cytokinesis is impaired, resulting in binucleate cells (**Figure 1A**) (**Richter et al., 2007**). Late-secretory traffic from the TGN to the plane of cell division requires the formation of AP-1 complex-coated transport vesicles, which depends on the action of four functionally overlapping ARF-GEFs BIG1 to BIG4 (**Park et al., 2013**; **Richter et al., 2014**). Mutational inactivation of the sole BFA-resistant ARF-GEF BIG3 renders AP-1 vesicle formation BFA-sensitive. KNOLLE is thus retained at TGN membrane aggregates called BFA compartments and cytokinesis is impaired, resulting in binucleate cells (**Figure 1A**) (**Richter et al., 2014**). To examine in what form – monomeric or part of complex – KNOLLE is delivered to the plane of cell division, we inhibited secretory traffic by BFA treatment of *gnl1* and *big3* mutants. However, BFA treatment would inhibit secretory traffic in some dividing cells but not in others because the cells in the developing seedling root divide asynchronously. To overcome this limitation, we used β-estradiol (EST)-inducible expression of KNOLLE SNARE partners NPSN11 or SNAP33 fused to a fluorescent protein (**Zuo et al., 2000**). Importantly, neither YFP:NPSN11 nor GFP:SNAP33 was expressed without EST treatment (**Figure 1B–C**), which is a prerequisite for the detection of newly-made cytokinesis-specific SNARE complexes.

Arabidopsis *big3* mutant seedlings were treated with BFA for 30 min followed by 210 min of combined BFA and EST treatment to induce expression of YFP:NPSN11 or GFP:SNAP33 in cells whose traffic to the cell-division plane was blocked at the TGN. Seedlings were then live-imaged for YFP:NPSN11 or GFP:SNAP33. The two fusion proteins accumulated in TGN-containing BFA compartments; this was in contrast to the strong labeling of cell plates in wild-type seedlings expressing BFA-resistant BIG3 ARF-GEF or in *big3* mutant seedlings not treated with BFA (**Figure 1B–C**). The frequency of cells undergoing cytokinesis was not altered by BFA treatment of wild-type or mutant seedlings, as evidenced by immunostaining of phragmoplast microtubules (**Figure 1—figure supplement 1**; **Supplementary file 1a**).

Co-immunoprecipitation analysis of BFA-treated *big3* mutant seedlings expressing EST-inducible YFP:NPSN11 revealed the presence of Qb-SNARE NPSN11 fused to YFP, Qa-SNARE KNOLLE, Qc-SNARE SYP71 and R-SNARE VAMP721/722 as well as the absence of Qbc-SNARE SNAP33 in the anti-GFP precipitate (**Figure 2A**). Thus, only the members of the KNOLLE-NPSN11-SYP71-VAMP721/722 complex were co-immunoprecipitated whereas the SNARE partner SNAP33 from the other KNOLLE-containing SNARE complex was not. The converse was observed in the co-immunoprecipitation analysis of *big3* mutant seedlings expressing the EST-inducible Qbc-SNARE member of the other KNOLLE complex, GFP:SNAP33. Qc-SNARE SYP71 was not detected in the co-immunoprecipitate, in contrast to the members of the trimeric KNOLLE complex Qbc-SNARE GFP:SNAP33, Qa-SNARE KNOLLE and R-SNARE VAMP721/722 (**Figure 2B**). Thus, the interaction detected by co-immunoprecipitation was exclusively confined to members of the KNOLLE-containing complex that contained the EST-induced SNARE partner, strongly suggesting that only direct

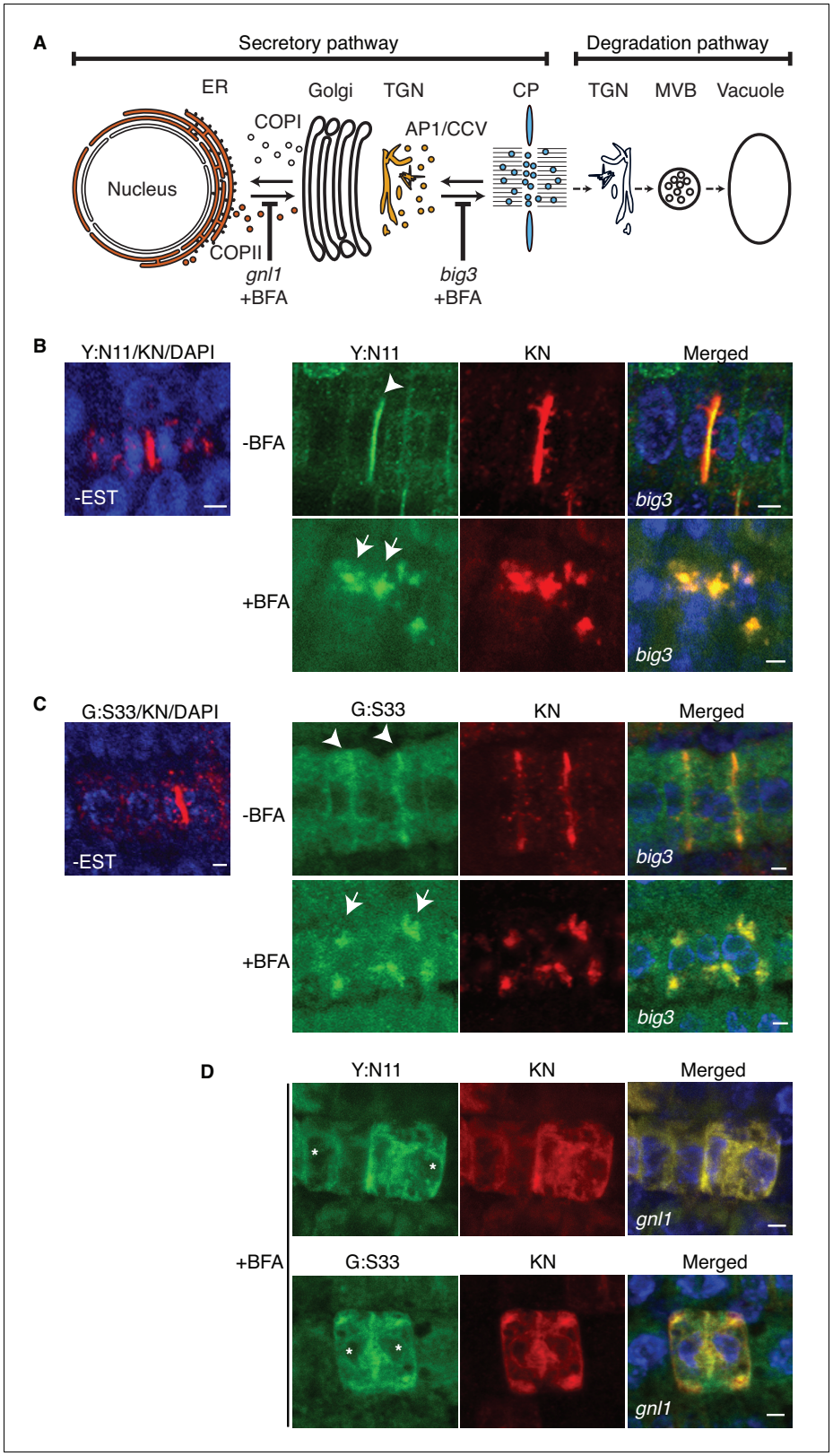

Figure 1. Site-specific inhibition of SNARE protein trafficking to the cell-division plane. (**A**) Qa-SNARE KNOLLE trafficking route in cytokinesis (***Reichardt et al., 2007***). ER, endoplasmic reticulum; TGN, *trans*-Golgi network; CP, cell plate; MVB, multivesicular body; COPI, COPII, AP1/CCV, membrane vesicles with specific coat protein complexes; *gnl1*, *big3*, knockout mutations of ARF-GEFs rendering those trafficking steps sensitive to brefeldin A

Figure 1 continued on next page

Figure 1 continued

(BFA). (**B–D**) Subcellular localisation of estradiol-inducible YFP:NPSN11 (**B**, **D**; green) and GFP-SNAP33 (**C**, **D**; green), and KNOLLE (**B–D**; red) in *big3* (**B**, **C**) and *gnl1 GNL1*$^{BFA\text{-}sens.}$ (**D**) mutant seedling roots treated with 50 µM BFA for 30 min, followed by 50 µM BFA + 20 µM estradiol for 210 min. Note that YFP:NPSN11 (Y:N11) or GFP:SNAP33 (G:S33) accumulates with KNOLLE (KN) at the BFA compartments in BFA-treated *big3* mutant whereas YFP:NPSN11 or GFP:SNAP33 colocalises with KNOLLE at the ER in BFA-treated *gnl1 GNL1*$^{BFA\text{-}sens.}$ mutant. Note also no expression of YFP:NPSN11 (Y:N11, **B**) or GFP:SNAP33 (G:S33, **C**) without estradiol treatment. Nuclei of overlays (**B–D**) were counterstained with DAPI (blue). -BFA, mock treatment; +BFA, BFA treatment; -EST, no estradiol treatment. Arrowheads, cell plates; arrows, BFA compartments; asterisks, ER. Scale bar, 5 µm. The experiments were technically repeated three times.

DOI: 10.7554/eLife.25327.002

The following figure supplements are available for figure 1:

Figure supplement 1. Cytokinetic cells in *big3* and *gnl1 GNL1*$^{BFA\text{-}sens.}$ mutant seedling roots.

DOI: 10.7554/eLife.25327.003

Figure supplement 2. Subcellular localisation (**A**, **B**) and co-immunoprecipitation analysis (**C**) of pKNOLLE::mRFP:PEP12 (aka SYP21) (red) in *big3* mutant seedling root cells expressing estradiol-inducible YFP:NPSN11 (**A**, **C**) and GFP:SNAP33 (**B**, **C**).

DOI: 10.7554/eLife.25327.004

Figure supplement 3. Site-specific inhibition of SNARE protein trafficking to the cell-division plane and loss of COPI from Golgi membrane in *gnl1 GNL1*$^{BFA\text{-}sens.}$ seedlings.

DOI: 10.7554/eLife.25327.005

interactions between SNARE complex members were detected. Further co-immunoprecipitation experiments with non-EST-induced seedlings demonstrated that co-immunoprecipitation of KNOLLE indeed required the EST-induced expression of YFP:NPSN11 or GFP:SNAP33 (***Figure 2—figure supplement 1A***). In addition, to rule out that these complexes might have formed during the immunoprecipitation procedure, we mixed the protein extracts with varying amounts of extract from *KNOLLE::mCherry:KNOLLE* transgenic seedlings before immunoprecipitation with anti-GFP beads. Neither 1x nor 10x mCherry:KNOLLE addition changed the amount of KNOLLE-containing SNARE complex formed (***Figure 2—figure supplement 1B***). We also addressed whether BFA treatment might stimulate the formation of KNOLLE-containing SNARE complexes. To this end, we compared protein extracts from untreated wild-type seedlings with those from BFA-treated wild-type seedlings. No obvious difference in KNOLLE complex formation was detected between treated and untreated seedlings (***Figure 2—figure supplement 1C***). As an additional control, we examined whether EST-induced KNOLLE-partners GFP:SNAP33 and YFP:NPSN11 co-immunoprecipitated the Qa-SNARE PEP12 (aka SYP21). PEP12 is normally located at the multivesicular body (MVB) (***da Silva Conceição et al., 1997***; ***Müller et al., 2003***), and was also relocated to the same BFA compartments as was YFP:NPSN11 in BFA-treated *big3* mutant seedlings (***Figure 1—figure supplement 2A–B***). Neither SNAP33 nor NPSN11 interacted with mRFP-tagged PEP12 whereas both did interact with KNOLLE, confirming the specificity of the co-immunoprecipitation assay (***Figure 1—figure supplement 2C***). These results indicate that KNOLLE forms part of a SNARE complex before the initiation of the fusion process at the plane of cell division. Thus, KNOLLE seems to be transported as part of two different *cis*-SNARE complexes from the TGN to the plane of cell division. These assembled SNARE complexes comprise either (i) KNOLLE, SNAP33 and VAMP721/722 or (ii) KNOLLE, NPSN11, SYP71 and VAMP721/722.

To determine where along the secretory pathway the KNOLLE-containing *cis*-SNARE complexes are assembled, we blocked traffic already at the ER-Golgi interface by BFA treatment of *gnl1* mutant seedlings expressing engineered BFA-sensitive GNL1$^{BFA\text{-}sens.}$ (***Richter et al., 2007***) and EST-inducible SNAREs YFP:NPSN11 or GFP:SNAP33. By subcellular localisation, all relevant SNARE components (YFP:NPSN11, GFP:SNAP33, KNOLLE) were detected at the ER (***Figure 1D***), indicating effective inhibition of traffic between ER and Golgi stacks. As an additional control, we analysed the subcellular localisation of COPI subunit γCOP, which is normally associated with the Golgi membrane whereas BFA treatment caused accumulation of γCOP in the cytosol (***Figure 1—figure supplement 3***) (***Richter et al., 2007***). Co-immunoprecipitation with anti-GFP beads of protein extracts from BFA-treated BFA-sensitive *GNL1*$^{BFA\text{-}sens.}$ seedlings revealed that KNOLLE already exists as part

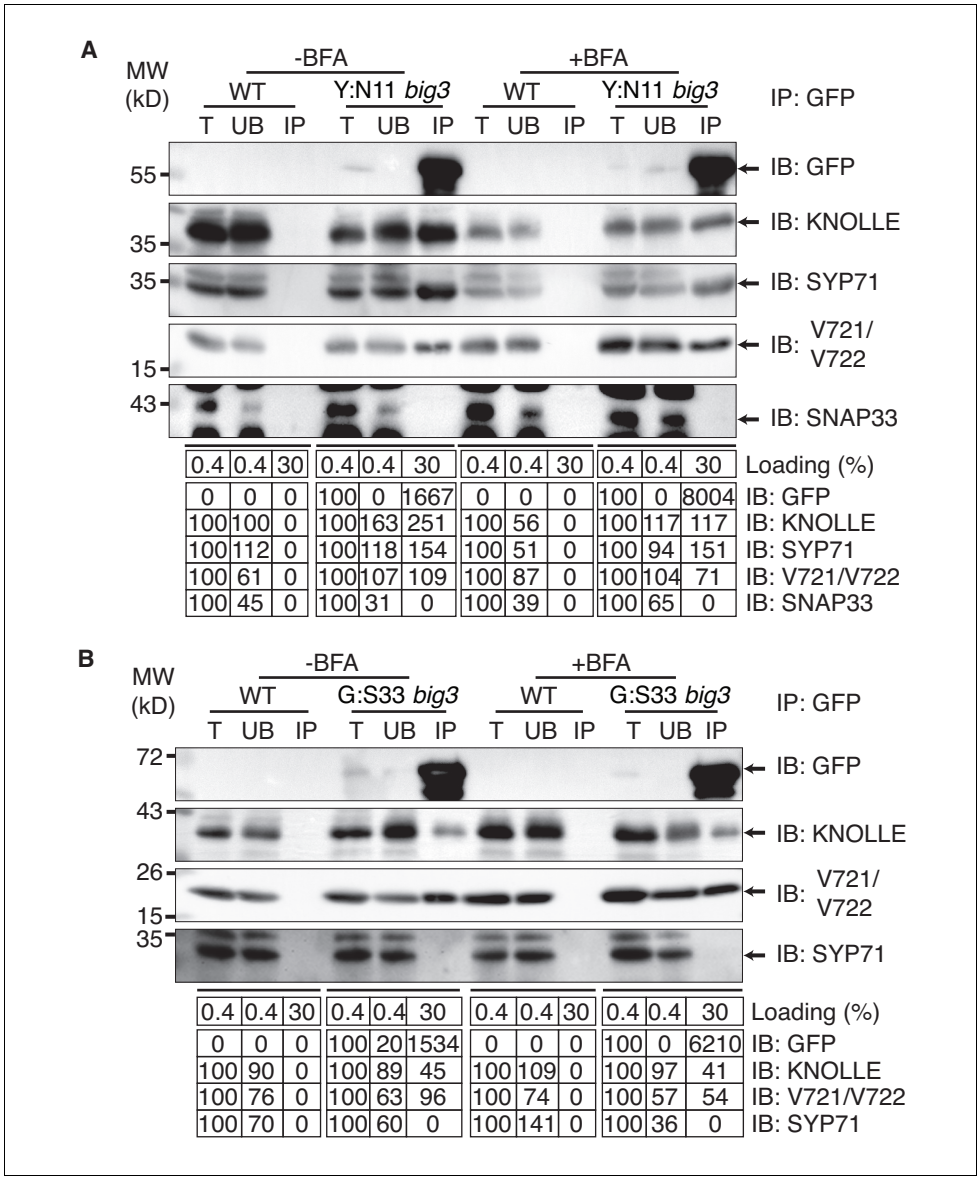

0.4	0.4	30	0.4	0.4	30	0.4	0.4	30	0.4	0.4	30	Loading (%)
0	0	0	100	0	1667	0	0	0	100	0	8004	IB: GFP
100	100	0	100	163	251	100	56	0	100	117	117	IB: KNOLLE
100	112	0	100	118	154	100	51	0	100	94	151	IB: SYP71
100	61	0	100	107	109	100	87	0	100	104	71	IB: V721/V722
100	45	0	100	31	0	100	39	0	100	65	0	IB: SNAP33

0.4	0.4	30	0.4	0.4	30	0.4	0.4	30	0.4	0.4	30	Loading (%)
0	0	0	100	20	1534	0	0	0	100	0	6210	IB: GFP
100	90	0	100	89	45	100	109	0	100	97	41	IB: KNOLLE
100	76	0	100	63	96	100	74	0	100	57	54	IB: V721/V722
100	70	0	100	60	0	100	141	0	100	36	0	IB: SYP71

Figure 2. Interaction analysis of cytokinetic SNAREs with traffic blocked at the TGN. Wild-type (WT) and *big3* mutant seedlings carrying estradiol-inducible *YFP:NPSN11* (**A**) or *GFP:SNAP33* (**B**) transgenes were treated with 50 µM BFA for 30 min followed by 50 µM BFA + 20 µM estradiol for 210 min (see ***Figure 1B–C***). Protein extracts were subjected to immunoprecipitation with anti-GFP beads, protein blots were probed with the antisera indicated on the right (IB): GFP, anti-GFP; KN, anti-KNOLLE; V721/V722, anti-VAMP721/722; SYP71, anti-SYP71; SNAP33, anti-SNAP33; kDa, protein size (left); MW, molecular weight; -BFA, mock treatment; +BFA, BFA treatment; T, total extract; UB, unbound; IP, immunoprecipitate. Loading (%), relative loading volume to total volume; relative signal intensity (input signal = 100% for UB and IP). The experiments were technically repeated more than six times.

DOI: 10.7554/eLife.25327.006

The following figure supplement is available for figure 2:

Figure supplement 1. Control experiments for co-immunoprecipitation analysis of cytokinetic SNAREs.

DOI: 10.7554/eLife.25327.007

of a *cis*-SNARE complex in the ER. Further co-immunoprecipitation analysis demonstrated interactions exclusively between components within each cytokinetic SNARE complex but not between members of the two different SNARE complexes, ruling out recovery of non-interacting proteins from the same membrane compartment (***Figure 3A–B***). Thus, KNOLLE is trafficked in two different *cis*-SNARE complexes along the secretory pathway from the ER to the plane of cell division.

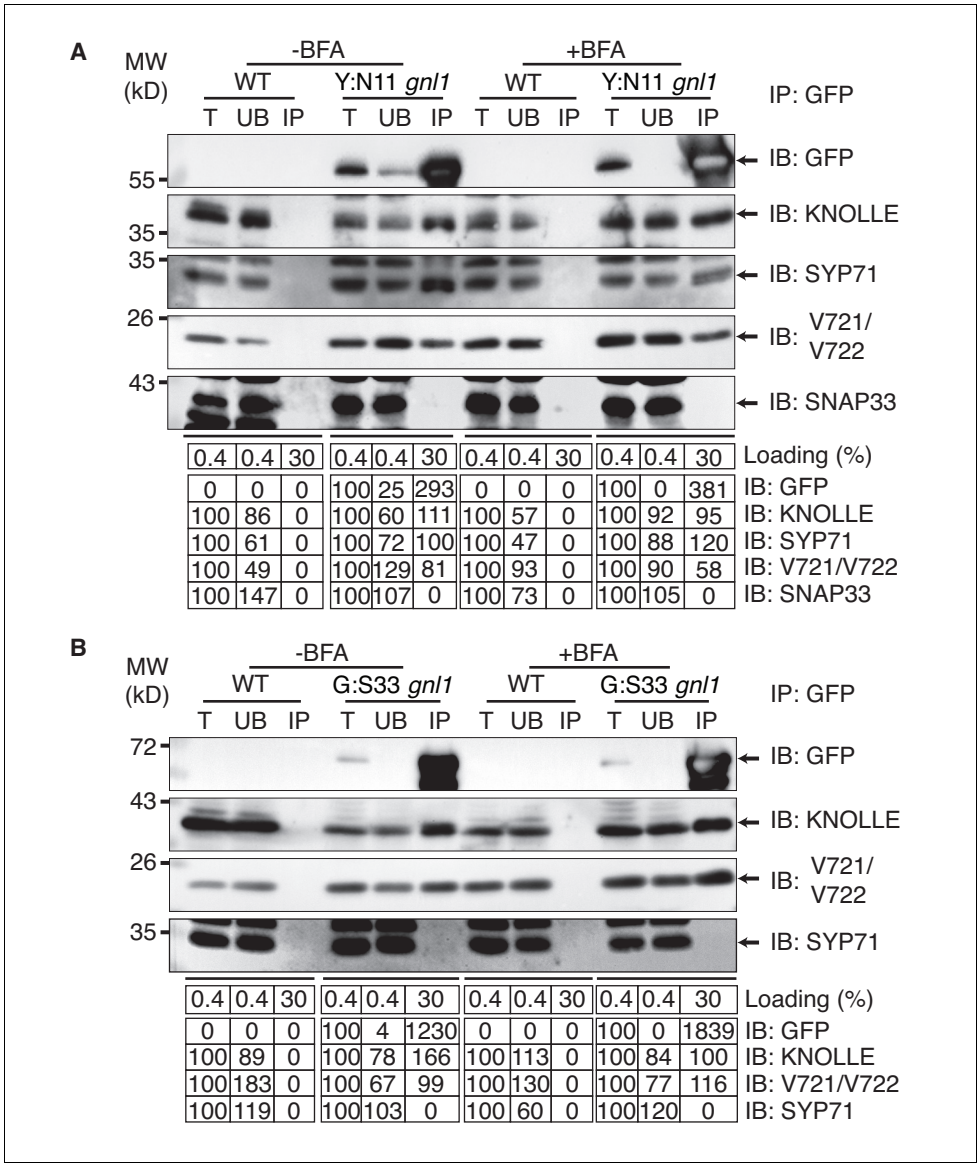

0.4	0.4	30	0.4	0.4	30	0.4	0.4	30	0.4	0.4	30	Loading (%)
0	0	0	100	25	293	0	0	0	100	0	381	IB: GFP
100	86	0	100	60	111	100	57	0	100	92	95	IB: KNOLLE
100	61	0	100	72	100	100	47	0	100	88	120	IB: SYP71
100	49	0	100	129	81	100	93	0	100	90	58	IB: V721/V722
100	147	0	100	107	0	100	73	0	100	105	0	IB: SNAP33

0.4	0.4	30	0.4	0.4	30	0.4	0.4	30	0.4	0.4	30	Loading (%)
0	0	0	100	4	1230	0	0	0	100	0	1839	IB: GFP
100	89	0	100	78	166	100	113	0	100	84	100	IB: KNOLLE
100	183	0	100	67	99	100	130	0	100	77	116	IB: V721/V722
100	119	0	100	103	0	100	60	0	100	120	0	IB: SYP71

Figure 3. Interaction analysis of cytokinetic SNAREs with traffic blocked at the ER. Wild-type (WT) and *gnl1* mutant seedlings complemented with *GNL1*$^{BFA\text{-}sens.}$ encoding a BFA-sensitive variant of GNL1 and carrying estradiol-inducible *YFP:NPSN11* (**A**) or *GFP:SNAP33* (**B**) transgenes were treated with 50 µM BFA for 30 min followed by 50 µM BFA + 20 µM estradiol for 210 min (see ***Figure 1D***). Protein extracts were subjected to immunoprecipitation with anti-GFP beads, protein blots were probed with the antisera indicated on the right (IB): GFP, anti-GFP; KN, anti-KNOLLE; V721/V722, anti-VAMP721/722; SYP71, anti-SYP71; SNAP33, anti-SNAP33; kDa, protein size (left); MW, molecular weight; -BFA, mock treatment; +BFA, BFA treatment; T, total extract; UB, unbound; IP, immunoprecipitate. Loading (%), relative loading volume to total volume; relative signal intensity (input signal = 100% for UB and IP). The experiments were technically repeated more than six times.
DOI: 10.7554/eLife.25327.008

Our results indicate that cytokinetic SNARE complexes are assembled on the ER and from there delivered as *cis*-SNARE complexes rather than monomeric SNARE proteins along the secretory pathway, via Golgi stack and TGN, to the plane of cell division (***Figure 4***). This implies that *cis*-SNARE complexes (i.e. residing on the same membrane) are delivered to the division plane where they are transformed into fusogenic *trans*-SNARE complexes linking adjacent membrane vesicles. These observations also explain the requirement for the SM protein KEULE during cell-plate formation (***Park et al., 2012***). Breaking up *cis*-SNARE complexes by the action of NSF ATPase, which normally

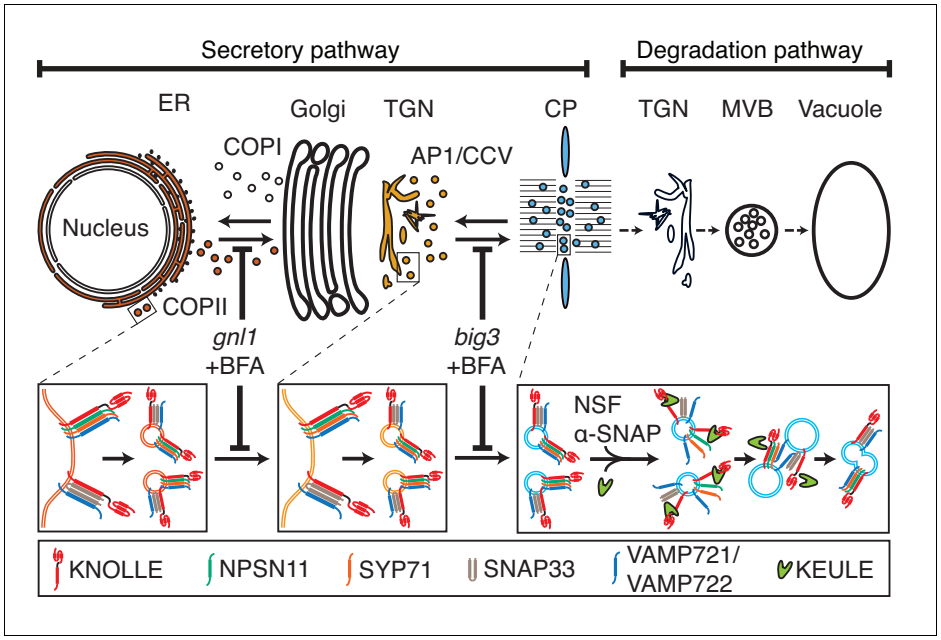

Figure 4. Trafficking of *cis*-SNARE complexes during cytokinesis (model). Two different types of cytokinetic *cis*-SNARE complexes are assembled on the ER, recruited into COPII vesicles and passed on to the Golgi stack/TGN. At the TGN, they are incorporated into AP1/CCV vesicles for delivery to the division plane. Following their disassembly by NSF ATPase, monomeric Qa-SNARE KNOLLE is assisted by SM protein KEULE in the formation of *trans*-SNARE complexes mediating fusion of adjacent vesicles during cell-plate formation and expansion (***Park et al., 2012***).

DOI: 10.7554/eLife.25327.009

occurs following the fusion of membrane vesicles with the target membrane (***Rizo and Südhof, 2012***) would result in back-folding of the monomeric Qa-SNARE to prevent re-formation of the *cis*-SNARE complex. In cytokinesis, however, SM protein KEULE interacts with Qa-SNARE KNOLLE to keep it open as a prerequisite for the formation of the fusogenic *trans*-SNARE complex (***Park et al., 2012***).

Trafficking of *cis*-SNARE complexes has two major advantages: (i) the *cis*-SNARE complex is an energetically favoured inactive form (***Jahn et al., 2003***) that is well-suited for transport and also ensures equal amounts of SNARE partners being delivered to the site of action. The four-helical bundle of the SNARE domains is very stable, requiring ATP hydrolysis for its disassembly. Because of its stability, the assembled *cis*-SNARE complex is physiologically inactive, not interacting with other SNARE proteins. (ii) Moreover, this might be a highly economic strategy of meeting the sharply rising demand for membrane-fusion capacity during cytokinesis when the equivalent of about one-third of the cell surface area has to be produced in the plane of cell division in a narrow time frame of about 30 min. In animal cytokinesis, the problem is largely solved by reducing the surface area through the constriction by the contractile ring that pulls in the plasma membrane. The remaining gap in the centre of the division plane is then closed by vesicle fusion that is mediated by plasma membrane SNARE proteins present throughout the cell cycle (***Low et al., 2003***) and/or by ESCRTIII activity (***Mierzwa and Gerlich, 2014***). Apart from plant cytokinesis, any major expansion of the eukaryotic cell surface area requires enhanced membrane fusion capacity that cannot easily be matched by the local recycling of plasma membrane-resident SNARE proteins whereas the long-distance delivery of inactive *cis*-SNARE complexes proposed here would meet the requirement.

Materials and methods

Plant material, Growth Condition and Transformation

Arabidopsis thaliana [NCBITaxon:3702] wild-type (Columbia, Col), *pKNOLLE::mCherry:KNOLLE* or mutant plants were grown on soil or media (1/2 MS medium, 0.1% MES, pH 5.6) at 23°C in continuous light condition. *big3* homozygous plants were transformed with *pMDC7::GFP:SNAP33* or *pMDC7::YFP:NPSN11* using *Agrobacterium* [NCBITaxon:358]-mediated floral dipping (**Clough and Bent, 1998**; **Richter et al., 2014**). T1 seedlings were selected on Hygromycin (20 µg/ml, Duchefa Biochemie, Netherlands) plates to isolate *big3* mutant plants carrying transgenes *pMDC7::GFP:SNAP33* or *pMDC7::YFP:NPSN11*. The same transgenes were introduced into a BFA-sensitive *GNL1* genetic background by crossing these transgenic plants with *gnl1* homozygous plants bearing a $pGNL1::GNL1^{BFA\text{-}sens.}$ transgene (**Richter et al., 2007**). For interaction analysis of NPSN11 and SNAP33 with MVB-localised Qa-SNARE PEP12 (aka SYP21), *big3* homozygous plants bearing *pMDC7::GFP:SNAP33* or *pMDC7::YFP:NPSN11* were transformed with *pKNOLLE::mRFP:PEP12*. T1 plants were selected by spraying them three times with 1:1000 diluted BASTA (183 g/l glufosinate; AgrEvo, Düsseldorf, Germany). The homozygous background of *big3* or *gnl1* $GNL1^{BFA\text{-}sens.}$ was confirmed as previously reported (**Richter et al., 2007**, **2014**).

Molecular biology

For generating *pMDC7::GFP:SNAP33, GFP:SNAP33* was amplified with GFP-AttB1-5 and SNAP33-AttB2-3 primers from *p35S::GFP:SNAP33* (**Park et al., 2012**). According to the manufacturer's instruction (Invitrogen, Molecular Probes), the PCR product was cloned into a modified β-estradiol inducible *pMDC7* vector (**Zuo et al., 2000**) in which *Ubiquitin 10* promoter replaced the original promoter (kindly provided by Niko Geldner, Univ. Lausanne). For generating *pMDC7::YFP:NPSN11*, *YFP:NPSN11* was amplified by PCR with YFP-AttB1-5 and NPSN11-AttB2-3 primers from *pKNOLLE::YFP:NPSN11* (**El Kasmi et al., 2013**) and further cloned into the same *pMDC7* vector as described above. For generating *pKNOLLE::mRFP:PEP12*, *PEP12* coding sequence was amplified by PCR with PEP12-XbaI-5 and PEP12-EcoRI-3 primers. The PCR products were digested with *Xba*I and *Eco*RI (Thermo Fischer Scientific, Massachusetts, US) and cloned in-frame downstream of *mRFP* in the *KNOLLE* expression cassette (**Müller et al., 2003**). For primer sequences, see ***supplementary file 1b***.

Chemical treatment

Five-day-old seedlings grown on solid media (1/2 MS, 0.1% MES, pH 5.6, 0.9% Agar) were transferred to liquid media (1/2 MS, 0.1% MES, 1% sucrose, pH 5.6) with or without 50 µM brefeldin A (BFA, 50 mM stock solution in 1:1 DMSO/EtOH, Invitrogen). After 30 min, 20 µM β-estradiol (EST, 20 mM stock solution in DMSO, Sigma-Aldrich, St. Louis, US) was added, and the seedlings were then incubated for another 210 min with mild agitation.

Co-immunoprecipitation and immunoblot analysis

Co-immunoprecipitation was slightly modified from a published protocol (**Park et al., 2012**). In brief, 1–2 g of seedlings were frozen in liquid nitrogen (N_2) immediately after chemical treatment. The seedlings were thoroughly grounded and the powder suspended in ice-cold buffer (50 mM Tris pH 7.5, 150 mM NaCl, 1 mM EDTA, 0.5% Triton X-100) supplemented with EDTA-free complete protease inhibitor cocktail (Roche, Basel, Swiss Confederation). Cleared protein lysate was incubated with anti-GFP beads (GFP-trap, Chromotek, Planegg-Martinsried, Germany) for 2 hr in the cold room with mild rotation. The beads were washed six times with ice-cold buffer (50 mM Tris pH 7.5, 150 mM NaCl, 1 mM EDTA, 0.2% Triton X-100) supplemented with EDTA-free complete protease inhibitors cocktail and resuspended with 2x Laemmli buffer. For ***Figure 2—figure supplements 1B***, 0.3 ml of cleared protein extracts of YFP:N11 or GFP:SNAP33 were incubated with 0.3 ml or 3 ml of the cleared protein extracts of mCherry:KNOLLE for 2 hr as described above and subjected to immunoprecipitation with anti-GFP beads. For immunoblot analysis, primary antisera anti-GFP (1:1000, mouse, Roche [SCR:001326]), anti-KNOLLE (KN, 1:6000, rabbit) (**Lauber et al., 1997**), anti-VAMP721/VAMP722 (V721/V722) (1:5000, rabbit) (**Kwon et al., 2008**), anti-SNAP33 (1:5000, rabbit) (**Heese et al., 2001**), anti-SYP71 (1:4000, rabbit) (**El Kasmi et al., 2013**), anti-RFP (1:700, rat, Chromotek [RRID:AB_2336064]), anti-γCOP (aka SEC21) (1:5000, rabbit, Agrisera, Vännäs, SWEDEN

[SCR:013574]) and POD-conjugated secondary antibodies (1:5000 for anti-rabbit-POD, 1:2000 for anti-rat-POD, Sigma-Aldrich [SCR:008988]) were used. Membranes were developed using a chemiluminescence detection system (Fusion Fx7 Imager, PEQlab, Erlangen, Germany).

Immunofluorescence analysis

After chemical treatment, seedlings were immediately fixed in 4% (w/v) paraformaldehyde for 1 hr and stored at −20˚C until used for immunostaining. For immunofluorescence, primary antisera anti-KN (1:4000, rabbit) (***Lauber et al., 1997***), anti-γCOP (1:2000, rabbit, Agrisera), anti-α-tubulin (1:600, rat, Abcam, Cambridge, UK [SCR:012931]) and secondary antibodies anti-rabbit Cy3 (1:600, Dianova, Hamburg, Germany), anti-rat Cy3 (1:600, Dianova) were applied. Nuclei were stained with 1 µg/ml DAPI (1 mg/ml stock solution in H_2O). Samples were prepared manually or with an immunohistochemistry system (InsituPro VSi, Intavis, Cologne, Germany). Fluorescent images were taken using a confocal laser scanning microscope (Leica SP8 for ***Figure 1*** and ***Figure 1—figure supplements 1*** and ***2***; Zeiss LSM880 for ***Figure 1—figure supplement 3***).

Softwares

Sequences were analysed with CLC main workbench 6. Fluorescent images were maximally projected from Z-stack images using the Fiji ImageJ program. Images were further processed using Adobe Photoshop CS3 and Adobe Illustrator CS3. For quantifying signal intensity in immunoblot analysis, the Fiji (ImageJ, NIH) program was used.

Acknowledgements

We thank Jennifer Saile and Sandra Richter for technical assistance, Sandra Richter and Simon Klesen for construction of *pKNOLLE::mCherry:KNOLLE*, Niko Geldner for vector, Paul Schultze-Lefert, Tony Sanderfoot and Natasha V Raikhel for antisera and Thorsten Nürnberger, Martin Bayer, Christopher Grefen and Niko Geldner for critical reading of the manuscript. Funding by the Deutsche Forschungsgemeinschaft is gratefully acknowledged.

Additional information

Funding

Funder	Grant reference number	Author
Deutsche Forschungsgemeinschaft	Ju 179/19-1	Gerd Jürgens

The funders had no role in study design, data collection and interpretation, or the decision to submit the work for publication.

Author contributions

MK, Acquisition of data, Analysis and interpretation of data; MP, Acquisition of data, Writing-review and editing, Analysis and interpretation of data, Drafting and revising the article; UM, UH, Acquisition of data; GJ, Conceptualization, Funding acquisition, Writing-original draft, Writing-review and editing, Conception and design

Author ORCIDs

Gerd Jürgens, http://orcid.org/0000-0003-4666-8308

Additional files

Supplementary files

• Supplementary file 1. (a) Frequency of cytokinetic cells in mutant seedling roots. (b) Primers used in this study

DOI: 10.7554/eLife.25327.010

References

Clough SJ, Bent AF. 1998. Floral dip: a simplified method for Agrobacterium-mediated transformation ofArabidopsis thaliana. *The Plant Journal* **16**:735–743. doi: 10.1046/j.1365-313x.1998.00343.x

da Silva Conceição A, Marty-Mazars D, Bassham DC, Sanderfoot AA, Marty F, Raikhel NV. 1997. The syntaxin homolog AtPEP12p resides on a late post-golgi compartment in plants. *The Plant Cell* **9**:571–582. doi: 10.2307/3870508, PMID: 9144962

El Kasmi F, Krause C, Hiller U, Stierhof YD, Mayer U, Conner L, Kong L, Reichardt I, Sanderfoot AA, Jürgens G. 2013. SNARE complexes of different composition jointly mediate membrane fusion in arabidopsis cytokinesis. *Molecular Biology of the Cell* **24**:1593–1601. doi: 10.1091/mbc.E13-02-0074, PMID: 23515225

Heese M, Gansel X, Sticher L, Wick P, Grebe M, Granier F, Jurgens G. 2001. Functional characterization of the KNOLLE-interacting t-SNARE AtSNAP33 and its role in plant cytokinesis. *The Journal of Cell Biology* **155**:239–250. doi: 10.1083/jcb.200107126, PMID: 11591731

Jahn R, Lang T, Südhof TC. 2003. Membrane fusion. *Cell* **112**:519–533. doi: 10.1016/S0092-8674(03)00112-0, PMID: 12600315

Kwon C, Neu C, Pajonk S, Yun HS, Lipka U, Humphry M, Bau S, Straus M, Kwaaitaal M, Rampelt H, El Kasmi F, Jürgens G, Parker J, Panstruga R, Lipka V, Schulze-Lefert P. 2008. Co-option of a default secretory pathway for plant immune responses. *Nature* **451**:835–840. doi: 10.1038/nature06545, PMID: 18273019

Lauber MH, Waizenegger I, Steinmann T, Schwarz H, Mayer U, Hwang I, Lukowitz W, Jürgens G. 1997. The Arabidopsis KNOLLE protein is a cytokinesis-specific syntaxin. *The Journal of Cell Biology* **139**:1485–1493. doi: 10.1083/jcb.139.6.1485, PMID: 9396754

Low SH, Li X, Miura M, Kudo N, Quiñones B, Weimbs T. 2003. Syntaxin 2 and endobrevin are required for the terminal step of cytokinesis in mammalian cells. *Developmental Cell* **4**:753–759. doi: 10.1016/S1534-5807(03)00122-9, PMID: 12737809

Mierzwa B, Gerlich DW. 2014. Cytokinetic abscission: molecular mechanisms and temporal control. *Developmental Cell* **31**:525–538. doi: 10.1016/j.devcel.2014.11.006, PMID: 25490264

Mossessova E, Corpina RA, Goldberg J. 2003. Crystal structure of ARF1*Sec7 complexed with brefeldin A and its implications for the guanine nucleotide exchange mechanism. *Molecular Cell* **12**:1403–1411. doi: 10.1016/S1097-2765(03)00475-1, PMID: 14690595

Müller I, Wagner W, Völker A, Schellmann S, Nacry P, Küttner F, Schwarz-Sommer Z, Mayer U, Jürgens G. 2003. Syntaxin specificity of cytokinesis in Arabidopsis. *Nature Cell Biology* **5**:531–534. doi: 10.1038/ncb991, PMID: 12738961

Müller S, Jürgens G. 2016. Plant cytokinesis-No ring, no constriction but centrifugal construction of the partitioning membrane. *Seminars in Cell & Developmental Biology* **53**:10–18. doi: 10.1016/j.semcdb.2015.10.037, PMID: 26529278

Nakayama K. 2016. Regulation of cytokinesis by membrane trafficking involving small GTPases and the ESCRT machinery. *Critical Reviews in Biochemistry and Molecular Biology* **51**:1–6. doi: 10.3109/10409238.2015.1085827, PMID: 26362026

Park M, Song K, Reichardt I, Kim H, Mayer U, Stierhof YD, Hwang I, Jürgens G. 2013. Arabidopsis μ-adaptin subunit AP1M of adaptor protein complex 1 mediates late secretory and vacuolar traffic and is required for growth. *PNAS* **110**:10318–10323. doi: 10.1073/pnas.1300460110, PMID: 23733933

Park M, Touihri S, Müller I, Mayer U, Jürgens G. 2012. Sec1/Munc18 protein stabilizes fusion-competent syntaxin for membrane fusion in Arabidopsis cytokinesis. *Developmental Cell* **22**:989–1000. doi: 10.1016/j.devcel.2012.03.002, PMID: 22595672

Reichardt I, Stierhof YD, Mayer U, Richter S, Schwarz H, Schumacher K, Jürgens G. 2007. Plant cytokinesis requires de novo secretory trafficking but not endocytosis. *Current Biology* **17**:2047–2053. doi: 10.1016/j.cub.2007.10.040, PMID: 17997308

Renault L, Guibert B, Cherfils J. 2003. Structural snapshots of the mechanism and inhibition of a guanine nucleotide exchange factor. *Nature* **426**:525–530. doi: 10.1038/nature02197, PMID: 14654833

Richter S, Geldner N, Schrader J, Wolters H, Stierhof YD, Rios G, Koncz C, Robinson DG, Jürgens G. 2007. Functional diversification of closely related ARF-GEFs in protein secretion and recycling. *Nature* **448**:488–492. doi: 10.1038/nature05967, PMID: 17653190

Richter S, Kientz M, Brumm S, Nielsen ME, Park M, Gavidia R, Krause C, Voss U, Beckmann H, Mayer U, Stierhof YD, Jürgens G. 2014. Delivery of endocytosed proteins to the cell-division plane requires change of pathway from recycling to secretion. *eLife* **3**:e02131. doi: 10.7554/eLife.02131, PMID: 24714496

Rizo J, Südhof TC. 2012. The membrane fusion enigma: snares, Sec1/Munc18 proteins, and their Accomplices—Guilty as Charged? *Annual Review of Cell and Developmental Biology* **28**:279–308. doi: 10.1146/annurev-cellbio-101011-155818

Zheng H, Bednarek SY, Sanderfoot AA, Alonso J, Ecker JR, Raikhel N. 2002. NPSN11 is a cell Plate-Associated SNARE protein that interacts with the Syntaxin KNOLLE. *Plant Physiology* **129**:530–539. doi: 10.1104/pp.003970

Zuo J, Niu QW, Chua NH. 2000. Technical advance: an estrogen receptor-based transactivator XVE mediates highly inducible gene expression in transgenic plants. *The Plant Journal* **24**:265–273. doi: 10.1046/j.1365-313x.2000.00868.x, PMID: 11069700